HELSINKI POLYTECHNIC
Faculty of Technology

Electrical Engineering

Electronics and Automation

BACHELOR’S THESIS

RELAY CARD FOR CAPACITANCE MEASUREMENTS

Author: Sami Romo
Supervisor: Esa Häkkinen, Lic. Tech.
Instructor: Sami Salento, MSc

Approved: April ___, 2007

Esa Häkkinen
Lic. Tech.

PREFACE

This bachelor’s thesis was made for the research and development laboratory of VTI Technologies, which I would like to thank for giving me such an interesting subject for my study. I would like to thank all the people in the laboratory who helped me with the technical aspects of the study and who have been working with me, you have created an interesting, inspiring environment to work.

I would also like to thank Esa Häkkinen for his help on the theoretical side of the subject, of which he seems to have broad knowledge. Naturally I could not have completed this study without all the things learned from various teachers in my years at Helsinki Polytechnic Stadia and the one term I spent studying at Oregon Institute of Technology as an exchange student.

Last, but not least I would like to thank my girlfriend Heidi for helping me to have time to complete this study by upholding our household while I was buried in technical papers on relays, printed circuit board materials, electromagnetic compatibility and the like. I could not have done it without you.

The amount of new information I have gained during the making of this study is astonishing. I only hope to keep deepening my understanding on this interesting area of technology in the future.

Helsinki April 18, 2007

Sami Romo

STADIA
HELSINKI POLYTECHNIC

ABSTRACT

Name: Sami Romo

Title: Relay Card for Capacitance Measurements

Date: April 18, 2007
Number of pages: 75 + 25

Department: Electrical Engineering
Study Programme: Electronics and Automation

Supervisor: Esa Häkkinen, Lic. Tech.

Instructor: Sami Salento, MSc

In this bachelor's thesis a relay card for capacitance measurements was designed, built and tested. The study was made for the research and development laboratory of VTI Technologies, which manufactures capacitive silicon micro electro mechanical accelerometers and pressure sensors. As the size of the sensors is decreasing the capacitance value of the sensors also decreases. The decreased capacitance causes a need for new and more accurate measurement systems.

The technology used in the instrument measuring the capacitance dictates a framework how the relay card should be designed, thus the operating principle of the instrument must be known. To achieve accurate results the measurement instrument and its functions needed to be used correctly.

The relay card was designed using printed circuit board design methods that minimize interference coupling to the measurement. The relay card that was designed in this study is modular. It consists of a separate CPU card, which was used to control the add-on cards connected to it. The CPU card was controlled from a computer through a serial bus. Two add-on cards for the CPU card were designed in this study. The first one was the measurement card, which could be used to measure 32 capacitive sensors. The second add-on card was the MUX card, which could be used to switch between two measurement cards.

The capacitance measurements carried out through the MUX card and the measurement cards were characterized with a series of test measurements. The test measurement data was then analysed. The relay card design was confirmed to work and offer accurate measurement results up to a measurement frequency of 10 MHz. The length of the measurement cables limited the measurement frequency.

Keywords: Capacitance Measurement, PCB Design, Relay Card

TIIVISTELMÄ

Tekijä: Sami Romo

Työn nimi: Relekortti kapasitanssimittauksiin

Päivämäärä: 18.4.2007 Sivumäärä: 75 + 25

Koulutusohjelma: Sähkötekniikka Suuntautumisvaihtoehto: Elektroniikka ja automaatio

Työn valvoja: Yliopettaja tekn. lis. Esa Häkkinen

Työn ohjaaja: Tuotekehityslaboratorion johtaja DI Sami Salento

Tässä työssä suunniteltiin, rakennettiin ja testattiin relekortti kapasitanssimittauksiin VTI Technologies Oy:n tuotekehityslaboratoriolle. VTI valmistaa piistä kapasitiivisia mikromekaanisia paine- ja kiihtyvyysantureita. Uudet anturit ovat yhä pienempiä ja niiltä odotetaan suurempaa tarkkuutta kuin aiemmin. Tämä saa aikaan tarpeen yhä tarkemmille mittausjärjestelmille antureiden karakterisointiin niiden tuotekehitysvaiheessa.

Työssä käsitellään kapasitanssin mittauksessa käytetyn mittalaitteen tekniikkaa, sillä mittalaitteen ominaisuudet vaikuttivat relekortin suunnitteluun. Tästä syystä käytetyn mittalaitteen ominaisuudet tuli tietää ja niitä piti osata käyttää oikein.

Relekortti suunniteltiin käyttäen tekniikoita, jotka minimoivat ulkoisten häiriöiden vaikutukset mittauksiin. Jotta relekortti olisi helppo päivittää ja muokata erilaisiin mittauksiin sopivaksi, suunniteltiin se modulaariseksi. Relekortti koostui erillisestä prosessorikortista, jota ohjattiin tietokoneella sarjaväylän kautta. Prosessorikorttiin voitiin kiinnittää lisäkortteja, joilla itse mittaus tehtiin. Työssä suunniteltiin kaksi eri lisäkorttia, jotka liitetään prosessorikorttiin. Ensimmäinen lisäkortti oli kapasitanssimittakortti, jonka avulla voitiin mitata 32 kapasitivista anturia. Toinen lisäkortti oli vaihtokytkinkortti, jonka avulla voitiin käyttää kahta kapasitanssimittauskorttia ja mitata yhteensä 64 kapasitiivista anturia.

Relekortin toiminta todettiin testimittauksilla joiden tulokset analysoitiin. Relekortti todettiin toimivaksi ja sillä saatiin aikaan erittäin tarkkoja kapasitanssimittauksia aina 10MHz mittaustaajuudelle asti. Mittaustaajuutta rajoittaa mittauskaapelien pituus, joita lyhentämällä taajuutta voitaisiin nostaa.

Avainsanat: Kapasitanssin mittaus, piirilevysuunnittelu, relekortti

TABLE OF CONTENTS

APPENDICES

SYMBOLS AND ABBREVIATIONS

2T	Two Terminal
4TP	Four Terminal Pair
B	Susceptance
C	Capacitance
C_0	Characteristic Capacitance
CLK	Clock
CPU	Central Processing Unit
CS	Chip Select
CTE	Coefficient of Thermal Expansion
DPDT	Dual Pole Dual Throw
DUT	Device Under Test
ε_0	Dielectric Constant of Free Air
ε_{eff}	Effective Dielectric Constant
ε_r	Relative Dielectric Constant
EMC	Electromagnetic Compatibility
FET	Field Effect Transistor
G	Conductance
$\mathrm{H_c}$	High Current
$\mathrm{H_p}$	High Potential
$\mathrm{I^2C}$	Inter Integrated Circuit
IC	Integrated Circuit
ISP	In System Programming
λ	Wavelength
L	Inductance
L_0	Characteristic Inductance
$\mathrm{L_c}$	Low Current
$\mathrm{L_p}$	Low Potential

MISO	Master In Slave Out
MOSI	Master Out Slave In
MUX	Multiplexer
PCB	Printed Circuit Board
θ	Phase
R	Resistance
SE	Shielding Effectiveness
SER	Reduction in Shielding Effectiveness
SPI	Serial Peripheral Interface
T_g	Glass Transition Temperature
τ_{pd}	Propagation Delay
USART	Universal Synchronous Asynchronous Receiver Transmitter
X	Reactance
Y	Admittance
Z	Impedance
Z_0	Characteristic Impedance

1 INTRODUCTION

This bachelor's thesis, Relay Card for Capacitance Measurements, was made to fill the need to improve the measuring accuracy of capacitance measurements in the research and development laboratory of VTI Technologies.

VTI is a forerunner in capacitive micro electromechanical systems pressure and acceleration sensors and manufactures millions of sensors per year. VTI Technologies' accelerometers are used mainly in automotive industry for various systems including Antilock Braking Systems, Electronic Stability Control, but also in medical applications like cardiac pacemakers and in inertial navigational devices and nowadays a growing sector is sports and fitness where the sensors are used to measure sport activity level or to help make the perfect swing in golf.

The trend in the sensor market is that new sensors need to be smaller and at the same time more accurate than before. Smaller size yields to lower production price and better profit. As a side product the capacitance value of the sensors decreases. The decreasing capacitance values as well as the increased accuracy requirements make characterizing these new sensors challenging and give improved accuracy requirements for the measurement systems.

In this study the facts contributing to the accuracy of the measurements are first identified and then the relay card is designed using the best possible methods. These facts include proper usage for the measurement instrument, the design of the relay card printed circuit board and selection of materials used in the relay card. The performance of the relay card is then confirmed with a series of test measurements.

As most of VTIs products go to the automotive industry, the measurements need to fill the requirements of the automotive industry. One requirement is that all components can withstand a broad operating temperature range from –40 °C to +125 °C. These high temperatures are challenging for electronic components as well as the printed circuit boards where they are mounted.

For the measurement system used to characterize these sensors needs to measure multiple samples, or DUTs (Device Under Test), the measurement system needs to be automated. In today’s laboratory, this means that a computer controls the measurement system.

The measurement instruments used to characterize the sensors measure impedance. Impedance is a complex quantity, which makes the instruments rather complicated. Capacitance is an imaginary component of impedance.

The measurement instruments operate in a specific way, which dictates how the measurement can and will be carried out. One of the most used instruments to measure impedance is the LCR bridge. LCR bridges are used because of their flexibility to measure all aspects of impedance: inductance L, capacitance C and resistance R, as the name implies. The high precision LCR bridges used in the laboratory are based on the four terminal pair auto balancing bridge.

The auto balancing bridge uses four terminal pairs to connect to the device under test, whose impedance is to be measured. For optimal performance the 4TP (Four Terminal Pair) configuration needs to remain intact all the way to the device under test. A coaxial cable forms one terminal pair, thus four coaxial cables are used to contact the device under the test. However sometimes it is necessary to extend the cables using fewer cables. The shielded 2T (Two Terminal) configuration is used when the 4TP configuration is impractical. Basically this method uses two coaxial cables with their outer conductor connected together to form two shielded terminals.

The surroundings can induce an error to the measurement. Guarding is used to reduce this error. Guarding uses the outer conductor of the coaxial cables to shield against stray capacitance from the surroundings of the device under test.

Before the actual measurements can be performed, the remaining error can be compensated for. Two different error compensation methods are used. The first method is the open / short compensation, it uses the results from open and short circuit measurements to compensate the error caused by the test cables and test fixture. On more complex measurement circuits the open / short / load compensation method is used. In the open / short / load method, an additional reference load measurement is used to give a reference point near the value of the device under test. This yields to lower error in complex measurement circuits.

To efficiently do the characterization measurements, multiple DUTs need to be connected to the measurement instrument. The instrument can however measure only one DUT at a time, thus relays are used to switch one DUT to the measurement instrument at a time. The printed circuit board of this relay card needs to be designed in a specific way, minimizing the errors that improper design would cause to the measurement. Improper design could not only cause errors to the measurement but also render the device useless.

Because the measurement instruments can be operated using high frequencies, controlled impedance throughout the measurement cables is imperative. Most instruments are designed to use coaxial cables with a characteristic impedance of 50 Ω. The characteristic impedance of the cables should stay the same all the way to the device under test. This means that the measurement signals on the relay card should also have the same impedance. Two basic methods are used to create controlled impedance traces in printed circuit boards. The first one is the microstrip where a trace lies above a reference plane. The second is the stripline where the trace is located between two reference planes. The dimensions of the trace and the planes, as well as the dielectric material in between determine the characteristic impedance of the trace.

One important thing in sensitive high accuracy measurements is shielding. Usually this means enclosing the electronic device in a conducting case. However, shielding can also be used within the printed circuit board of the electronic device. Any practical enclosure needs apertures for wires or displays. These apertures hinder the shielding and dictate the shielding effectiveness of the enclosure. Keeping the apertures as small as possible compared to the wavelength of the noise to be shielded against increases the shielding effectiveness.

Today’s electronic devices use printed circuit boards with multiple layers, the way the printed circuit board is constructed is called the stackup of the printed circuit board. The stackup of printed circuit boards with multiple layers can be constructed in many different ways. The stackup consists of layers of so called core and prepreg laminates and the way these laminates are used to construct the printed circuit board is the stackup, which is some times also called build-up.

The printed circuit board can be made from different materials. The most used material is the FR4, which offers adequate performance for most applications. However, the high temperature the relay card needs to withstand rules out the use of FR4. Rogers is a material used in high-speed electronics devices, but it also outperforms the FR4 material in temperature durability.

Theory and proper usage of the equipment used to measure capacitance in the laboratory are explained in Chapter 2. Chapter 3 introduces some fundamental design techniques for printed circuit boards to achieve electromagnetic compatibility. Chapter 4 details the design of the cards designed in this study and Chapter 5 explains how the cards are used. The relay card is then characterized in Chapter 6.

2 CAPACITANCE MEASUREMENTS

Capacitance measurements are in fact complex impedance measurements. Figure 1 below illustrates the complex nature of impedance.

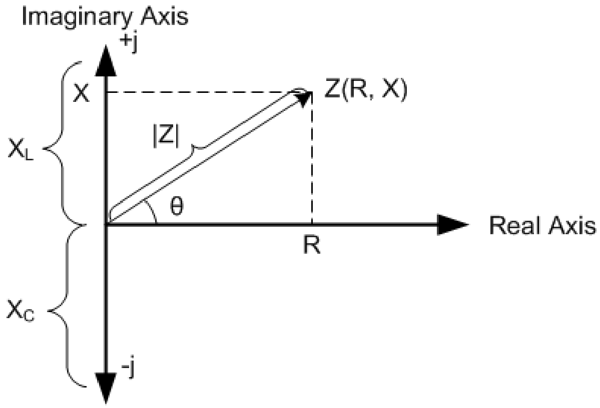

Figure 1. *Definition of impedance. The real part of impedance is resistance R and the imaginary part is reactance X. Reactance can be divided in to inductive part X_L and capacitive part X_C.*

Reactance can be divided in to positive side X_L created by Inductance L, and the negative side X_C created by capacitance C. The reciprocal of impedance is the admittance Y. Different ways of representing the impedance are shown in Equation 1.

$$Z = R + jX = \frac{1}{Y} = \frac{1}{G + jB} = |Z|\angle\theta \qquad (1)$$

Where *Z* is the impedance, *Y* the admittance, *R* the resistance, *X* the reactance, *j* the imaginary unit, *G* the conductance, *B* the susceptance and |*Z*| the magnitude and θ the phase angle of the impedance.

The complex nature of impedance and its frequency dependency makes the instruments used to measure it fairly complicated. The most common and versatile instrument used to measure impedance is the LCR-bridge. LCR-bridge can measure all the forms of impedance: Inductance *L*, capacitance *C* and resistance *R*, as the name implies. Depending on the model of the instrument a range of other options is available. These commonly include settings for frequency, measurement voltage, DC (Direct Current) offset voltage, averaging functions, DUT impedance range settings and powerful error compensation settings, which make LCR-bridges very versatile and accurate instruments for various impedance measurements. The auto balancing bridge method is the most used impedance measurement technology in high performance LCR-bridges. Other common methods used to measure impedance are the bridge method, RF I-V method and the network analysis method which all have their own characteristics.

Chapter 2.1 briefly explains how the Auto Balancing Bridge Method of measuring capacitance works and Chapter 2.2 concentrates on different techniques used to achieve accurate measurements by using the instrument correctly in different situations. Chapter 3 explains various printed circuit board design techniques. The information on Chapters 2 and 3 is combined in Chapter 4 in the design of the relay card.

2.1 Auto Balancing Bridge Method

The auto balancing bridge method offers accurate measurements with a broad frequency range and is thus the most used high performance method of measuring impedance up to around 100 MHz. Different instruments use different configurations of the auto balancing bridge method and even in the same instrument the low frequency measurements are performed with a different configuration from the high frequency measurements. The main operating principle of the auto balancing bridge method and its contact to the DUT are illustrated in Figure 2.

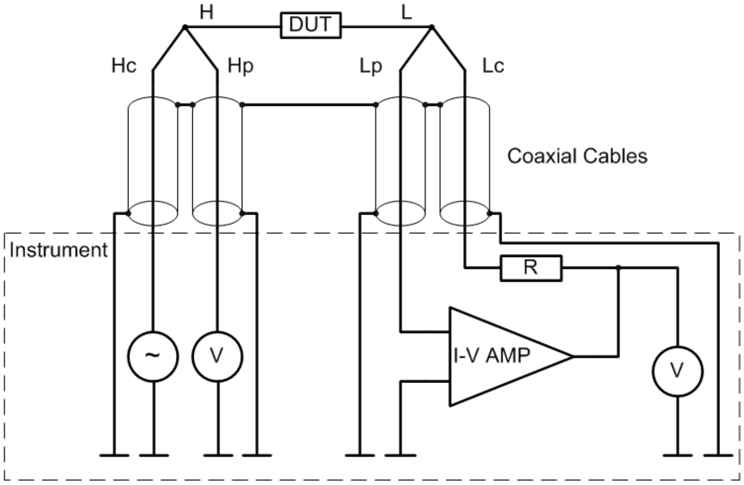

Figure 2. *The four terminal pair auto balancing bridge [Adopted from reference 1, p. 61]. The I-V converter amplifier maintains potential L at a virtual ground. The impedance of the DUT is calculated from the measured potential at H and the voltage across the resistor R.*

The current flowing through the DUT also flows through the resistor R. The potential L on the right side of the DUT is maintained at a virtual ground. The virtual ground is maintained because the I-V converter amplifier balances the current flowing through R with the current flowing through the DUT. The impedance if the DUT is calculated from the measured potential at H and the voltage across the resistor R. All of the measurements result in vectors, or complex numbers, as both the magnitude and the phase of the signal are measured. The vector nature of the measurements makes the actual instruments rather complicated.

There are two conductors, current c and potential p, going to each point L and H from the instrument. To achieve optimum measurement accuracy, these conductors are connected together as close to the DUT as possible. The current flows through the DUT in the H_C and L_C conductors and the measurement is performed with the H_P and L_P conductors, this way the current flowing through the DUT will not affect the actual measurement and cause an error to the measurement. The outer conductors of the coaxial cables must be connected together. This is done as close as the DUT as possible.

Because the instrument can be used in high frequencies, controlled impedance throughout the instrument and its cables is necessary. Coaxial cables with a characteristic impedance of 50 Ω are most commonly used to connect the instrument to the DUT since they give high performance throughout the whole frequency range of the instrument. The auto balancing bridge illustrated in figure 1 is also called the four terminal pair auto balancing bridge because of the four coaxial cables. The inner and the outer conductor of each of the coaxial cables form a terminal pair, thus the 4TP name. The four conductor pairs are labelled low current (L_C), low potential (L_P), high current (H_C) and high potential (H_P). A more detailed description of an actual instrument and how it works can be found in Okada and Sekino (2003, p. 19).

2.2 Achieving Accurate Measurements Using Proper Techniques

The measurement results of any high precision instrument can be ruined by improper usage. This Chapter explains the most important procedures that assure reliable and accurate measurements with an LCR-bridge using the 4TP auto balancing bridge method.

2.2.1 Guarding

Guarding is one of the most important factors in obtaining reliable and accurate measurement results; it dramatically decreases the stray capacitance from the surroundings of the DUT. Stray capacitance causes an error to the measurement and its effects can be reduced with guarding. Figure 3 shows how the outer conductor of the coaxial cables in the 4TP configuration can be used as a guard.

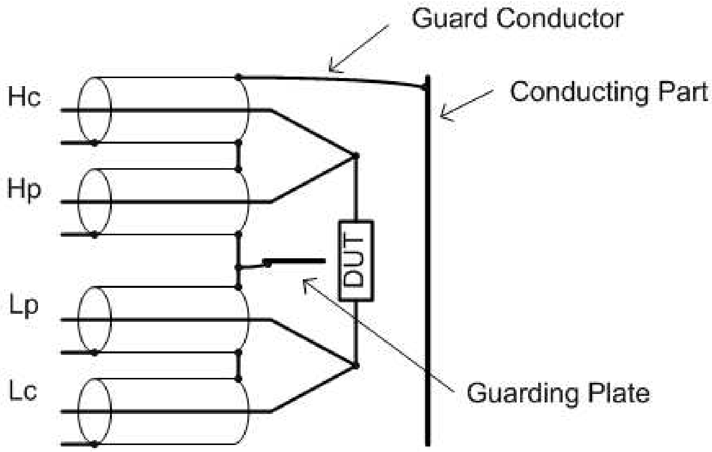

Figure 3. *Guarding against stray capacitance [Adopted from reference 1, p.48]. All conducting parts near the DUT should be connected to the guard. A guarding plate can be connected between the H and L terminals if possible.*

The outer conductors of the coaxial cables, which are connected together, are connected to any conducting parts near the DUT to reduce stray capacitance from the conducting parts to the measurement terminals. A guarding plate can be added between the H and L terminals to reduce stray capacitance between the measurement terminals. Adding a guarding plate may not be possible when measuring physically very small DUT.

2.2.2 Cable Extensions

4TP to 4TP Cable Extension

The cables used in the 4TP measurement can be extended. However, the length of the cable must be shorter than one half of the wavelength for the 4TP configuration to work properly. Okada and Sekino (2003, p. 41) give the following guideline to determine the maximum usable length for the cable.

$$f \times l \leq 15 \qquad (2)$$

Where *f* is the measurement frequency in MHz and *l* the length of the cable in meters.

When extending the existing cables, the extension must be done in a specific way to achieve the best performance. When measuring at low frequencies the 4TP to 4TP extension method illustrated in Figure 4 is preferred [1, p. 39].

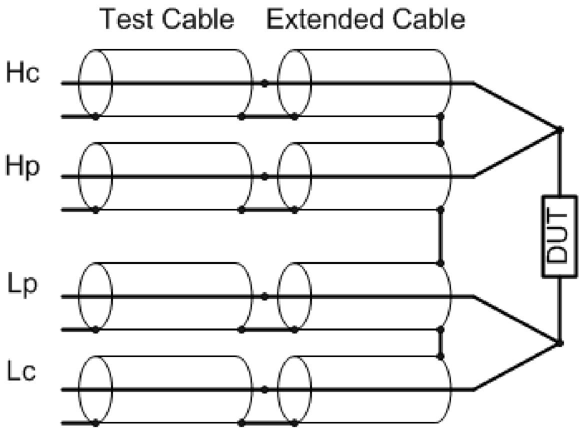

Figure 4. *4TP to 4TP cable extension method [Adopted from reference 1, p. 40]. By extending the outer conductor of the cables also, the 4TP configuration is maintained all the way to the DUT. However, the outer conductors must be connected together at the end of the cables.*

In the 4TP to 4TP extension method, the outer conductor of the coaxial cable is also extended and not connected together with the other outer conductors at the extension joint. The outer connectors are connected together at the end of the cables, just before the DUT for optimal performance. This way the 4TP configuration is maintained all the way to the DUT.

Shielded 2T Cable extension

The 2T extension method can be used if longer extension or higher measurement frequency is needed. The shielded 2T extension is usable to around 15 MHz [1, p. 45]. Figure 5 illustrates the shielded 2T cable extension method.

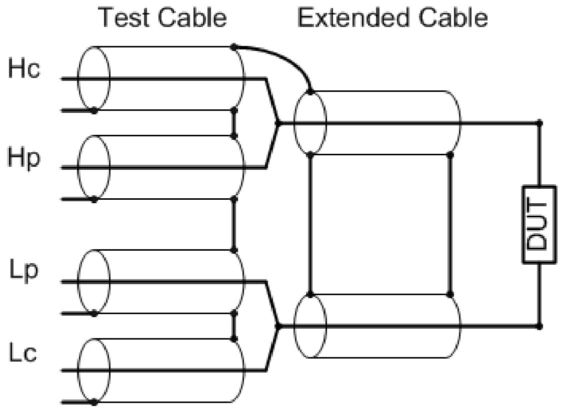

Figure 5. *Shielded 2T cable extension method [Adopted from reference 1, p. 46]. The 4TP configuration is terminated at the extension joint, and the outer conductors of the extended cable act as a guard between the two extended inner conductors.*

The 4TP configuration is terminated at the extension joint, and the outer conductors of the extension cables are connected together at both ends. The outer conductor of the cables acts as a guard between the inner conductors of the extended cable, hence the shielded 2T name. The residual impedance of the extension cable will cause an error to the measurement as it is directly added to the measurement result. The error is negligible if the impedance of the DUT is much greater than the residual impedance of the extension cable.

2.2.3 Error Compensation

After eliminating all possible sources of inaccuracies and minimizing the error to the measurement, the remaining error can be compensated. There are two different methods of error compensation that can be used depending on the measurement setup. The open / short compensation is the easier, but sufficient when using standard cables and the measurement circuit is very simple. The open / short / load compensation is used when non-standard or extended cables or user made test fixture is used. The open / short / load compensation is also effective when using switch boxes or other complicated test circuits. Error compensation needs to be performed before the actual measurement, except when connecting the DUT straight to the instrument using no cables or very short cables. Every time the test fixture or test leads are changed the error compensation needs to be carried out again to ensure accurate measurements. In a laboratory environment it is vital that the error compensation is performed properly because of the tests and test fixtures keep evolving.

Open / Short Compensation

Open / short compensation assumes that the residuals of the test fixture can be represented by a simple equivalent circuit featured in Figure 6.

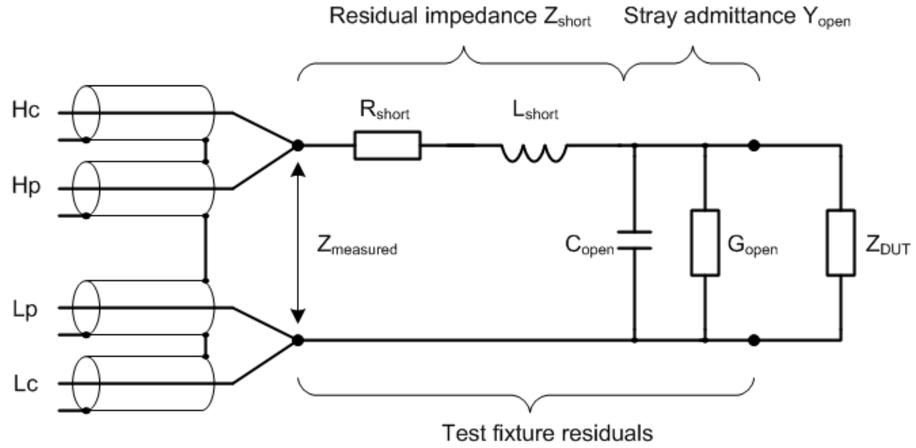

Figure 6. *Test fixture residuals [Adopted from reference 1, p. 43]. When measuring the impedance of the DUT, the residual impedance and the stray admittance of test fixture cause an error to the measurement. The induced error can be compensated using the open / short compensation method.*

Open / short compensation represents the text fixture residuals as a combination of residual impedance formed by R_{short} and L_{short} in series with the DUT and stray admittance formed by C_{open} and G_{open} parallel to the DUT.

Open measurement needed to calculate the compensation is illustrated in Figure 7.

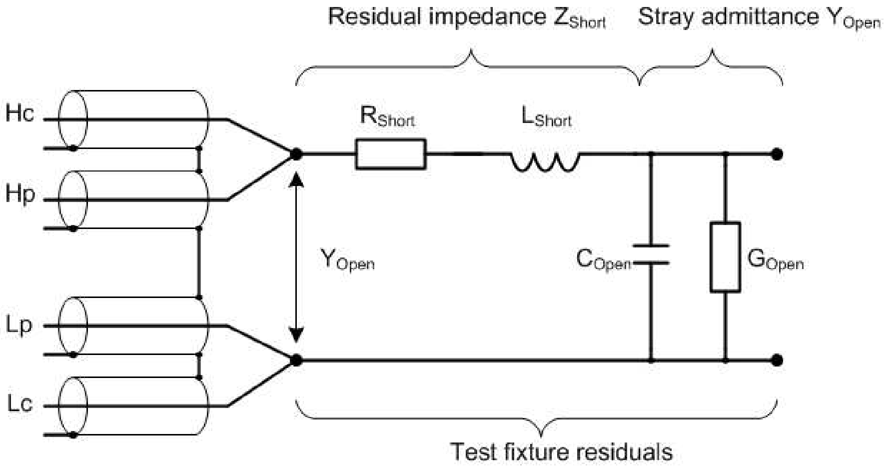

Figure 7. *Open measurement for error compensation [Adopted from reference 1, p. 43]. The stray admittance is measured leaving the measurement terminals open.*

When measuring the open compensation the residual impedance Z_{short} is negligible and the stray admittance is measured as Y_{open}. Figure 8 illustrates the short measurement.

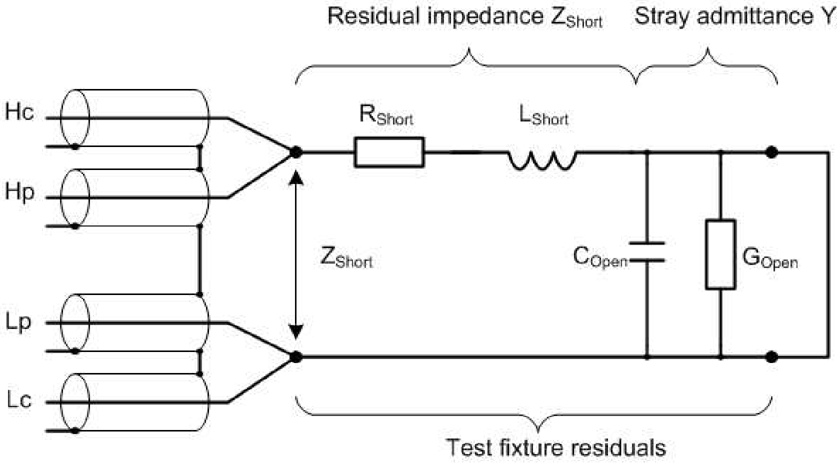

Figure 8. *Short measurement for error compensation [Adopted from reference 1, p. 43]. The residual impedance is measured by shorting the measurement terminals.*

When measuring the short compensation Y_{open} is bypassed and residual impedance is measured as Z_{short}.

Open and short measurements give the parameters for a simple equivalent circuit representing the residual impedances in Figure 9.

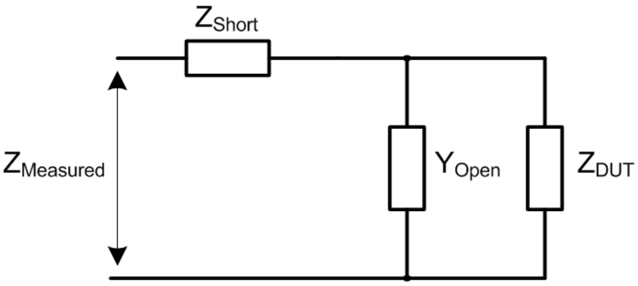

Figure 9. *Equivalent circuit of the open / short compensation method [Adopted from reference 1, p. 43]. The open and short measurement results are used to create an equivalent circuit where the impedance of the DUT can be solved.*

Now each residual parameter is known and can be represented as series impedance Z_{short} and parallel admittance Y_{open} in the equivalent circuit.

The unknown impedance of the DUT can now be calculated from Equation 3:

$$Z_{DUT} = \frac{Z_m - Z_s}{1 - (Z_m - Z_s)Y_o} \tag{3}$$

Where, $Y_o = G_o + j\omega C_o$ is the stray admittance, $Z_s = R_s + j\omega L_s$ is the stray impedance and Z_{DUT} is the impedance of the DUT.

Open / Short / Load Compensation

The open / short / load compensation is preferred over the open / short compensation if the measurement is carried out through a complicated test circuit or extended cables. The unknown four -terminal network circuit illustrated in Figure 10 represents the characteristics of the measurement circuit and test leads.

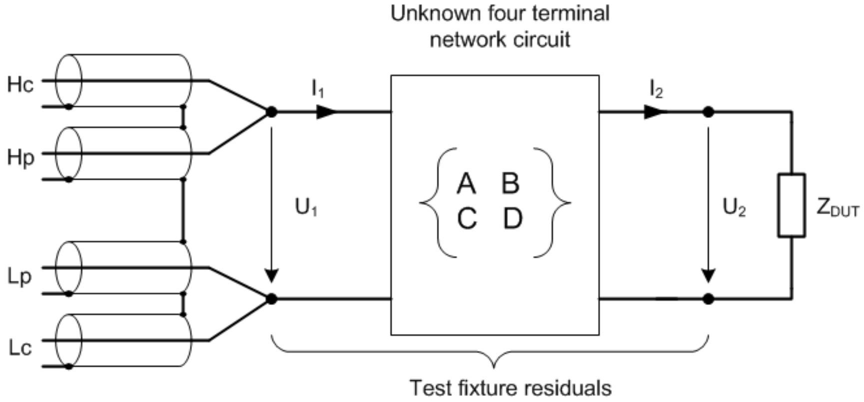

Figure 10. *Open / short / load compensation method [Adopted from reference 1, p. 57]. The residuals of the test fixture are modelled as an unknown four terminal network circuit.*

This advanced method of compensation is used when the complicated residual circuit cannot be modelled as the simple equivalent circuit shown earlier in Figure 9. Instead the open / short / load method models the residuals as a four-terminal network circuit.

If Z_2 is the impedance of a DUT connected to the instrument, the instrument would measure impedance Z_1 as:

$$Z_1 = \frac{AU_2 + BI_2}{CU_2 + DI_2} = \frac{AZ_2 + B}{CZ_2 + D} \tag{4}$$

Where A, B, C and D are the parameters of the four terminal network circuit, U_2 the voltage of the DUT, I_2 the current of the DUT, U_1 the voltage of the measurement, I_1 the current of the measurement. Using the following vector definitions the parameters A, B, C and D can removed from the equation.

$\mathrm{Z_{Open}}$: Measured open value
$\mathrm{Z_{Short}}$: Measured shorted value
$\mathrm{Z_{Load}}$: Measured standard load value
$\mathrm{Z_{Expected\ load}}$: Expected value of the load
$\mathrm{Z_{Measured}}$: Measured value of DUT
$\mathrm{Z_{DUT}}$: Corrected value of the DUT

$\mathrm{Z_{Open}}$ is the measured open circuit impedance, $\mathrm{Z_{Short}}$ is the measured shorted circuit impedance, $\mathrm{Z_{Load}}$ is the measured value of a standard load connected to the circuit, $\mathrm{Z_{Expected\ load}}$ is the accurate expected impedance of the load,

$Z_{Measured}$ is the impedance measured from the circuit and Z_{DUT} the corrected impedance of the DUT. The analysis yields to Equation 5, which corrects for impedance error factors in the measurement [1, p. 121].

$$Z_{DUT} = \frac{Z_{Expected\,load}(Z_{Open} - Z_{Load})(Z_{Measured} - Z_{Short})}{(Z_{Load} - Z_{Short})(Z_{Open} - Z_{Measured})} \qquad (5)$$

The component used in the load measurement needs to have an accurately known value of the same class and type as the actual measured component. The physical size of the load has also to be close to the size of the DUT and it must be connected to the instrument in a similar way as the actual DUT.

Figure 11 represents how the open / short / load compensation improves the accuracy of the measurement compared to open / short method on complex measurements.

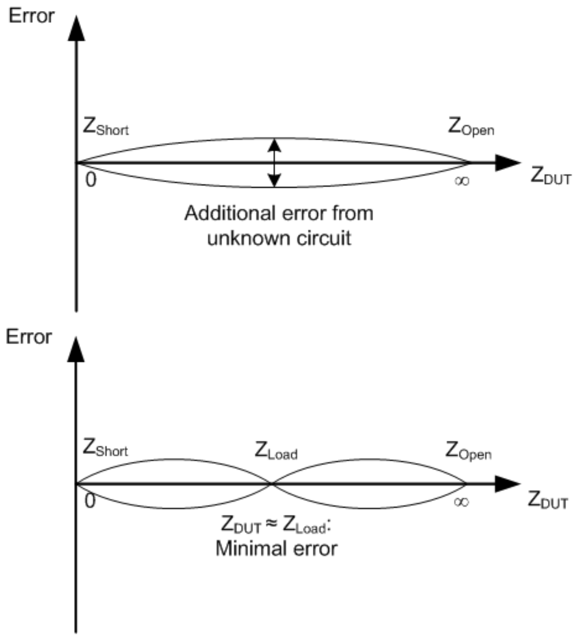

Figure 11. *Differences between the two compensation methods in complex circuits [Adopted from reference 1, p. 58]. The load measurement gives an additional reference point near the impedance of the DUT, thus minimising the error in the measurement.*

The load compensation gives an additional reference point near the impedance value of the DUT, thus improving the accuracy of the measurement considerably especially in complex circuits. The induced error increases if the impedance of the load is much different from the impedance of the DUT.

3 PRINTED CIRCUIT BOARD DESIGN TECHNIQUES

A good PCB (Printed Circuit Board) layout and design is an integral part of any functioning electronic device. Bad PCB design can cause the device to be totally useless, cause erroneous operation or electromagnetic noise to be radiated and thus hinder other electronic devices.

Some printed circuit board design practices are briefly introduced in Chapter 3.1 while Chapter 3.2 explains the controlled impedance technologies used in printed circuit boards. Chapter 3.3 explains how ground traces and planes can be used to shield the PCB from outside noise and how apertures in the shield decrease the shielding effectiveness. Chapter 3.4 explains the construction of modern multilayer printed circuit boards and Chapter 3.5 focuses on the properties of PCB materials and their effects.

3.1 Printed Circuit Board Design Practices

Signal Return Path

When designing PCBs it is important to minimize signal loops and their area. The return current path of the signal must be kept as short and close as possible to the signal trace. The best way to achieve this is to use a dedicated ground plane, thus all signal traces have a their return current path right under them. In a multilayer PCB with multiple ground planes it is important to think of the return current path when a signal trace changes layers. Figure 12 illustrates two methods of assuring a complete return current path.

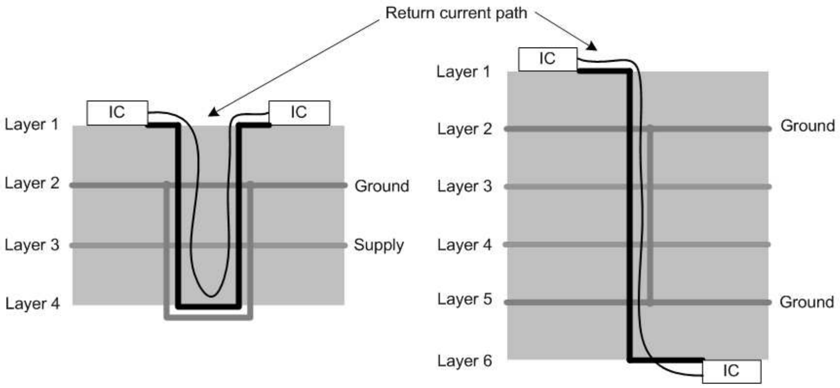

Figure 12. *Assuring a complete return current path using ground traces and vias in multilayer PCBs. The return current of the signal should have a path through the different layers of the PCB as close as possible.*

Ground trace and vias provide a return current path if the signal trace routed above a ground plane needs to change the routing layer temporarily. If the ground plane to which the signal is referenced changes, a ground via for the return current should be placed near the signal via [2].

Planes and Segmentation

The dedicated supply and ground planes should be kept as intact as possible and via concentrations and other split apertures in the plane should be avoided. The current in the plane should have a channel between the pads of the components and vias.

Splitting the ground plane in to two or more parts should be avoided. A single solid ground plane will offer better performance. Components and signal traces should however be segmented. This means that components and traces susceptible to interference should be kept away from components and traces causing noise [3]. Figure 13 illustrates this technique.

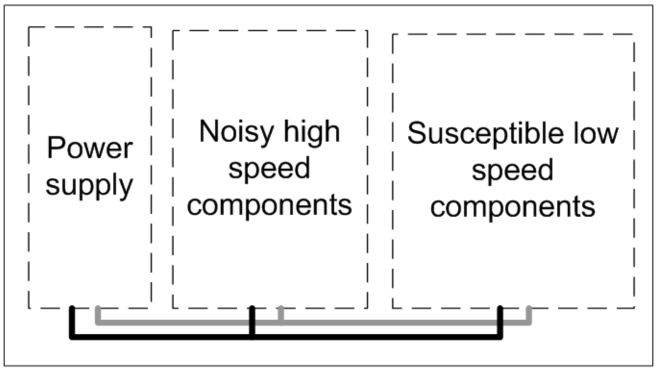

Figure 13. *Segmentation of the PCB. Segmenting the PCB by function or speed of the circuits helps to prevent EMC problems within the PCB.*

The segmentation should be done by function or speed of the circuits. Fast and noisy components should also be located closer to the power supply. This reduces the power surges from sudden power peaks of fast components. Fast transients in the power demand cause EMC (Electromagnetic Compatibility) problems.

All copper in the PCB should be connected and no floating conducting parts should appear. Floating copper can act as an antenna and cause EMC problems. Unused inputs on logic gates should also be grounded.

If the PCB has several different supply voltages, the supply planes with different potentials should not be placed on adjacent layers. A ground plane should always separate the supply voltage planes.

Placing the Decoupling Capacitors

Decoupling capacitors should be added for each IC (Integrated Circuit), large ICs should have more than one decoupling capacitor. Sometimes it is necessary to have one larger value decoupling capacitor and one smaller value decoupling capacitor. In this case the smaller value capacitor should be placed closer to the IC. The supply trace should be kept as short as possible. A good design practice to also have all ground and supply traces as wide as possible to minimize the impedance of the traces.

High Speed Traces and Crosstalk

Stubs in high-speed traces should be avoided as they cause signal reflections. Figure 14 shows how stubs can be avoided.

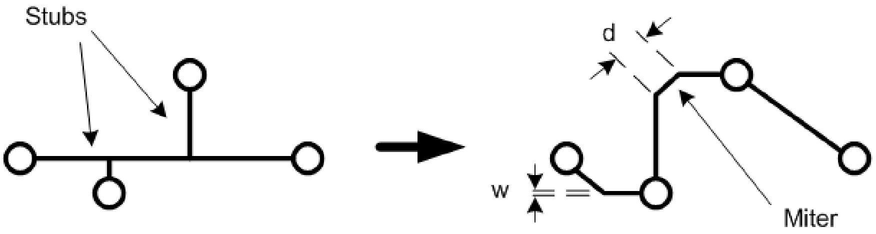

Figure 14. *Routing high speed traces to multiple components [adopted from 4, p. 137]. Stubs in high-speed traces should be avoided and a single continuous trace used instead. Trace corners should be mitered.*

Very short stubs that are much shorter than the wavelength have minimal effects, but the effects of many stubs add up. Instead of using stubs, a continuous trace should link all the components. All corners in the traces should have a mitre. The miter length d should be greater than the trace width w [4, p. 136].

Crosstalk can become a problem in high-speed circuits especially in long parallel traces. Good ground plane reduces crosstalk, however sometimes this is not enough. Parallel traces should not be routed right next to each other to reduce crosstalk. Figure 15 illustrates a technique called the 3w rule to reduce crosstalk.

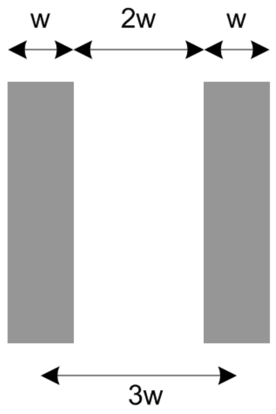

Figure 15. *Reducing crosstalk using the 3w rule. The centers of adjacent traces of width w should be placed 3w apart to avoid crosstalk between the traces.*

Traces of width w should be separated by a gap of 2w. This technique is often referred to as the 3w rule as the trace centres are 3w apart. Using the 3w rule, the fringing field reaching the adjacent trace has fallen 96 % from its value immediately next to the trace [4, p. 160]. Traces on adjacent layers should be routed orthogonally to reduce crosstalk. This means that traces on one layer should be routed horizontally and traces on the second layer should be routed vertically if possible.

3.2 Controlled Impedance

Controlled impedance of the tracks on the PCB becomes a necessity at high frequencies. Controlled impedance tracks are also called transmission lines. The impedance of a transmission line is called characteristic impedance. At high frequencies any impedance mismatch between the source, transmission line and the sink causes reflections to occur. Reflections cause unwanted effects such as ringing, undershoot and overshoot to the circuit.

Characteristic impedance of a transmission line is defined as the ratio of characteristic inductance and characteristic capacitance per unit length of the trace as shown in Equation 6.

$$Z_0 = \sqrt{\frac{L_0}{C_0}} \tag{6}$$

Where Z_0 is the characteristic impedance, L_0 the characteristic inductance and C_0 the characteristic capacitance. The characteristic impedance of the transmission line needs to match the impedance of the source and sink.

The dielectric medium causes the electromagnetic signal to slow down. This causes a propagation delay for the signal. Equation 7 shows the propagation delay expressed with characteristic inductance and capacitance per unit length.

$$\tau_{pd} = \sqrt{L_0 C_0} \qquad (7)$$

Where τ_{pd} is the propagation delay of the signal. The trace is considered electrically long if the propagation time of the signal down the trace and back again is longer than the rise time of the signal. The length at which this happens is called the critical length. In the case of an electrically long trace, line termination needs to be considered.

Branches in controlled impedance traces need to be dealt with in a certain way. Two different methods are illustrated in Figure 16.

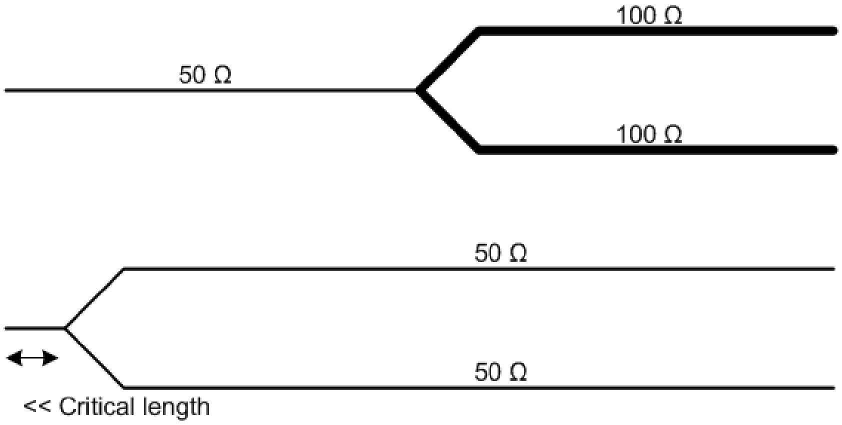

Figure 16. *Branches in controlled impedance traces [Adopted from 5, p. 219]. Branching a single 50 Ω trace to two parallel 100 Ω traces will act as a single 50 Ω trace. Branching the trace well within the critical length will have very little discontinuity effects.*

Branching a single 50 Ω trace to two parallel 100 Ω traces will act as a single 50 Ω trace like two parallel resistors and causes no reflections. The discontinuity from branching the trace close to the driver will have very little effect if it is done well within the critical length [5, p. 219].

The controlled impedance technologies used in printed circuit boards are the surface microstrip tracking and the stripline tracking. Surface microstrips are located on either side of the printed circuit board, above a ground plane and striplines are located in between two ground planes. A supply plane also provides a coupling reference for tracking, thus a stripline can be conveniently located between a ground plane and a supply plane.

3.2.1 *Surface Microstrip*

A microstrip trace and parameters defining the characteristic impedance of the trace is illustrated in Figure 17.

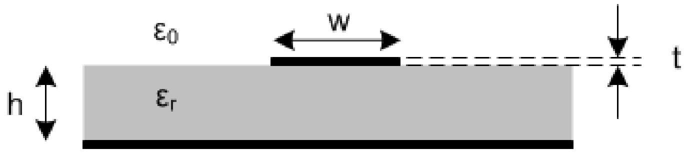

Figure 17. *Microstrip trace and parameters. The characteristic impedance is defined by the width and thickness of the trace, the distance between the trace and the ground plane and the effective dielectric constant of the substrate.*

The characteristic impedance of a microstrip is defined by the width and thickness of the trace, the distance between the trace and the ground plane and the effective dielectric constant of the substrate, which is formed by the relative dielectric constant of the substrate and the dielectric constant of free air. The characteristic impedance of the trace can be calculated from Equation 8 below.

$$Z_0 = \frac{87}{\sqrt{\varepsilon_{eff} + 1.41}} \ln\left(\frac{5.98h}{0.8w + t}\right) \tag{8}$$

Where ε_{eff} is the effective relative dielectric constant of the substrate, *h* the distance between the trace and the ground plane, *w* the width of the trace and *t* the thickness of the trace. Equation x assumes that $0.1 < \frac{h}{w} < 3.0$ and $1 < \varepsilon_{eff} < 15$ [6].

Because the trace is located on the outer most layer of the printed circuit board, some of the signal field travels through the substrate and some through the air. The effective dielectric constant can be calculated from the dielectric constant of the substrate using Equation 9 [4, p. 144].

$$\varepsilon_{eff} = \left(\frac{\varepsilon_r + 1}{2}\right) + \left(\frac{\varepsilon_r - 1}{2}\right)\left(\frac{1}{\sqrt{1 + 10\frac{h}{w}}}\right) \tag{9}$$

Where ε_r is the relative dielectric constant of the substrate. Usually the surface of a printed circuit board is covered with a solder resist mask, which has a dielectric constant of its own. The solder mask covering the traces reduces the characteristic impedance of the trace between 1 Ω and 3 Ω [4, p. 144].

The propagation delay of a microstrip can be calculated using Equation 10 [6].

$$\tau_{pd} = 3.337\sqrt{\varepsilon_{eff}} \tag{10}$$

The propagation delay can be used to determine whether the trace is electrically long or not.

3.2.2 Stripline

Balanced Stripline

A balanced stripline trace and parameters defining the characteristic impedance of the trace is illustrated in Figure 18 below.

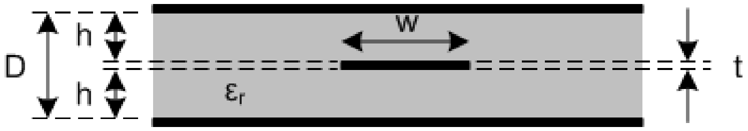

Figure 18. *Balanced stripline trace and parameters. The characteristic impedance is defined by the width and thickness of the trace, the distance between the two ground planes and the dielectric constant of the substrate.*

The stripline illustrated above is called balanced stripline because its symmetry, the distance from both planes to the trace is the same. The characteristic impedance of a stripline is defined by the width and thickness of the trace, the distance between the trace and the two ground planes and the dielectric constant of the substrate. Equation 11 below can be used to determine the characteristic impedance of the trace.

$$Z_0 = \frac{60}{\sqrt{\varepsilon_r}} \ln\left(\frac{1.9D}{0.8w + t}\right) \qquad (11)$$

Where $D = 2h + t$ is the distance between the two ground planes. The impedance of a stripline is less than half of that of a microstrip. Equation 11 assumes that $0.1 < \frac{w}{h} < 2.0$, $\frac{t}{h} < 0.25$ and $1 < \varepsilon_r < 15$ [6].

Equation 12 determines the propagation delay of a stripline [6].

$$\tau_{pd} = 3.337\sqrt{\varepsilon_r} \qquad (12)$$

The propagation delay of a stripline is slightly higher than that of a microstrip because the signal field is contained within the printed circuit board.

Asymmetric Stripline

If the distance between the trace and the two planes is different depending on the plane, the stripline is called asymmetric stripline. Asymmetric stripline characteristic impedance can be calculated from Equation 13 below.

$$Z_0 = \frac{80}{\sqrt{\varepsilon_r}} \ln\left(\frac{1.9(2h_2 + t)}{0.8w + t}\right)\left(1 - \frac{h_2}{4h_1}\right) \qquad (13)$$

Where h_1 and h_2 are the distances from the trace to the bottom and top planes, respectively. Equation 13 assumes that $h_1 > h_2$, $0.1 < \frac{w}{h} < 2.0$, $\frac{t}{h} < 0.25$ and $1 < \varepsilon_r < 15$ [6].

3.2.3 Dual Stripline

When one controlled impedance routing layer is not enough, a dual stripline technology can be used. Two layers with controlled impedance striplines between two ground planes form a dual stripline. Dual stripline and parameters are illustrated in Figure 19.

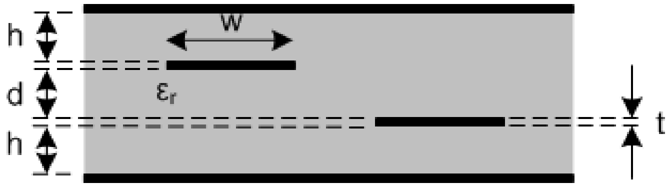

***Figure 19**. Dual stripline traces and parameters. The characteristic impedance is defined by the width and thickness of the traces, the distance from the ground plane to the trace, the distance between the traces and the dielectric constant of the substrate.*

The characteristic impedance of dual stripline can be calculated from Equation 14.

$$Z_0 = \frac{80}{\sqrt{\varepsilon_r}}\left(1 - \frac{h}{4(h+d+t)}\right)\ln\left(\frac{1.9(2h+t)}{0.8w+t}\right) \qquad (14)$$

Where d is the distance between the two signal planes. The propagation delay of dual stripline technology is the same as that of the balanced stripline technology as the same dielectric material is used. Equation 14 assumes that $\frac{w}{h-t} < 0.35$, $\frac{t}{h} < 0.25$ and $1 < \varepsilon_r < 15$ [6].

The characteristic impedance Equations 8, 11, 13 and 14 have their limitations but they offer a good approximation for most cases. One limitation is that the Equations only use one dielectric material. Advanced PCBs can use multiple dielectric materials. In the case of multiple dielectric materials commercial multiple dielectric characteristic impedance software has to be used to achieve accurate results. The software numerically solves Maxwell's equations and offer very accurate results on variety of complex controlled impedance configurations.

3.3 Shielding and Apertures

There are some techniques that can be used to shield critical signals on a printed circuit board from being interfered by an outside source of noise. Shielding techniques work both ways. The same technique can be used to shield a device from causing noise to the outside world, or shield the device against noise coming from the outside world.

One simple technique is the guard ring. A guard ring is a ground trace surrounding a part of the PCB. Figure 20 illustrates the use of the guard ring.

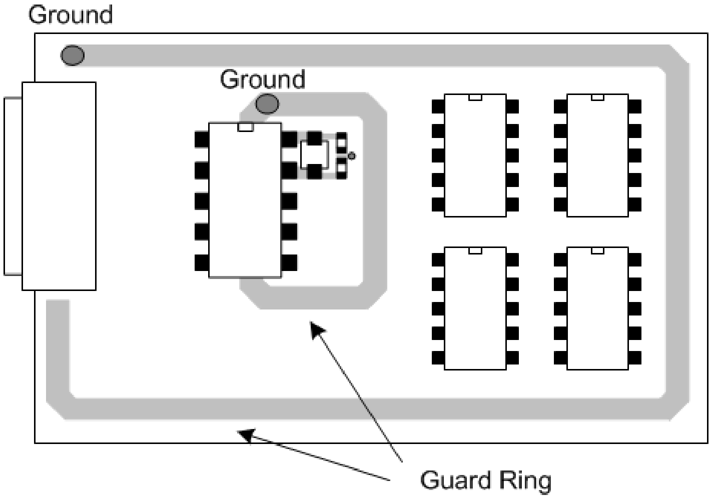

Figure 20. *The guard ring. Guard ring can be used to surround a whole layer or parts of it to shield critical circuits.*

The guard ring can be used to surround a single component, a segment on the PCB or a whole supply plane or routing layer. In normal operation no return current flows in the guard ring, but it catches incoming or outgoing RF noise [4, p. 128].

Another technique is creating a faradays cage by placing multiple vias on the edges of ground planes, creating a cage for the traces on layers between the two ground planes. This is very effective if the ground planes are intact and do not contain many holes and the vias are placed close to each other.

As with actual enclosures, the shielding effectiveness is determined by the necessary apertures in the shield. The longest dimension of an aperture and the minimum wavelength of the frequency band to be shielded against define the shielding effectiveness of the aperture. The SE (Shielding

Effectiveness) of an aperture can be calculated from Equation 15 below [7, p. 188].

$$SE = 20\log\left(\frac{\lambda}{2d}\right) \qquad (15)$$

Where *SE* is the shielding effectiveness in dB, *d* the longest dimension of the aperture and λ the wavelength of the minimum frequency band to be shielded against. For wavelengths less than or equal to twice the longest aperture dimension there is effectively no shielding. The frequency at which this occurs is called the cut-off frequency of the aperture. A good approximation is that for frequencies below the cut-off frequency the shielding effectiveness increases 20 dB per decade up to the maximum of the material used in the shield [8, p. 280]. Figure 21 illustrates different types of apertures in the shield.

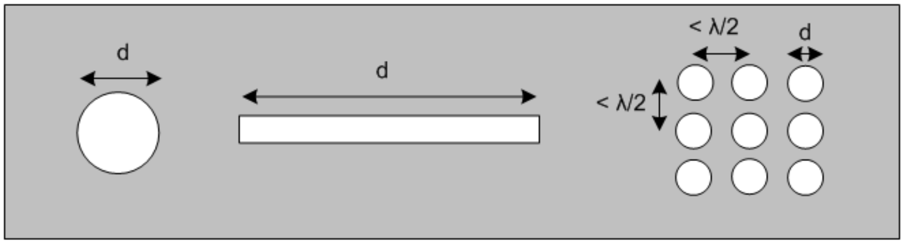

Figure 21. *Different types of apertures. The longest dimension of the aperture and the minimum wavelength of the frequency band to be shielded against define the shielding effectiveness of apertures. Apertures placed closer than half the wavelength together cause an additional reduction to the shielding effectiveness.*

Some times it is necessary to have multiple apertures close to each other. When the distance between the apertures is more than half the wavelength the apertures can be treated separately. If the distance between the apertures is less than half the wavelength then the SER (Shielding Effectiveness Reduction) compared to a single aperture is approximately proportional to the square root of the number of apertures as shown in Equation 16.

$$SER = -20\log\left(\sqrt{n}\right) \qquad (16)$$

Where *SER* is the reduction in shielding effectiveness and *n* the number of adjacent apertures of equal size [7, p. 190].

3.4 Multilayer Stackup

A multilayer PCB stackup consists of multiple layers of dielectric material and copper layers bonded together. A double layer PCB consists of a single core laminate with copper bonded to each side. A four-layer board consists of two thinner core laminates with copper on each side separated by a very thin layer of dielectric material, which is called the prepreg, or one thicker layer of core laminate with a prepreg laminate on each side. Figure 22 illustrates these three standard PCB stackups.

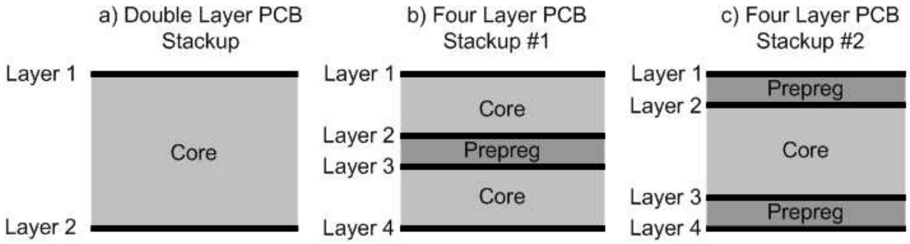

Figure 22. *Common PCB stackups. Four layer PCB can be made in two different ways while a double layer PCB can be made only in one way.*

Double layer PCB can only be made in one way, but four layer PCB can be made in two different ways, each offering certain benefits. If the inner layers in the stackup illustrated in Figure 22b are used as dedicated ground and supply planes it offers an extra bypass capacitance formed by the two parallel plates. However the distance from the traces on the outer layers is longer, thus offering a longer return current path. Four layer PCB stackup illustrated in Figure 22c corrects this problem but does not offer the extra capacitance. However, it can be used to shield the traces on the inner layers if the outer layers are used as dedicated ground and supply planes.

Core and prepreg laminates come in a variety of standard thicknesses. A certain total PCB thickness can be achieved by using laminates with appropriate thickness and possibly stacking more than one layers of prepreg material together to form a thicker layer of prepreg laminate. The thickness of the copper layers is also variable. Usually the copper on the inner layers is thinner than on the outermost layers, but each thickness can be varied. An outer layer copper thickness of 35 μm is normally used.

Sometimes the core and the prepreg are made from the exact same material and have the same dielectric constant but it is not uncommon that they are made from slightly different materials having slightly different dielectric constants. On complex printed circuit boards two or more totally different material technologies can be mixed, using a few layers of high frequency material for radio frequency signals and normal material for other layers.

3.5 Printed Circuit Board Material Properties

A variety of different PCB materials exist, each having their own characteristics. The most common PCB material is the FR4, which is adequate for most applications. However, in some applications the characteristics of FR4 are inadequate. The most important characteristics of PCB materials are their thickness, dielectric constant ε_r, moisture absorption, coefficient of thermal expansion (CTE), and glass transition temperature (T_g).

Thickness and dielectric constant of the PCB materials are used when calculating the characteristic impedance of transmission lines. Sometimes a certain thickness of the PCB is also required and can be the only deciding factor.

If the PCB material absorbs moisture the dielectric constant of the material changes, thus changing the stray capacitance induced to the measurement. Absorbed moisture can also cause unwanted effects in rapid temperature changes.

The coefficient of thermal expansion describes how significant the thermal expansion of the material is. The CTE is usually given to all three axes separately. Thermal expansion can cause a surface mount component or its solder joints to crack.

The glass transition temperature is the temperature where a thermoset material transitions from glass-like to becoming rubbery. This transition from glass-like below T_g to rubbery above T_g has major effects on the properties of the material. Surpassing PCB material's T_g results in decreased copper bond and reduced reliability of plated-through holes.

4 RELAY CARD DESIGN

The relay card was designed to be easily modifiable for different purposes, thus the design consists of a separate CPU (Central Processing Unit) card and various add-on cards for the actual relay switching. The CPU card was fairly complex but stays the same no matter what type of add-on card was attached to it. The CPU card was controlled via EIA-485 serial link that can be found standard in almost any industrial computer. EIA-485 is a half duplex, differential multi drop serial link. EIA-485 was previously known as RS-485, a name still in common use. Two different add-on cards were designed in this study. The first one was the measurement card, which can be used to measure 32 capacitances. The second add-on card was a simple MUX (Multiplexer) card that switches between two measurement cards. This way it was possible to measure a total of 64 capacitances using one MUX card and two measurement cards each controlled by a CPU card.

Chapters 2 and 3 explained the facts that need to be considered in the design to achieve optimum performance for the Relay Card. The design of each card, the CPU Card, the MUX Card and the Measurement Card is detailed in Chapters 4.1, 4.2 and 4.3, respectively.

4.1 PCB Material and Stackup

The relay card needs to withstand low and high temperatures, rapid temperature changes and moisture caused by the temperature changes. A normal temperature range for measurements in the VTI laboratory is from -40 °C to +125 °C. The same measurements are performed in different temperatures to determine the temperature dependency of the DUT. If the temperature cycles affect the relay card used to measure the DUT, it is possible to confuse the characteristics of the relay card and the DUT. Thus, it is important to minimize the effect of the relay card to the measurement.

Components used in the relay card were chosen to withstand a broad temperature range, but continuous exposure to rapid temperature changes and temperature extremes is also severe for the PCB. Thus the choice of the PCB material was also important, too. The most important properties of a typical FR4 material and a high speed PCB material called Rogers are shown in Table 1. Rogers PCB material has been commonly used in VTIs laboratory in high temperature tests, especially if humidity is a concern.

Table 1. *Comparison of FR4 and Rogers PCB materials [9, 10 and 11]. Rogers offers superior high frequency characteristics as well as better durability in high temperatures and rapid temperature changes.*

Parameter		**Isola FR402 core and prepreg**	**Rogers RO4350B Core**	**Rogers RO4403 Prepreg**
Standard thicknesses		0.05 mm to 3.2 mm	0.101 mm to 1.524 mm	0.101 mm
Dielectric constant, ε_r		4.6 at 1 MHz 4.25 at 1 GHz	3.66 ± 0.05	3.17 ± 0.05 up to 10 Ghz
Moisture absorption		0.30 %	0.04 %	0.05 %
Coefficient of thermal expansion, CTE	x	15 ppm/°C (Post T_g 17 ppm/°C)	14 ppm/°C	16 ppm/°C
	y	15 ppm/°C (Post T_g 17 ppm/°C)	16 ppm/°C	19 ppm/°C
	z	50 ppm/°C (Post T_g 250 ppm/°C)	50 ppm/°C	80 ppm/°C
Glass transition temperature, T_g		110 °C to 150 °C, typically 140 °C	> 280 °C	> 280 °C

Rogers PCB material was chosen mainly because of its ability to withstand high temperatures and its low moisture absorption rather than its high-speed properties. When FR4 material is constantly exposed to high temperatures, the resin from the resin-fibreglass mixture of the laminate starts to vaporize and the laminate starts to deteriorate rapidly. The large tolerance of the glass transition temperature of FR4 can also cause problems at a typical test temperature of 125 °C. Delamination of the FR4 laminate occurs at constant exposure to high temperatures. In rapid temperature changes the relatively high moisture absorption of FR4 changes the properties of the laminate causing errors to sensitive capacitance measurements. The post T_g Z –axis CTE is very high and can cause vias and other plated through holes to break. The ceramic based Rogers PCB materials do not deteriorate in high temperatures and they absorb far less moisture and thus endure high temperatures and rapid temperature changes.

Six layer PCB stackup was chosen for the relay card because of the measurement cards complexity. The six layer stackup offered two planes for controlled impedance traces located between two ground planes. The remaining two layers were used for the control signals and supply voltage for the relays. The same stackup, illustrated in Figure 23, is used in all three PCBs designed in this study, but each card has its own layer definition.

Figure 23. *Relay card PCB stackup. Four layers of prepreg separated three core laminates. The dielectric constant of the core laminate and the prepreg was different.*

To achieve a typical total PCB thickness of around 1.55 mm, four 0.101 mm prepreg layers were laminated together to create a 0.404 mm layer of prepreg. The thickness of the core material was only 0.254 mm. The outer layers had a copper thickness of 35 µm and the inner layers had a thickness of 18 µm. The core material was Rogers RO4350B and the prepreg material was Rogers RO4403.

4.2 CPU Card

The CPU card controls the add-on cards connected to it. It was designed in a way that any kind of an add-on card can be attached to it and no modifications need to be done to the CPU card. Figure 24 shows the simplified block diagram and connections of the CPU card.

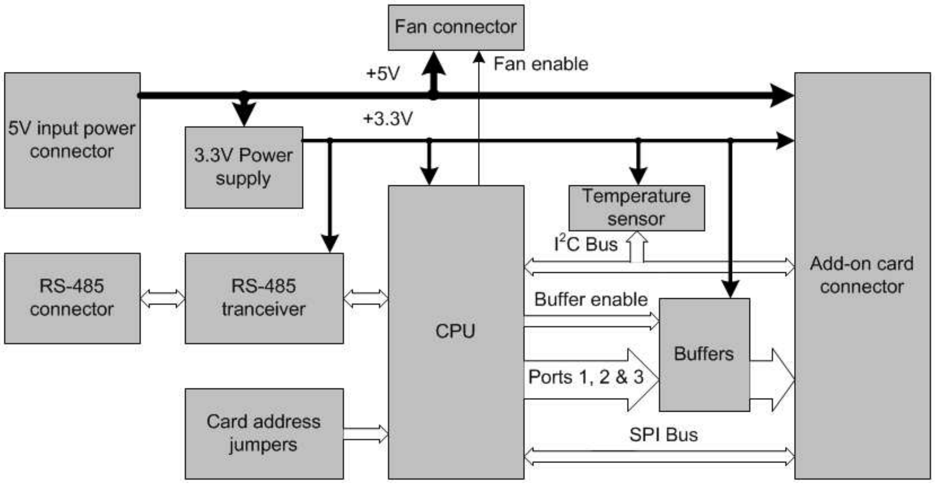

Figure 24. *Simplified block diagram of the CPU card. A linear regulator was used to make the 3.3 V supply voltage for the CPU card from the 5 V input voltage. The CPU card was controlled via EIA-485 serial link. All of the important buses and supply voltages were routed to the add-on card connector.*

All the main components on the CPU card worked with a 3.3 V supply voltage, but the relays used in the add-on cards used a 5.0 V supply voltage. An onboard 5.0 V supply was considered, but linear regulators capable of supplying the worst case current for the CPU card and the relays in the temperature of +125 °C were physically too large to fit the PCB of the CPU card. Instead an outside 5.0 V supply was chosen. The outside voltage supply can be of any size and does not need to withstand the high temperature.

Each CPU card connected to the same EIA-485 serial communication line was given an individual address with the card address jumpers. The relay card was controlled via the EIA-485 serial bus from an industrial computer. Three output ports were routed to the buffers. The buffers protected the microcontroller from damage and can drove more current than the microcontrollers output pins. The buffers were used to drive the relays located on the add-on cards. There was an onboard digital temperature sensor connected to the I^2C (Inter Integrated Circuit) bus, which was also routed to the add-on card connector. More temperature sensors can be added on the add-on cards.

The CPU card had a fan connector for future purposes. The speed of the fan can be adjusted with pulse width modulation if needed, at present the fan can only be controlled on or off, as the feature was not necessary needed. The SPI (Serial Peripheral Interface) serial bus was also routed to the add-on card connector for future purposes and nothing was actually connected to the SPI bus. These preparations for future applications make physical modifications to the CPU card unnecessary, as only the firmware needs to be modified for added functionality in the future.

4.2.1 Schematic

The CPU card was build around the Atmel AT90CAN128 microcontroller. The AT90CAN128 microcontroller was chosen over the more widely used ATmega128 for its automotive temperature specification, it is one of the only microcontrollers able to handle the automotive temperature range from -40 °C to +125 °C. All other components used in the CPU card were also selected to withstand the same temperature range. Figure 25 illustrates the detailed block diagram of the CPU card. The full schematic of the CPU card can be found in Appendix A.

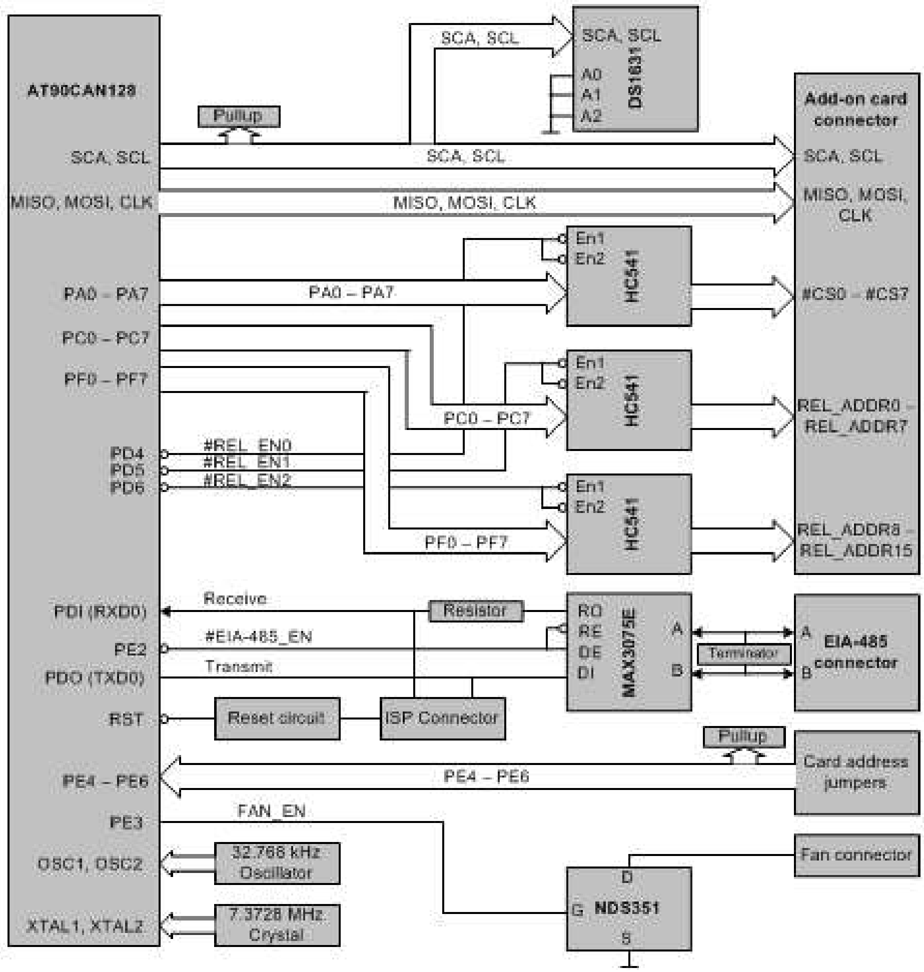

__Figure 25.__ Detailed block diagram of the CPU card. Only logical parts are illustrated and the supply voltage regulators and connections are omitted.

The microcontroller used an external 7.3728 MHz crystal for its main clock source. This particular frequency was used since the baud rates used in serial communications were easily derived from it. A separate 32.768 kHz low frequency oscillator was also used to provide a real time clock for the microcontroller. This clock will run even if the microcontroller itself is in power save mode.

The reset circuitry provided a pull-up for the zero active reset signal and a capacitor to prevent noise from activating the reset. It also had a diode to protect the reset pin of the microcontroller. The reset pin is internally protected to ground and only the supply side needs external protection [12].

The ISP (In System Programming) connector is used to program the firmware to the internal flash memory of the microcontroller. It uses the same clock signal as the SPI bus, but has separate transmit and receive pins. ISP stands for In System Programming, which means that the microcontroller can be programmed when it has already been soldered to its place on the PCB.

The SPI bus was routed straight to the add-on card connector. Neither one of the add-on cards designed in this study used the SPI bus, but it was added for possible future use. The SPI bus consists of a master and multiple slaves. The master selects the slave it wants to communicate with a separate chip select signal. This way only the wanted component will react to the communication sent through the bus. The serial communication takes place through three signals: MOSI (Master Out Slave In), MISO (Master In Slave Out) and CLK (Clock). This way the direction of the signals is always known. The CLK signal is the clock that the master provides for the bus. A separate chip select signal is needed for every slave in the bus.

The I^2C serial bus has separate pull-up resistors because the components using the I^2C bus do not actively drive the bus high. The components connected to the I^2C bus all have an address, which is used to select which component reacts to the commands sent through the bus. The master selects the slave it wants to communicate with by first sending the address to the bus, which is followed by the command. The address of the slave is 7-bits long, and one bit determines if it is a read or a write operation. Thus one byte, where the least significant bit is the read or write bit and the 7 other bits the address is used to select the slave, is sent first. Each command is one byte long. The I^2C bus uses only two signals, SCA for data and SCL for the clock. The master provides the clock for the bus.

The I^2C bus was routed to the add-on card connector and a Maxim DS1631 digital temperature sensor. The address of the DS1631 temperature sensor is fixed with three address pins on the sensor. The high nibble of the address is fixed to 0x9 and three most significant bits of the lower nibble are user definable. The address of the onboard temperature sensor was selected as 0x90 for write and 0x91 for read operations. The DS1631 digital temperature sensor offers a 12-bit resolution and a measurement error of only ±0.5 °C for a temperature range from 0 °C to +70 °C. For the whole operational temperature range of -55 °C to +125 °C the error is ±2.0 °C [13].

Ports A, C and F of the microcontroller were used to control the relays on the add-on cards. These relay control ports were buffered before the add-on card connector. The 74HC541 non-inverting buffers protect the microcontroller and can drive and sink more current than the microcontroller. Each 8-bit buffer can be activated separately with a zero active output enable signal or be left floating in high impedance state.

Maxim MAX3075E EIA-485 serial transceiver was connected to the same serial transmit and receive pins as the ISP connector. A resistor was used to prevent collisions with the ISP in case both are used simultaneously. The EIA-485 serial bus is a half duplex serial communication bus; the direction of the communication is selected with a separate signal. On normal situation the transceiver is in receive mode and only switches to transmit mode when it needs to transmit something. EIA-485 bus is multi droppable, which means multiple devices, can be connected to it at the same time. In the case of a collision, the bus waits a random amount of time and transmits the data again. The bus needs to be terminated from both ends and a termination resistor was placed between the A and B pins of the connector. A jumper can be used to switch on the termination if needed. Only the ends of the bus need to be terminated and transceivers in the middle of the bus must not be terminated [14].

Each CPU card on the same EIA-485 bus can be given an address by three jumpers connected to the microcontroller. The signals going to the jumpers had pull-up resistors. Using jumpers to determine the address of the CPU card made it easy to configure several cards to work in the same bus in a changing laboratory environment.

An external fan, or other high current component can be attached to the CPU card and controlled by the microcontroller. Since the current driving capability of the pins on the microcontroller are limited, an N channel NDS351 FET (Field Effect Transistor) was used to drive the fan. The NDS351 FET can drive up to 1.4 A of current continuously [15].

4.2.2 Printed Circuit Board Layout

The CPU card used the same stackup as the add-on cards although fewer layers could have been used. Having ground layers on both sides of the PCB helped to prevent noise from the CPU card to reach the measurement. A separate 3.3 V supply plane and a ground plane were located in the middle of the stack. Figure 26 illustrates the use of the layers on the PCB.

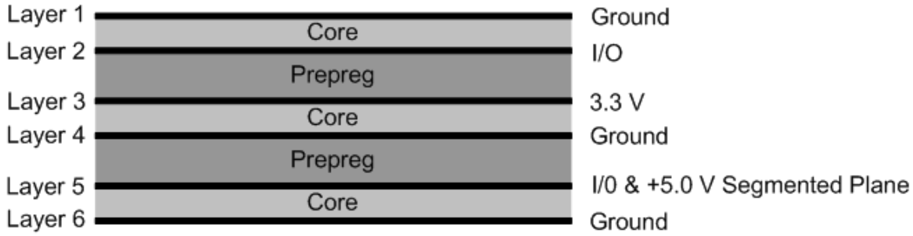

Figure 26. *Layer definition of the CPU card. Layers 1, 4 and 6 were ground planes, layer 3 was the 3.3 V supply plane and layers 2 and 5 were the actual routing layers. A part of routing layer 5 was dedicated as a 5.0 V supply plane.*

The 5.0 V input voltage had a segmented plane on layer 5. A ground plane separated the 3.3 V and 5.0 V supply planes. Only part of layer 5 was used as a supply plane as illustrated in Figure 27.

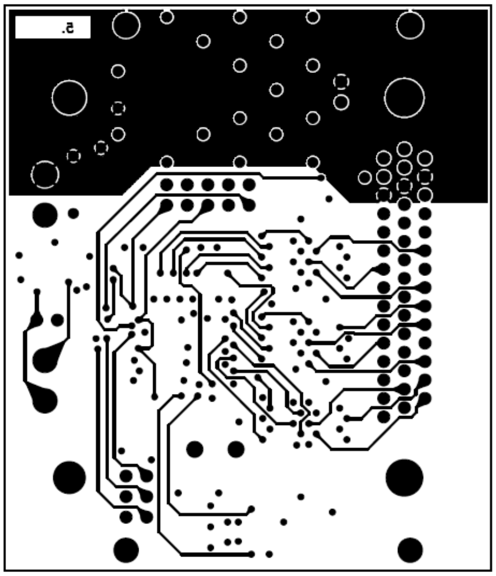

Figure 27. *Segmented 5.0 V input supply plane. The input voltage had a segmented plane on layer 5. The separate plane area offered the benefits of a plane and left most of the layer for routing signals.*

The segmented supply plane was located on the upper third of the PCB and the rest was used for routing other signals. The segmented plane offered a low impedance route for the current of the relays. Three pins on the add-on card connector were used to route the input voltage to the relays.

Only the relays on the add-on cards used the 5.0 V input voltage and the rest of the components used 3.3 V, which was regulated from the input voltage. The output current capacity of linear regulators drops in high temperatures. The MC33269 linear regulator is rated at 800 mA but can only supply a fraction of it in ambient temperature of +125 °C. The maximum operating die temperature of MC33269 is +150 °C, which leaves only a little margin for the component to heat from the electric current flowing through it. Figure 28 shows a heatsink solution within the PCB.

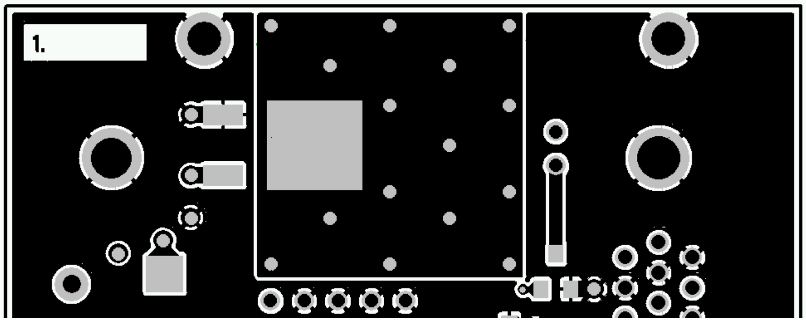

Figure 28. *Heatsinking the power supply. The large pad on the 3.3 V linear regulator was connected to a 20 mm by 20 mm square of copper to help cool down the regulator. The copper square was connected to the 3.3 V supply plane with multiple vias to minimise impedance.*

The large output pad of the regulator was connected to a large square of copper; this helped to transfer the heat from the regulator to air more effectively. The MC33269 can supply 155 mA of current in the ambient temperature of +125 °C without the die temperature rising beyond the maximum of +150 °C, if the output pad is connected to a copper square of 20 mm by 20 mm [16, p. 6].

The CPU card PCB was segmented by function of the circuits, this helped to trouble shoot the device as well as offered better EMC performance. Locating only the power supply and the fan connector to the upper part of the PCB allowed the use of the segmented input supply plane discussed earlier. The segmentation of the CPU card is shown in Figure 29.

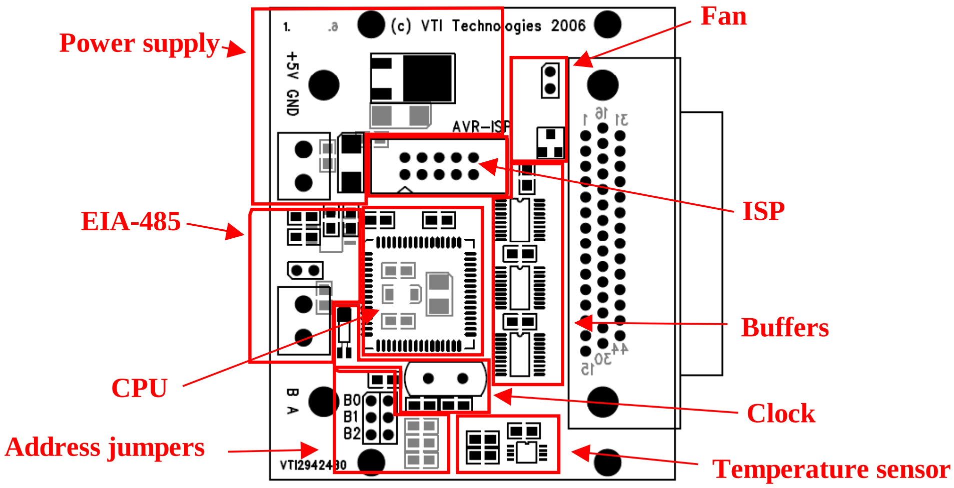

Figure 29. *Segmentation of the CPU card. Components on the top side of the PCB are marked on black and components on the bottom side with grey.*

Fast speed circuits like the clock sources and the EIA-485 transceiver were located close to the CPU and further away from the add-on card connector. Bypass capacitors were located as near as possible to the pins they are supplying current for. Components were located on both sides of the PCB because of the size limitations of the PCB as well as being able to minimize trace lengths. The 44 pin high density D connector on the right was used to connect the add-on cards to the CPU card. The complete PCB drawings of the CPU card can be found in Appendix B. Figure 30 shows the completed prototype of the CPU card.

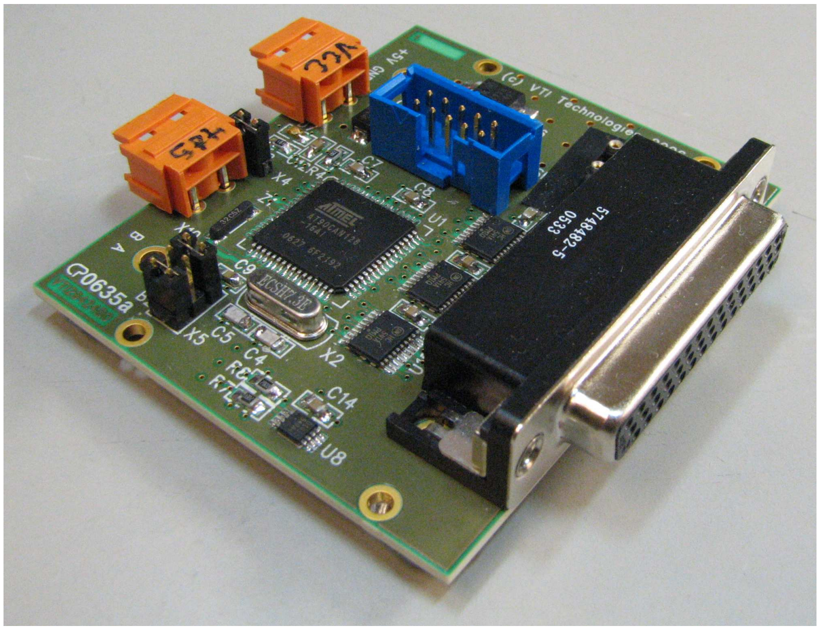

__Figure 30.__ A photo of the CPU card. The largest component on the PCB was the 44 pin high density D connector that was used to connect the add-on cards.

By far the largest component on the PCB was the add-on card connector. It offered just enough pins for all the signals and a few extra ground pins. All components, including the connectors, resistors and capacitors were rated for the temperature range from -40 °C to +125 °C. A complete bill of materials for the CPU card can be found in Appendix C.

4.2.3 Firmware

The CPU card ran a program called firmware, which controlled the operation of the CPU card. The firmware is loaded and ran every time the system boots up and it controls the microcontroller and I/O subsystems connected to it. The firmware for the Atmel AT90CAN128 microcontroller used in the CPU card was coded in C language. The code was cross-compiled to work with the 8-bit Atmel AVR architecture of the AT90CAN128 microcontroller. Like in any other embedded systems, the firmware ran in an infinite loop after initiating the system. A flow chart of the operation of the firmware is illustrated in Figure 31.

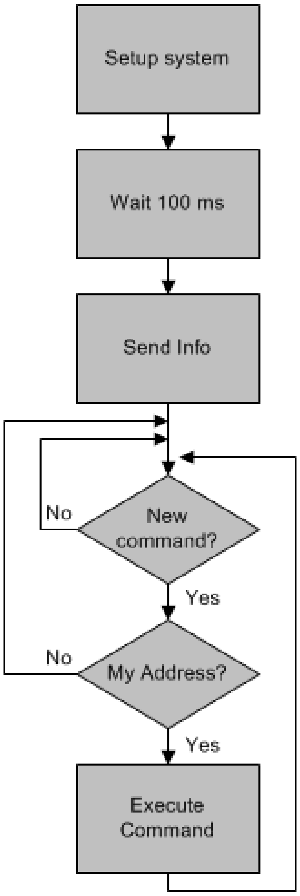

Figure 31. *Flow chart of the CPU card firmware. First the system was initiated and then the system checked for a new command with its address in an infinite loop.*

The program started by initiating the system. All the subsystems were initiated separately. The initiation included setting the direction of the microcontrollers I/O ports, initiating the timer registry, initiating the USART (Universal Synchronous Asynchronous Receiver Transmitter) registry for the EIA-485 serial communications, turning on the interrupts, reading the card address jumpers and finally initiating the output ports which controlled the relays on the add-on card. After a 100 ms delay the relay card sent information about itself to the EIA-485 serial bus. This information included the version of the firmware and support contact information. After these steps the normal operation of the program started. The program started to query the input register of the USART to see if a new command had arrived. It then decoded the command and checked the address, to which the command was intended. If the address checked out, the command was executed. After executing the command, the program queried the input registry of the USART again. This loop continued until a new command was received.

The speed of the EIA-485 serial bus was defined with the USART registers of the AT90CAN128 microcontroller. Table 2 shows the settings selected for the serial communication.

Table 2. *The settings of the AT90CAN128 microcontrollers USART for EIA-485 serial communication.*

Setting	Value
Bits per second	57600
Data bits	8
Stop bits	1
Parity	None
Flow control	None

The commands are sent from a computer through the EIA-485 serial bus. All commands must start with a character ‘*’ and end with the character ‘#’. This way the firmware knew when a new command started and when it ends. The relay card recognized the commands described in Table 3.

Table 3. *The commands of the relay card. The relay card recognized 9 different commands. The basic use of the relay card only needed the first 3 commands.*

Command	Action
Set port	Sets specified output port to specified value
Buffer enable	Enables specified output buffer
Buffer disable	Disables specified output buffer
Fan enable	Enables the fan
Fan disable	Disabled the fan
Read temperature	Reads the temperature of specified temperature sensor and sends it to the controlling PC
Send status	Sends the status of the relay card to the controlling PC
Send help	Sends a help screen to the controlling PC

The address of the relay card to be commanded was sent before the command and after the start command character. The onboard address jumpers fixed the address of the relay card. Only the relay card whose address was specified executed the command.

The source code of the firmware was divided in to several files by the function of the code to help to comprehend the code more easily. The firmware was based on the source code of another embedded system developed for measurement automation at VTI, but it had gone through an extensive revision and rework. For example the original code was made for another type of microcontroller, the ATmega128. More detailed discussion about the firmware is out of scope of this study, as this study concentrates on measurement technique and hardware design.

4.3 Measurement Card

The measurement card was designed for the measurement of 32 DUTs. Although all four cables of the 4TP measurement configuration were connected to the measurement card, the measurement card used the shielded 2T configuration. The use of 4TP configuration on the measurement card would have been difficult if not impossible to implement. The 4TP configuration would double the amount of relays needed and routing four separate terminal pairs with controlled impedance would be impractical or even impossible. Simplified block diagram in Figure 32 illustrates the design of the measurement card.

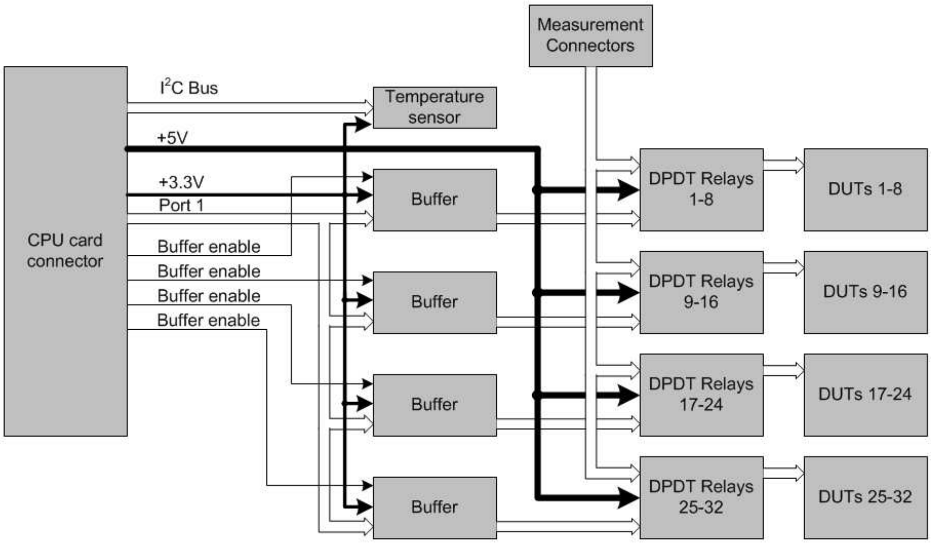

Figure 32. *Simplified block diagram of the measurement card. One 8-bit port was used to control the relays and four signals were used to select the appropriate buffer. Relays controlled by the buffers were used to switch the measurement signals to the appropriate DUT.*

The relays had a 5.0 V coil but the buffers and the temperature sensor used 3.3 V supply voltage. Both supply voltages came from the CPU card. One digital temperature sensor was connected to the I^2C serial bus. Four buffers drove the relays and each buffer controlled eight relays. The buffers were connected in parallel and buffered a single 8-bit port. Each buffer had its own chip select signal. The measuring instrument was connected to the measurement connectors. The 4TP measurement configuration was terminated at the connectors and the measurement card used the shielded 2T configuration. The relays were DPDT type; each relay controlled one DUT. DPDT stands for dual pole, dual throw. Dual pole means that the switching is made between two output poles, always switching from one to the other. Dual throw means that there are two separate sets of contacts; so two different signals can be switched simultaneously. Using DPDT relays saved space on the PCB and both the H and L terminals of the shielded 2T configuration were switched simultaneously.

4.3.1 Schematic

The measurement card design was straightforward. The design could be considered to consist from two parts, the digital control section and the analog measurement section. Block diagram in Figure 33 illustrates the control section of the measurement card. The full schematics for the measurement card are found in Appendix D.

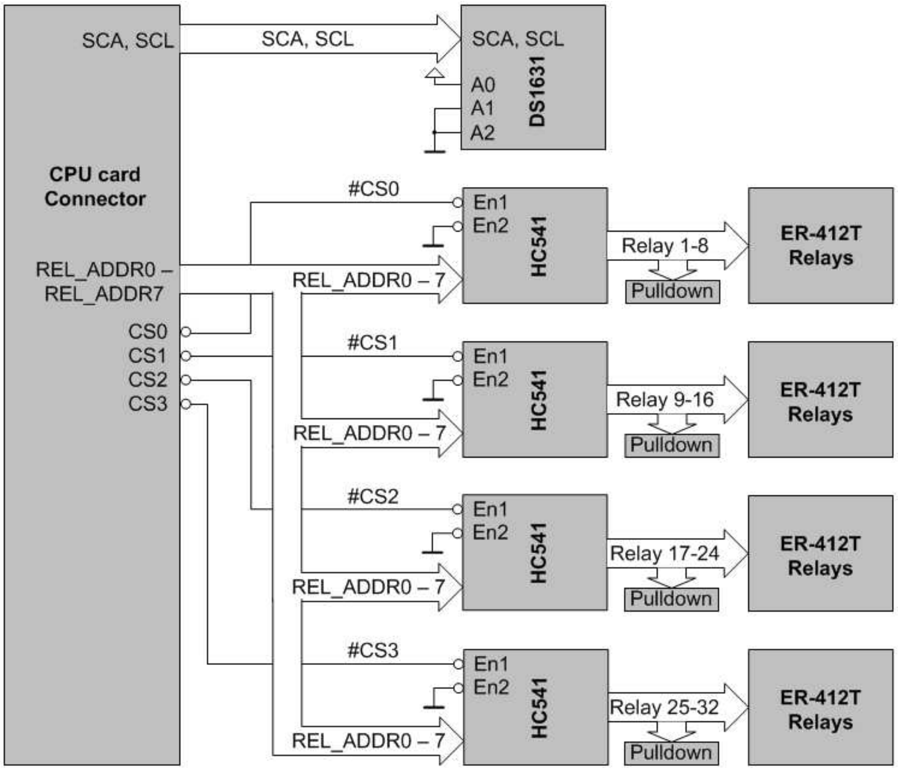

Figure 33. *Detailed block diagram of the control part of the measurement card. The outputs of the HC541 buffers were pulled down and were not left floating if the output of the buffer happened to be in high impedance state.*

The same DS1631 temperature sensor as used in the CPU card was connected to the I^2C bus. The address of the sensor was 0x92, which was fixed by the A0, A1 and A2 pins [13].

The HC541 buffers have two chip select pins, one of them was connected permanently to ground and the other one was controlled by the CS (Chip Select) signals from the CPU card. The output of the HC541 will be in high impedance state when the chip is not selected; therefore pull-down resistors were connected to the outputs of each buffer. If the outputs were allowed to float the relays could have been activated randomly [17].

The measurement card used hermetically sealed Teledyne ER-412T relays, which have an operating temperature range from -65 °C to +125 °C. The ER-412T relays also have an internal transistor driving the coil, the base current for the internal transistor should be at least 3.0 mA but limited to 15 mA [18]. The minimum high-level voltage of the 74HC541 buffer is 2.1 V, thus a resistor in the order of 500 Ω sufficed.

A total of 32 DUTs could be connected to the measurement card. The relays switched the appropriate DUT to the measurement terminals of the measurement card. The analog section performing the switching is illustrated in Figure 34.

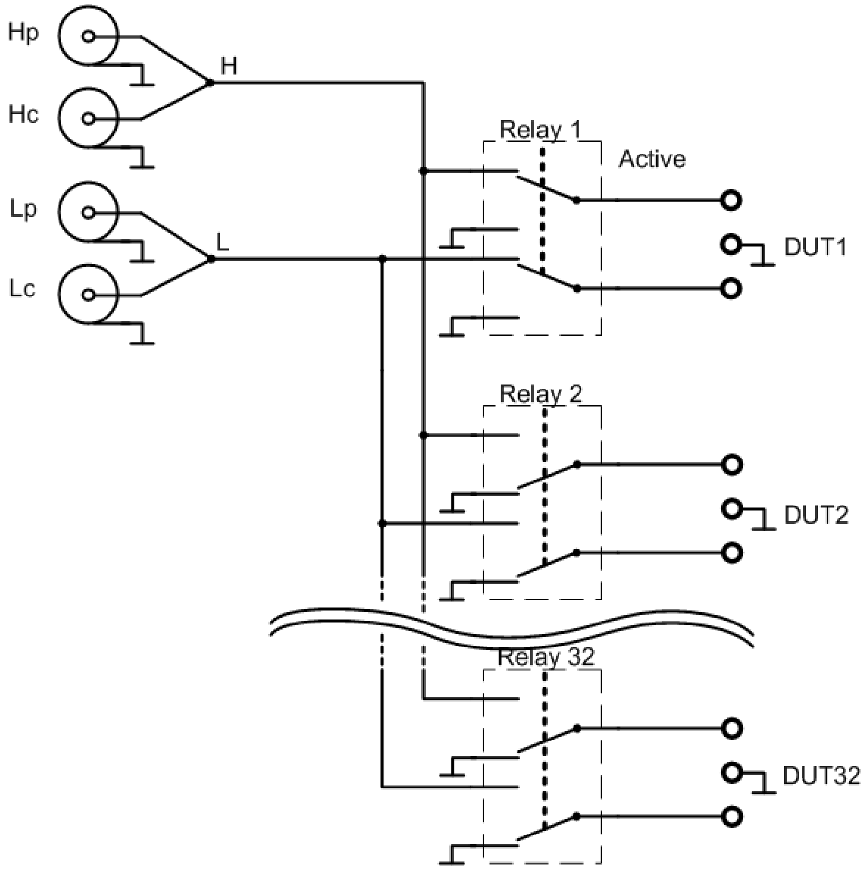

Figure 34. *Analog part of the measurement card. The 4TP configuration was terminated at the connectors and the measurement was performed using shielded 2T configuration. In the figure relay 1 is active and DUT1 can be measured.*

The four coaxial cables of the measuring instrument were connected to the measurement cards coaxial SMB connectors. The 4TP measurement configuration was then terminated at the connectors and the measurement signals continued in the shielded 2T configuration. One relay switched both the H and L terminals for one DUT. When the relays were not activated they connected the DUT to the guard on the outer conductor of the coaxial cables. Connecting the DUTs that were not being measured to the guard produced a more controlled environment for the measurement. The DUTs were connected to a 3-pin connector; the measurement was carried out using two pins and the third pin located in the middle was for the guard. Using this technique a guarding plate could be located near the DUT for optimum performance.

4.3.2 Printed Circuit Board Layout

The main concept of the measurement card PCB was the controlled impedance traces used in the measurement. The PCB was designed to offer controlled impedance traces for better measurement results when using higher measurement frequencies and to offer shielding for the measurement. Therefore the dual stripline method was chosen. The traces between the reference planes were protected against noise coming from the outside, thus improving the measurement accuracy. The layer definition of the measurement card is illustrated in Figure 35.

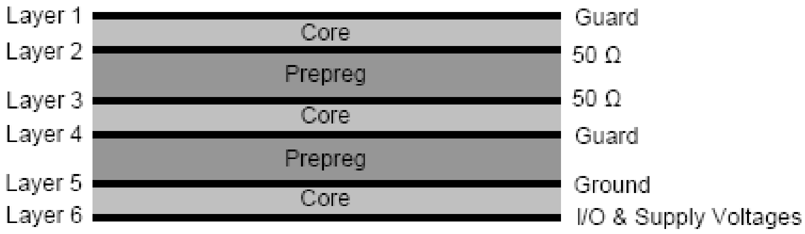

Figure 35. *Layer definition of the measurement card. The dual striplines were located on layers 2 and 3.*

The reference planes connected to guard were located on layers 1 and 4. The top layer housed as few components as possible to keep the guard layer as intact as possible. The actual striplines were on layers 2 and 3. Layer 5 was a ground plane and layer six was used for routing the signals and the 3.3 V supply voltage. The rest of layer 6 was flooded with copper connected to the 5.0 V supply voltage to offer lower impedance for the relatively high currents of the relay coils.

Because of the multiple dielectric materials used in the stackup of the PCB, the equations for calculating the characteristic impedance shown in Chapter 3.2 give erroneous results. Therefore Polar Instruments Si8000 multiple dielectric controlled impedance design system was used to determine the characteristic impedance of the traces. The Si8000 solves the characteristic impedance by numerically solving Maxwell's equations. The solver gives very accurate results and is widely used in the industry. Figure 36 illustrates the graphical user interface of the Si8000 software and the parameters that yielded in to the characteristic impedance of 50 Ω, which was used.

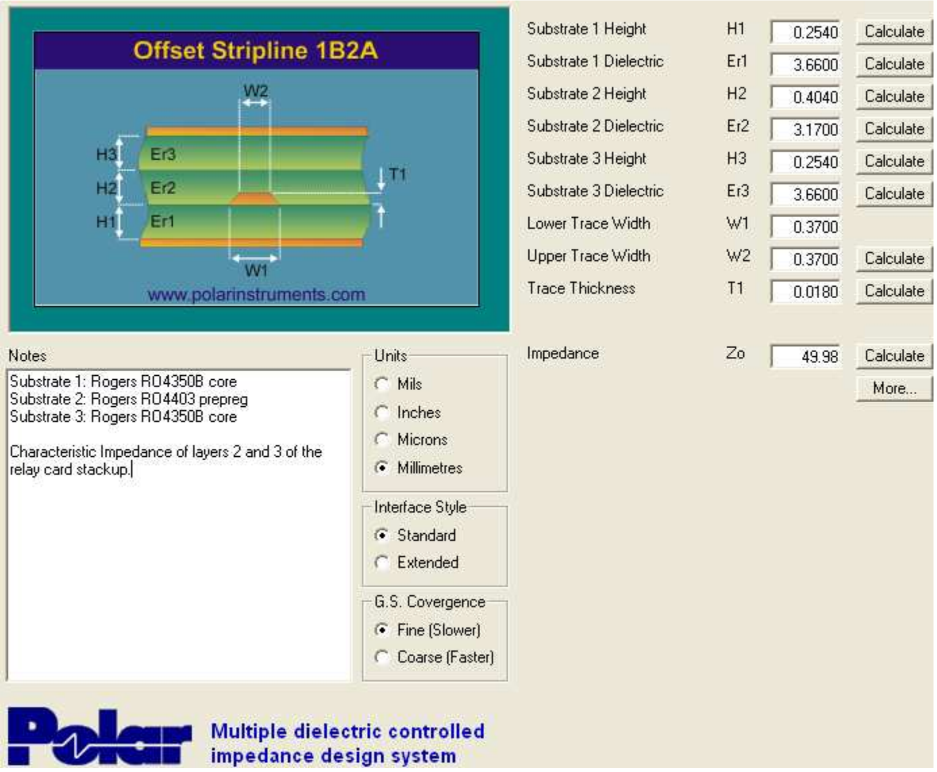

Substrate 1 Height	H1	0.2540
Substrate 1 Dielectric	Er1	3.6600
Substrate 2 Height	H2	0.4040
Substrate 2 Dielectric	Er2	3.1700
Substrate 3 Height	H3	0.2540
Substrate 3 Dielectric	Er3	3.6600
Lower Trace Width	W1	0.3700
Upper Trace Width	W2	0.3700
Trace Thickness	T1	0.0180
Impedance	Zo	49.98

Notes

Substrate 1: Rogers RO4350B core
Substrate 2: Rogers RO4403 prepreg
Substrate 3: Rogers RO4350B core

Characteristic Impedance of layers 2 and 3 of the relay card stackup.

Units
○ Mils
○ Inches
○ Microns
● Millimetres

Interface Style
● Standard
○ Extended

G.S. Covergence
● Fine (Slower)
○ Coarse (Faster)

Figure 36. *Polar instruments Si8000 controlled impedance solver software screenshot. Substrate 1 and 3 were Rogers Ro4350B core and substrate 2 was Rogers RO4403 prepreg. The PCB stackup was symmetric, thus the calculated characteristic impedance value could be used for both layers 2 and 3.*

Using a trace width of 0.37 mm for traces on layers 2 and 3 yielded to characteristic impedance of 50 Ω. The same trace thickness could be used on both layers because of the symmetry of the stackup.

The controlled impedance traces were shielded against noise coming from the top or bottom of the PCB by the guard planes. However, the planes did not shield the ends and sides of the PCB. Therefore the edges of the guard planes were protected by guard vias placed close to each other creating a faradays cage. The shielding effectiveness of the ends and sides of the PCB could be approximated by Equations 15 and 16 discussed earlier in Chapter 3.3. Figure 37 illustrates the shielding effectiveness by function of the frequency.

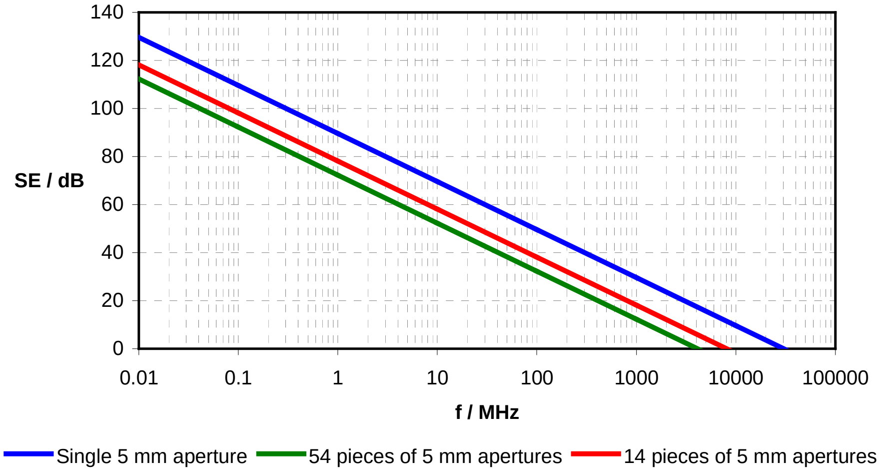

Figure 37*. Approximate shielding effectiveness of the faradays cage, which shielded the controlled impedance traces. Single aperture is added to the figure for comparison. Both ends of the measurement card had 14 apertures and both sides 54 apertures.*

Different sides of the faradays cage can be treated separately. The guard vias were placed 5 mm apart from each other and the aperture between the vias was approximated being 5 mm long. The ends of the PCB had 14 pieces of 5 mm apertures and the sides had 54 apertures. The closely placed vias offered adequate shielding effectiveness for the measurement signals. A guarding ring surrounded the controlled impedance routing layers. The faradays cage can be seen in Figure 38. The full PCB layout drawings for the measurement card are found in Appendix E.

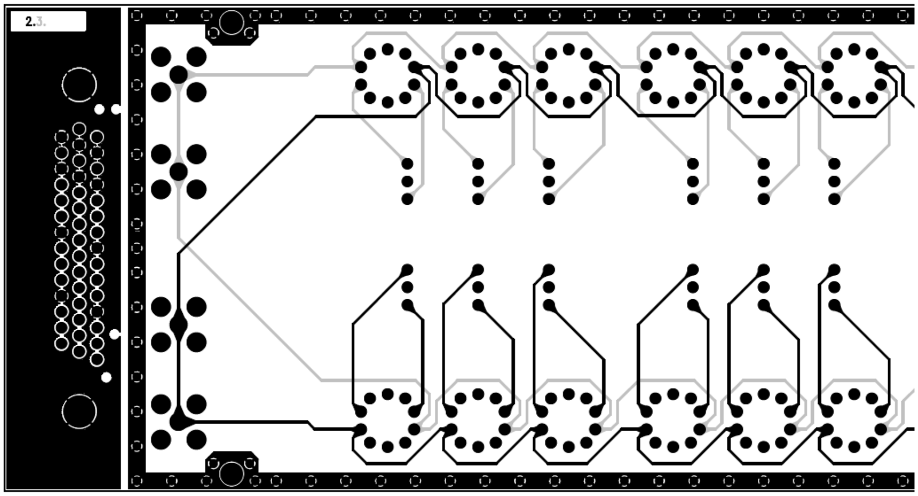

Figure 38. *Shielding of the controlled impedance traces. Traces on different layers are in different colours. The faradays cage formed by the guard vias and a guarding ring surrounded the traces.*

The controlled impedance traces were routed without any stubs and with appropriate miters in the corners. The traces were routed on different layers and any crossing of the signals in different layers was perpendicular.

The DUTs were connected to the measurement card with zero integration force sockets. The sockets illustrated in Figure 39 below had only 18 pins from 81 possible mounted, as can be seen in Figure 38 above. Use the zero integration force sockets enabled the DUTs to be changed easily.

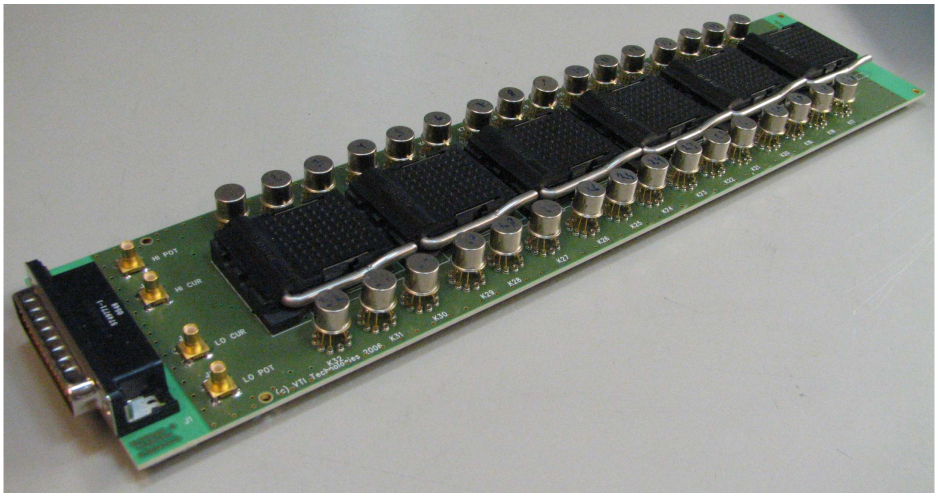

Figure 39. *Photo of the measurement card. The relays were located on the sides of the PCB and the DUT sockets were in the middle. Each socket except the right most one held 6 DUTs. The last socket on the right held only 2 DUTs.*

The digital temperature sensor was located on the far right of the PCB. Another temperature sensor was located on the CPU card, thus the temperature could be measured from both ends of the relay card. The temperature can then be determined to be constant throughout the relay card.

Each relay had a 100 nF bypass capacitor placed nearby. Pairs of 100 nF and 10 μF capacitors for both 5.0 V and 3.3 V supply voltages were placed equally along the measurement card PCB because the length of the PCB. One 100 nF capacitor was placed near the 3.3 V voltage pins of the CPU card connector to keep possible digital noise from the CPU card reaching the measurement card. The bill of materials for the measurement card is found in Appendix F.

4.4 MUX Card

The MUX card was designed to switch between two measurement cards. However, it could also be used in other applications requiring multiplexing or de-multiplexing of four coaxial cables. For optimum performance of the impedance measuring carried out through the MUX card, it was designed to keep the 4TP measurement configuration intact. This meant that not only the inner conductor of the coaxial cable was switched, but also the outer conductor and that all four measurement cables were treated separately. Four relays were used to do the switching, one for each cable of the measurement instrument. The MUX card was attached to and controlled by the CPU card. The simplified bock diagram of the MUX card is shown in Figure 40.

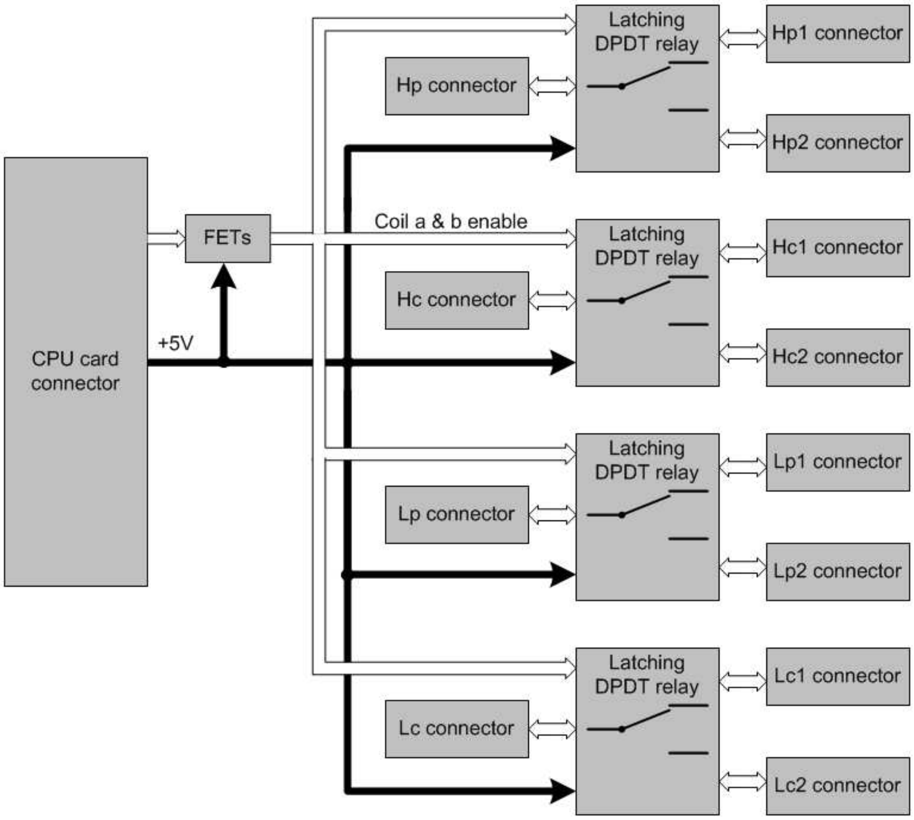

Figure 40. *Simplified block diagram of the MUX card. One latching DPDT relay per cable was used to do the switching. All parts operated on a 5.0 V supply voltage.*

The relays had 5.0 V coils but not an internal transistor driver. External transistors were used to drive the relay coils. The MUX card acted as a one to two switch, where both the inner and outer conductor of the cables are switched. The Teledyne RF-170 relays used in the MUX card have an operating temperature range from –55 °C to only +85 °C [19, p. 1]. However, this does not cause any problems since the MUX card could be used outside the high temperature area. In fact, even smaller temperature range would have sufficed.

4.4.1 Schematic

The MUX card used RF-170 magnetically latching relays, which have two coils: A and B. The position of the relay changes after receiving a pulse to the coil that was not previously activated. Reactivating the same coil again has no effect. The position holds magnetically even if the control signal for the coil is lost. The logical block diagram of the MUX card is shown in Figure 41.

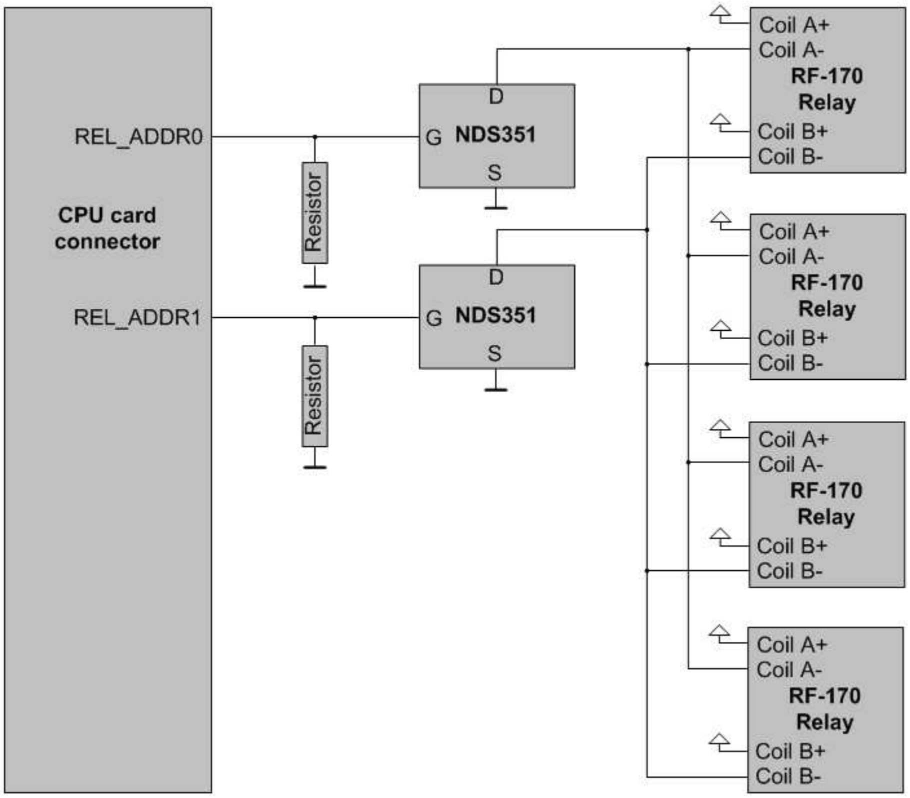

Figure 41. *Detailed block diagram of the control section of the MUX card. All four relays were controlled in parallel. A FET was used to drive both coils.*

The A and B coils of all four relays were controlled in parallel and driven with a FET respectively. One signal was used to control the A coils of all four relays and another signal controlled the B coils. After activating coils A, the measuring could be carried out from the first set of output connectors and when coils B were activated the measurement would be carried out from the second set of output connectors.

Each coil draws an approximate of 82 mA of current [19, p. 2]. Four parallel coils drew 328 mA of current; therefore a FET was used to control the coils. The absolute maximum current per output pin of the 74HC541 buffers on the CPU card is only 35 mA [17, p. 3]. The maximum coil set and reset voltage of the RF-170 relays is 3.5 V and the 74HC541 buffers on the CPU card have a minimum high-level voltage of 2.1 V, therefore the buffers could not be used to control the relay coils directly, even if they sourced enough current. The gates of the FET had pull-down resistors.

The schematic in Figure 42 shows the analog part of the MUX card that does the actual switching. When coil A is activated the switch moves to position A and to position B when coil B is activated.

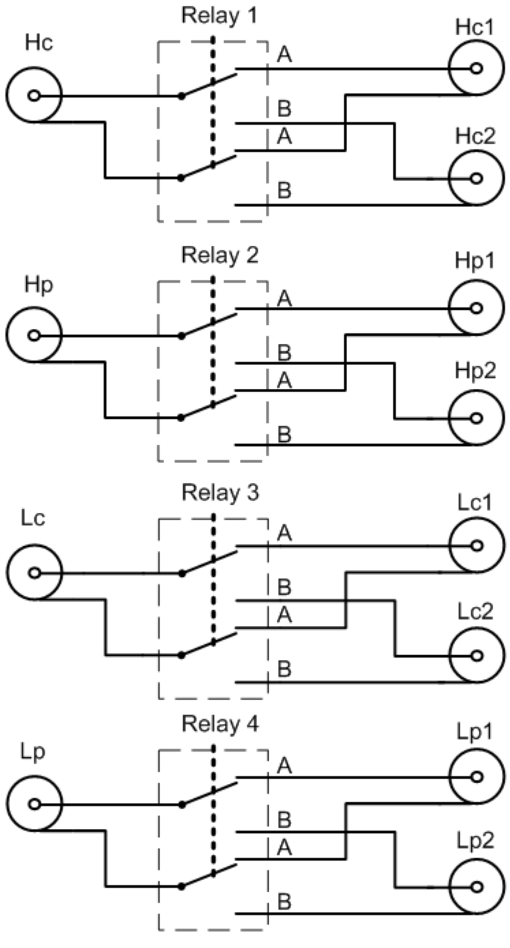

Figure 42. *Analog part of the MUX card. Each cable was individually switched and there was no connection between the four cables measurement cables.*

Each of the four relays switched the inner and outer conductors of one coaxial cable to keep the 4TP measurement configuration intact. Putting the MUX card between the DUT and the measurement instrument could be considered as a 4TP to 4TP cable extension. The full schematic of the MUX card is located in Appendix G.

4.4.2 Printed Circuit Board Layout

The PCB of the MUX card was simple and it used the same stackup as the measurement card. However, only layer 2 was used for controlled impedance traces. The layer definition of the MUX card is illustrated in figure 43 below.

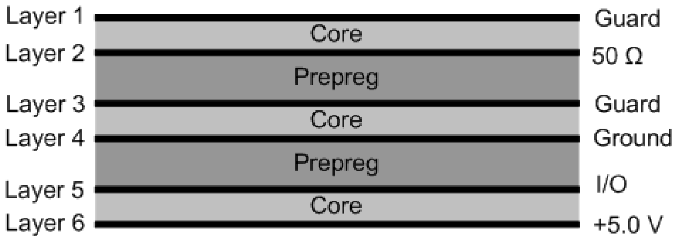

Figure 43. *Layer definition of the MUX card. The asymmetric striplines from the connectors to the relays were on layer 2, while layers 1 and 3 were the guard planes.*

Again the Polar Instruments Si8000 software was used to determine the appropriate trace width for the 50 Ω controlled impedance traces. Using the PCB stackup described in Chapter 4.1, the width of the asymmetric stripline traces on layer 2 was determined to be 0.32 mm. Bypass capacitors of 100 nF and 10 µF were located near the CPU card connector. The four identical relay circuits were located on the right. A photo of the MUX cards prototype is shown in Figure 44.

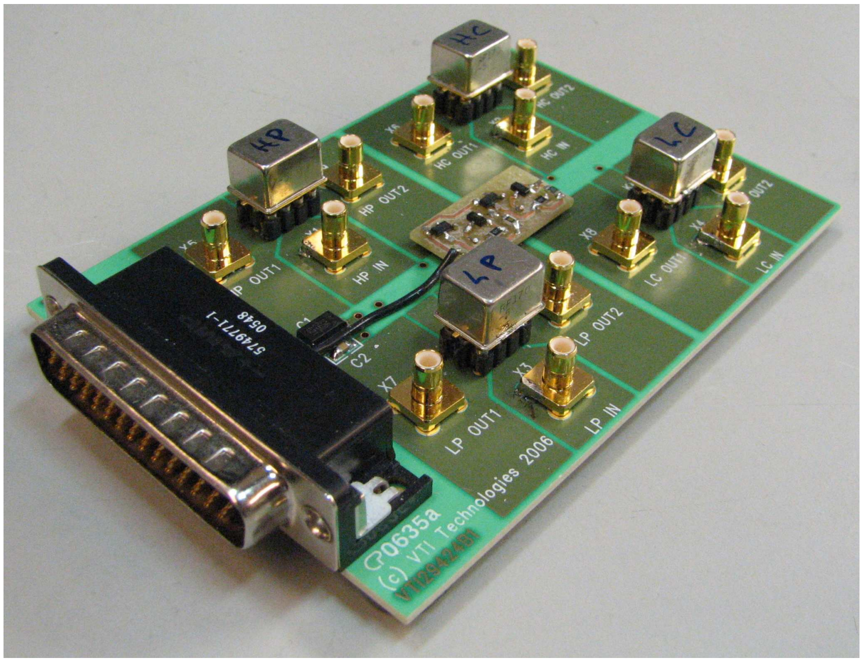

Figure 44. *Photo of the MUX card. The segmented guard planes for each coaxial SMB connector can be seen. The prototype in the photo had an error in the PCB, which was corrected with the small self milled PCB mounted on top.*

Each coaxial SMB connector had a small, segmented guard plane on layers 1 and 3. The 50 Ω transmission lines were located on layer 2. The traces were kept as short as possible so that the MUX card would have minimal effects on the measurement. The length of the traces was well within the critical length of the measurement signal. Guard vias that would have surrounded the segmented guard planes were not needed; as the SMB connectors' pins and the relays' pins provided shielding for the measurement signals. Complete PCB drawings for the MUX card are located in Appendix H and the bill of materials in Appendix I.

5 USING THE RELAY CARD

The relay card was designed for accurate impedance measurements. However, improper usage can render the results far from the intended measurement accuracy. The cables need to be connected properly and the address of the relay card needs to be set for the relay card to work. Error compensation on the measurement instrument needs to be performed to achieve accurate measurements. The computer controlling the relay card needs to have the same serial bus settings as the relay card. The serial bus settings used by the relay card are shown in Table 2 in Chapter 4.2.3.

The factors contributing to the design of the relay card were discussed in Chapters 2 and 3 while Chapter 4 describes how the actual relay card was designed. Chapter 5 describes a proper usage of the relay card for accurate measurements. Chapter 5.1 describes how the relay card should be connected to the measurement setup, Chapter 5.2 details how the relay card is controlled with the computer and Chapter 5.3 describes how the measurement instrument is used properly to achieve accurate results.

5.1 Cabling

Before any measuring can be carried out, the relay card needs to be connected to a functioning 5.0 V power supply, the EIA-485 serial link needs to be connected and properly terminated and the measurement cables need to be connected.

Figure 45 illustrates how the relay card is to be used. The LCR bridge is connected to the MUX card with four coaxial SMB cables. The MUX card is connected to two measurement cards enabling measurements for total of 64 capacitances.

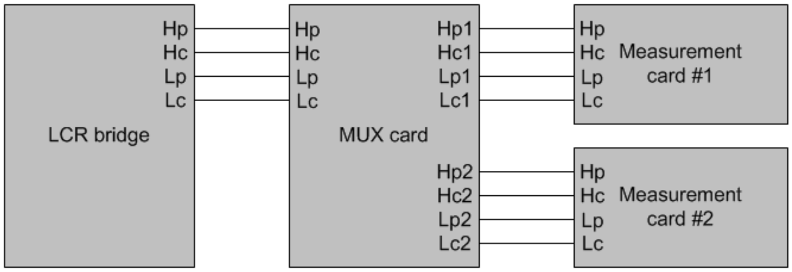

Figure 45. *Measurement connections for the relay card system. The MUX card is used to switch between two measurement cards.*

The total length of the coaxial cables should be limited according to Equation 2. For practical measurements the total length of the cables is around 1.5 m yielding in to a maximum measurement frequency of 10 MHz.

The EIA-485 serial bus is a differential, multi droppable half duplex bus. It uses 120 Ω twisted pair cable, which can be up to 1200 m long. For typical laboratory applications a few meters of cable will suffice. Each end of the bus needs to be terminated accordingly. Figure 46 illustrates how to connect the EIA-485 bus when using one MUX card and two measurement cards in the same bus.

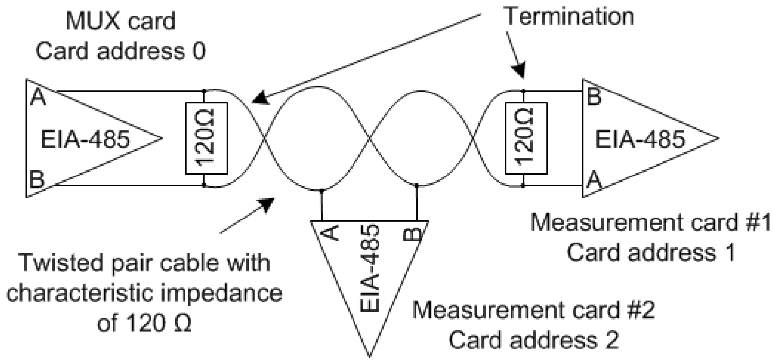

Figure 46. *Connecting the EIA-485 serial bus. Each end of the bus in terminated and each card needs to have a unique address.*

The termination of the bus is done with the termination jumper on the CPU card. The bus is terminated with the jumper in place and un-terminated when the jumper is not in place. Each card has a unique address selected by the address jumpers on the CPU card. Three jumpers used to determine the address can provide 8 different addresses from 0 to 7 for the relay cards.

5.2 Commands

As discussed earlier in Chapter 4.2.3, the relay card recognizes 9 different commands. However, some commands have parameters, and the address of the command has to be determined also by the same command string. The format of the commands is illustrated in Table 4.

Table 4. *The format of the relay cards commands. All commands do not need the data field in the command string.*

Start command	**Card Address**	**Command**	**Data**	**End command**
*	n	XX	xx	#

Each command starts with the '*' character and ends with the '#' character. The address is defined with one character and the command by one or two characters. Some commands need additional data like the value of the output port. The commands and their characters are illustrated in Table 5.

Table 5. *Command characters of the relay card. Both upper case and lower case characters are recognized as the same command.*

Command		**Data**	**Action**
s	1	Byte specifying the port data	Sets the data to the specified port
	2		
	3		
e	1	-	Enables the specified port or ports, 'a' stands for all ports
	2		
	3		
	a		
d	1	-	Disables the specified port or ports, 'a' stands for all ports
	2		
	3		
	a		
t	1	-	Reads the specified temperature sensor and sends temperature data in hex back to the controlling PC
	2		
	3		
	4		
f		-	Enables the fan
o		-	Disables the fan
v		-	Sends status information of the relay card to the controlling PC
h		-	Sends help message to the controlling PC

The set command must be sent separately for each port. Enable port and disable port commands can be configured to work for one or all ports. The read temperature command can read the temperature from four different sensors, one at a time. The rest of the commands are unambiguous.

5.3 Preparations for Measurements

Before any actual measuring, the error compensation on the measurement instrument needs to be performed. As the measuring will take place through the MUX card and the measurement card, only the open / short / load compensation method offers the required level of measurement accuracy.

The load should be similar to the DUTs in value and size. However the value of the load needs to be accurately known and stable. Hermetically shielded components offer the best stability over temperature and humidity. If the hermetical shielding is done with a conducting enclosure, the component is shielded against electromagnetic noise as well.

The measurement instrument used with the relay card should have the function to save and use multiple different compensation datasets. This means that the compensation will be performed to each and every DUT connector. Figure 47 illustrates the compensation procedure.

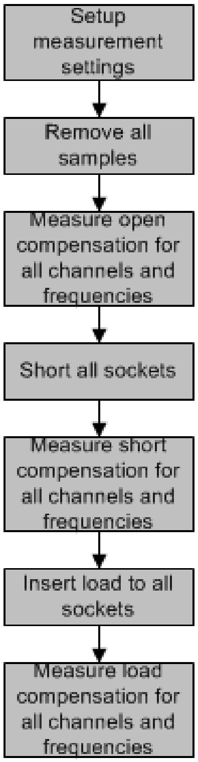

Figure 47. *Flow chart of the compensation procedure. The open / short / load compensation needs to be performed separately to each DUT channel and repeated for all frequencies. The most efficient way is to do the open compensation to all channels and frequencies first and then repeat the procedure for the short and load compensations.*

The open / short / load compensation data for each DUT connector is saved to a different channel on the measurement instrument. First the relay and compensation channel is chosen. Then the measurement is carried out for all frequencies. This is repeated until all relays and compensations are carried out. After the compensation if performed properly the actual measurement can be carried out accurately. First the compensation channel for the appropriate relay connector is selected and then the relay is activated and the measuring takes place.

In some cases it is reasonable to measure the stray capacitance of the empty sockets before measuring the actual DUT. Saving these results to the same file as the actual measurement data offers a way to troubleshoot the measurement. Errors caused by broken relays or sockets are easy to discover from high stray capacitance of the empty socket.

The type of DUTs that can be measured is determined by the pin order of the measurement card. Table 6 shows the pin order on for the DUTs.

Table 6. *Pin order for the DUTs. The measuring is carried out from pins 1 and 3, while the casing or other guard on the DUT can be connected to pin 2.*

Pin Number	Function
1	H
2	Guard
3	L

The actual measuring is carried out from pins 1 and 3. Pin 2 can be used to connect the case or other conducting parts of the DUT to guard.

6 RELAY CARD CHARACTERIZATION

A series of test measurements were made to characterize the relay card. The test measurements gave an approximation of the effect the relay card has on the measurement and if it causes an additional error to the results. Errors in measurement systems can be divided into two categories: systematic and random. Analysis of random errors requires the use of statistical methods and tools. Statistical analysis also require more DUTs to be measured multiple times by more than one operator and is thus beyond the scope of this study. Systematic errors however, can be easily detected by a series of simple test measurements using fewer DUTs and a single operator can make the measurements.

The use of the relay card is described in Chapter 5 and the characterization of the relay card is detailed in Chapter 6. The test measurements performed with the relay card are detailed in Chapter 6.1. The relay to relay variation is discussed in Chapter 6.2, bias and linearity are discussed in Chapter 6.3 and the frequency dependency is discussed in Chapter 6.4.

6.1 Test Measurements

Three separate measurements are needed and proper compensation is to be carried out before each measurement. In the first measurement the value of the reference DUTs is determined with no test cables. In the second measurement the same reference DUTs are measured using the cables that will be used in the actual measurement. The last test measurement is carried out through the MUX card using the measurement card with the same cables as the second test measurement. All test measurements are repeated for every DUT socket and measurement frequency.

The DUTs used in the test measurements were hermetically sealed capacitors. They offered a stable capacitance value in a laboratory environment and the results could be reproduced later using the same DUTs. The capacitors use high quality NP0 dielectric material, which offers stable value over temperature. Four hermetically sealed capacitors of different capacitance value were measured in the test. One of the capacitors used in the test measurements is illustrated in figure 48.

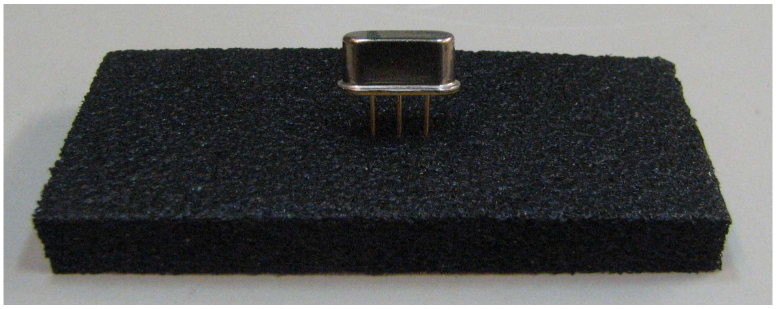

Figure 48. *One of the four hermetically sealed capacitors used in the test measurements. The hermetical casing made from a conducting material also offered electromagnetic shielding for the capacitor inside.*

The values selected should cover the operating range of the measurement system. One of the DUTs should be used as the load reference for the measurement instrument error compensation. The load reference should be selected from the middle of the operating range. The capacitance values for the DUTs were 3 pF, 6 pF, 9 pF and 12 pF. The 9 pF capacitor was used as the load reference.

For the measurement results to be reproducible the setting of the HP4285A LCR bridge are listed in Table 7.

Table 7. *HP4285A measurement settings for the test measurements.*

Parameter	Setting
Function	CsRs
Range	Auto
Level	500 mV_{RMS}
DC Bias	Off
Integration Time	Long
Trigger	Ext
ALC	Off
Average	4
Delay	0 ms

The settings used in the test measurements were the same as with normal measurements carried out at the VTI laboratory and would thus be used with the relay card in normal operation.

First the true value of the DUTs was determined by measuring them using very short test cables that have no effect on the measurement. When the measuring is carried out in this manner, only open / short compensation is necessary. The measurements were repeated for all relevant measurement frequencies. The frequencies selected for the measurements were 75 kHz, 100 kHz, 1 MHz, 3 MHz, 7 MHz and 10 MHz. The frequencies covered the operational range of the relay card. Frequencies above 10 MHz would require short cables, which would not be possible in practical measurements in the end application of the relay card.

In the second measurement, test cables with total length of 1.5 n were used. The cables consisted from one 0.5 m cable and one 1.0 m cable connected together with an extension piece. Using this kind of cables open / short / load compensation was needed. The results of the previous measurement were used as the reference value for the load. Again the measurement was repeated for multiple frequencies.

The last measurement was the actual characterization measurement for the relay card. Characterization was carried out through the MUX card and connecting the DUTs to the measurement card like in normal operation of the relay card. Both channels on the MUX card were assumed to be identical and the measurement was carried out using only channel 1 of the MUX card. First open / short / load compensation was performed to each relay, or DUT socket. Again the results from the first test measurement were used as the reference value for the load. First the empty sockets were measured. Each DUT was then measured in each socket using all 5 measurement frequencies. The measurement results of all 3 measurements can be found in Appendix J, all measurement results are in pico farads.

The instrument used in the measurements was the HP4285A LCR bridge, it offers high accuracy results in a frequency range from 75 kHz to 30 MHz. The measurement error of the HP4285A is illustrated in Table 8.

Table 8. *Calculated measurement error of the HP4285A LCR bridge when measuring a 10 pF DUT using 1.5 m long cables in room temperature with different frequencies [20].*

Frequency	Percent Error	Error in pF
100 kHz	±0.3 %	±0.03 pF
1 MHz	±0.3 %	±0.03 pF
10MHz	±1.6 %	±0.16 pF

The error depends on the measurement frequency. Using long cables the measurement accuracy of high frequency measurements deteriorates fast. Using 1.5 m cables the maximum measurement frequency of the instrument is limited to 10 MHz.

6.2 Relay to Relay Variation

Plotting the results of the measurements of the same DUT by function of the relay shows if the socket used in the measurement affects the measurement. If the different lengths of the measurement signals induced a systematic error, it is seen from the plot. The relay to relay variation for an empty socket is illustrated in Figure 49.

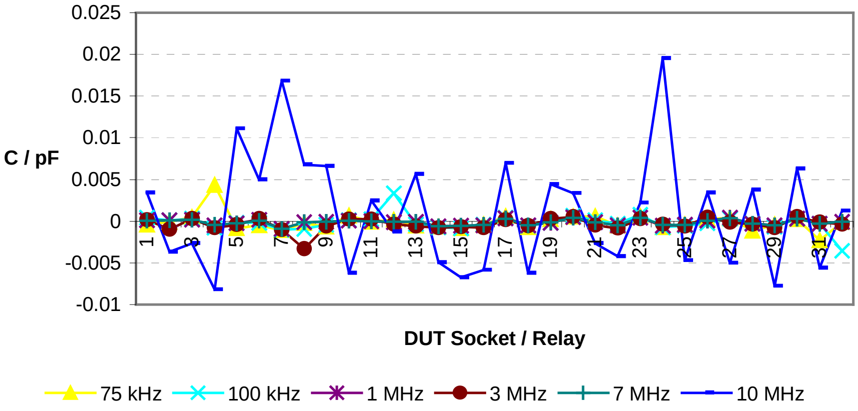

Figure 49. *Relay to relay variation of an empty socket. No systematic error could be seen, however the random variation in the 10 MHz measurement frequency stood out.*

No systematic error could be seen in the plot in any frequency. The random variation in the results of the 10 MHz measurements was however much larger than in lower frequencies. The relay to relay variation of the 6 pF DUT is illustrated in Figure 50. The 6 pF DUT represents a mid range value in the test measurement.

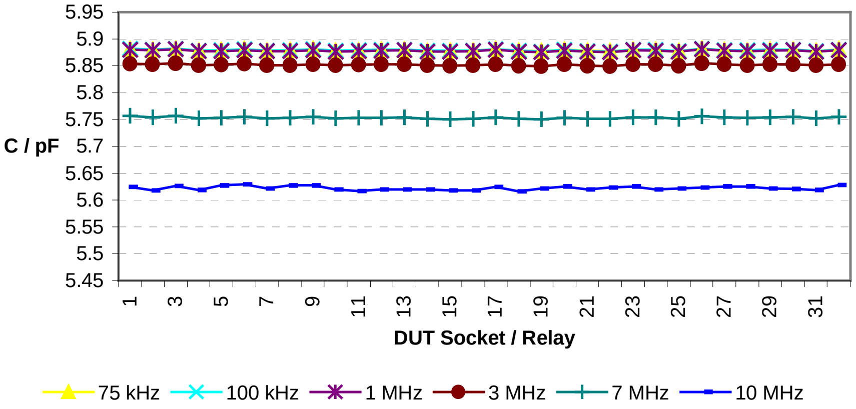

Figure 50. *Relay to relay variation of the 6 pF DUT. No systematic error could be seen. However, the small frequency dependency of the DUT was visible.*

It can be said that the location of the DUT, or the relay used did not affect the measurement. Each DUT socket could be treated as identical. This was a benefit of the open / short / load compensation carried out to each of the DUT sockets. If only open / short compensation would have been used a small systematic error would be visible when the distance the measurement signal travels increases going towards the far end of the measurement card. Sockets 16 and 17 were located on the far end and sockets 1 and 32 in the near end.

The variation of the measurement results was used as the only indication of the random error in the relay card. Variation is simply the remainder of the maximum and minimum values of each DUT. Variation gives an idea how widely the measurement results vary from measurement to measurement. Variation of the measurement was calculated from Equation 17.

$$C_{\text{var}iation} = Max(C_n) - Min(C_n) \tag{17}$$

Where $C_{\text{variation}}$ is the variation of the measurement results.

The variation of the relay card is illustrated in Figure 51 for each measurement frequency.

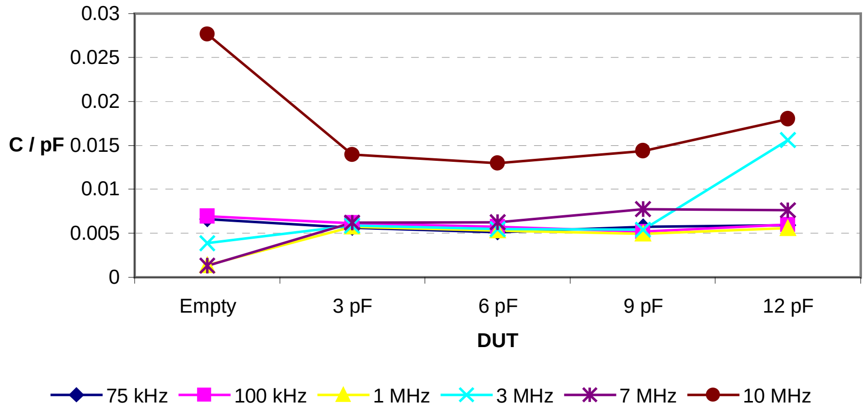

Figure 51. *Variation of the relay cards error. The variation was largest when measuring an empty socket. Again the 10 MHz measurements stood out especially in the case of the empty socket.*

The variation in an empty socket was much higher than when a DUT was connected. The variation increased noticeably on 10 MHz. However the variation fell well within the measurement accuracy of the HP4285A LCR bridge.

6.3 Bias and Linearity

Bias is a systematic error that induces an offset to the measurement. Bias can be removed from the measurement by first identifying it and then deducting it from any subsequent measurements.

The bias of the MUX card and measurement card could be identified by deducting the reference measurement carried out with 1.5 m cables from the measurement carried using the relay card and the same 1.5 m cables. The measurement results from different relays were deemed identical in the previous Chapter, thus the average of those results was used when determining the bias for better accuracy. The bias of the relay card was calculated using Equation 18.

$$C_{bias} = C_{ave} - C_{ref,1.5m} \qquad (18)$$

Where C_{bias} is the bias of the relay card, $C_{ave} = \frac{\sum_{n=1}^{32} C_n}{n}$ is the average result measured with all relays and $C_{ref,1.5m}$ is the reference value measured without using the relay card.

Linearity is the difference in bias of DUTs of different value. Linearity should be measured using DUTs in the whole operating range of the measurement system. When the linearity is plotted the ideal linearity is a horizontal line. If the bias is linear, the value of the DUT does not affect the bias. A linear bias error is easy to deduct from the measurement. Figure 52 illustrates the linearity error of the relay card.

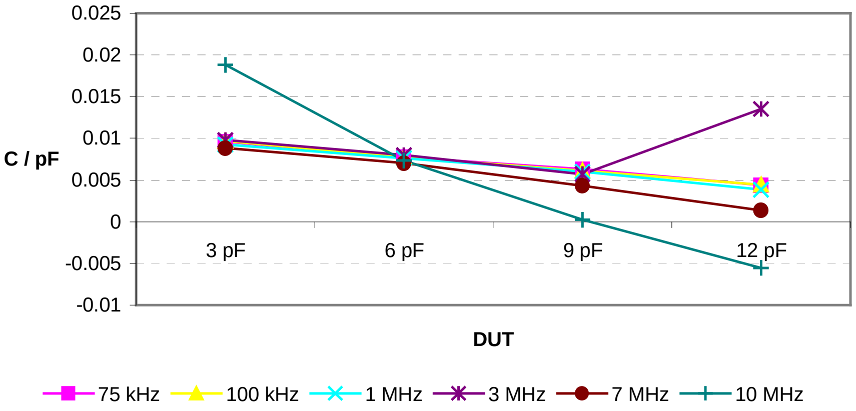

Figure 52. *Linearity error of the relay card plotted from the average readings of all relays. The linearity error of the relay card was small, but did increase with frequency. The linearity error in 10 MHz measurements was worse than in lower frequencies but it was still in well within acceptable limits.*

The linearity error of the relay card was small. Only the 10 MHz frequency stood out slightly, but was still well within acceptable limits.

6.4 Frequency Dependency

Frequency dependency of a measurement system can be determined by plotting the same the dataset used in the linearity plot by frequency. This shows the frequency dependency of the measurement system. Frequency dependency of the error can be used to determine if a certain measurement frequency offers inferior results compared to the other measurement frequencies. The frequency dependency of the relay card is plotted in Figure 53.

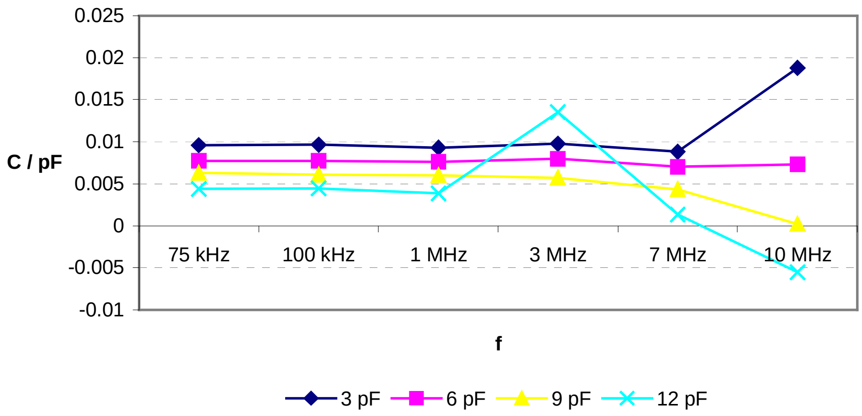

***Figure 53**. Frequency dependency of the relay card plotted from the average readings of all relays. The error increased at 10 MHz. However the measurement accuracy of the instrument was also noticeably weaker at 10 MHz.*

The error remained steady up to 7 MHz. At 10 MHz the error increased noticeably. The measurement accuracy of the HP4285A was also noticeably weaker at 10 MHz. Considering this fact, the frequency dependency of the relay card was negligible.

7 DISCUSSION AND CONCLUSIONS

The CPU card and its design are discussed in Chapter 7.1. Chapter 7.2 discusses the functionality of the MUX card while Chapter 7.3 concentrates on the measurement card and how it could be possible to improve its design. The results of the relay card characterization measurements are discussed in Chapter 7.4.

7.1 CPU Card

The modular design of the relay card worked. It was easy to design different add-on cards for different measurement applications using the CPU card to control the add-on cards. The CPU card proved to be versatile enough for most applications. Even though all the features in the CPU card were not used in this study, implementing them in the CPU card provides the possibility to use them in the future.

The SPI and I^2C serial buses can be used to connect countless different components to the CPU card. For example I/O chips connected to the SPI or I^2C serial buses could control the relays on the add-on cards.

Because the CPU card was controlled via the EIA-485 serial bus found on any industrial computer, there was no need for separate I/O cards in the computer anymore. A cost effective EIA-485 to USB converter can be made using only a few components and a self milled PCB to connect the relay card to modern laptops, which no longer have traditional serial or parallel ports.

Software such as LabView can be used to make a graphical user interface for the relay cards’ control. LabView is a graphical programming language, widely used in measurement automation. The whole measurement system can be automated using LabView programs controlling each instrument and device connected to the computer, which runs the LabView program.

7.2 MUX Card

The MUX card was a simple, yet effective tool for switching between any two devices using the 4TP (Four Terminal Pair) measurement configuration. The 4TP to 4TP extension method it uses offered improved measurement accuracy compared to other methods. Keeping the 4TP measurement configuration intact all the way to the measurement card was new in the laboratory. Previously expensive and physically large rack mounted relay boxes were used to do the switching. The relay boxes did not keep the 4TP measurement configuration intact, since the outer conductors of the cables were connected together at the relay box. Some of the relay boxes also induced noise to the measurement signals impairing the most sensitive measurements.

7.3 Measurement Card

The measurement card offered an effective way of measuring up to 32 capacitances. The shielded 2T (Two Terminal) method used was the only viable method to implement, which offered good measurement accuracy. The shielding of the measurement signals helped to achieve repeatable measurement results. The laboratory environment has a lot of instruments and thus multiple possible sources of interference. Using appropriate error compensation functions in the measurement instrument, very accurate measurement results could be achieved.

However the routing of the measurement signals on the measurement card could be done differently. Using the current design, the distance the measurement signals travel increases towards the right end of the PCB as illustrated in Figure 54.

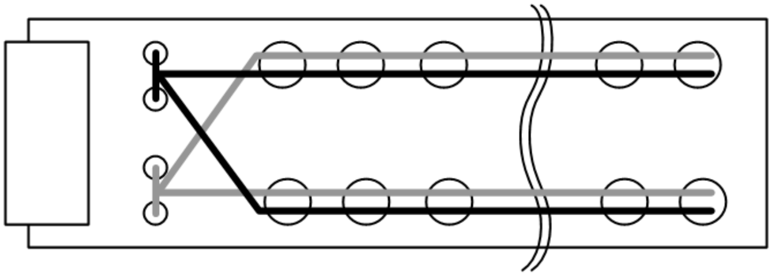

Figure 54. *The current measurement card design. The distance the measurement signal travels differed from relay to relay. The distance increases towards the right end of the PCB.*

Because the PCB was physically long the length difference of the traces is considerable. The distance the signal travelled from the connectors to the first relays is much less than the distance to the last relays and this induces a small bias error to the measurement, which depended on the relays position. The open / short / load compensation method compensated this bias. The measurement traces could be made to be the same length, regardless of the relays location using the technique illustrated in Figure 55.

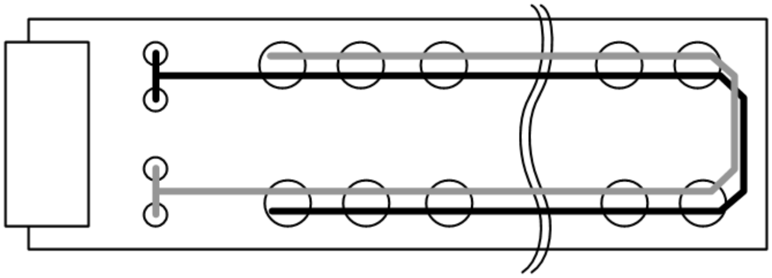

Figure 55. *Alternative way of routing the measurement signals in the measurement card. The distance the measurements signal travels stays the same regardless of the relays position.*

Not only the distance from the connector to all relays would be the same, but the signals would also be routed continuously. Using this technique the relays would seem identical, as the distance the measurement signal travels would be the same regardless of the relays position.

The open / short / load compensation is fairly inconvenient and time consuming to perform. If the relays could truly be considered identical, it might be possible to only use the open / short compensation method. To achieve accurate results the bias error should be determined and then the induced bias could be deducted from the measurement result. The linearity error should also be determined because DUTs of different capacitance value can be measured. If the linearity of the error were good, deducting the bias from the measurement results would be trivial.

7.4 Characterization

The characterization of the relay card was made using non-statistical methods. The test measurements that were carried out offered a sufficient way of estimating the measurement accuracy of the relay card without the need for additional measurements and statistical analysis.

Full statistical analysis of the relay card would not be feasible. However a compromise in the amount of DUTs and whether all relays are analyzed or not could be done. The analysis should also be done only at certain frequencies to reduce the amount of work and data needed in the analysis.

The analysis of the test measurement results supported the fact that the techniques used in the design of the relay card worked. Using proper error compensation techniques the small error induced by the changing distance the measurement signal travels depending on the relay was compensated. All relays and DUT sockets could be considered identical using proper error compensation.

The variation of the measurement results was higher when measuring an empty socket than when a DUT was connected to the socket. Some measurement systems at the VTI laboratory use a technique where one DUT socket is left empty when measuring the DUTs. The capacitance of the empty socket is then deducted from the other measurement results. As the variation of the stray capacitance of an empty socket was higher than when a DUT was connected, this technique would actually increase the error. If other errors such as bias would dominate, the technique would increase the accuracy of the measurement.

The 10 MHz measurement frequency stood out having slightly higher error in every analysis, but at this frequency the measurement was carried out at the limits of the measurement instruments capability using 1.5 m long cables. The wavelength of the measurement signal limited the usable length of the measurement cables. At 10MHz the maximum usable cable length was 1.5 m, which was used in the test measurements. The measurement accuracy of the HP4285A LCR bridge drops significantly due to long cables and high measurement frequency. However a small reduction in the measurement cables length could be enough to reduce the error to the same level as at lower frequencies or at least improve the linearity or the error. Reducing the measurement frequency from 10 MHz to 9 MHz would also improve the measurement accuracy.

The bias error of the relay card was minimal and the linearity error was also minor. The linearity error at 10 MHz was slightly higher than at lower frequencies, but could be expected because of the measurement cables length. The bias and linearity errors stayed within 0.03 pF at all frequencies.

The frequency dependency of the error could be seen at 10 MHz. Other than that there was no other frequency dependency in the error. Considering that the frequency dependent error came from the decreased measurement accuracy of the measurement instrument, the frequency dependency of the relay card is negligible.

The analysis of the measurement results concluded that the relay card could be used to measure capacitance with a measurement error of only ±0.02 pF with frequencies up to 7 MHz and with a measurement error of only ±0.03 pF with frequency of 10 MHz using 1.5 m long cables. The same figures for the HP4285A LCR bridge used to do the measurements were ±0.03 pF and ±0.16 pF, respectively. The measurement error of the HP4285A was however the long term stability for one year time period. The measurement error of an instrument could be decreased calibrating the instrument more often.

8 SUMMARY

To achieve accurate measurement results using instruments based on the auto balancing bridge, proper guarding against stray capacitance must be used. Cable extension should be made using the 4TP to 4TP extension method when possible. The measurement frequency limits the length of the extension. When 4TP to 4TP method cannot be used the shielded 2T extension method should be used.

The remaining error should be compensated for using the open / short compensation in simple measurement circuits and using the open / short / load compensation in complex measurement circuits. If any switching or multiplexing is performed in the measurement circuit it should be considered as a complex measurement circuit.

The printed circuit board of a measurement system should be designed using design techniques, which minimize interference coupling. The traces used in the measurement should have controlled impedance matched to that of the measurement instrument and its cables. The measurement traces should be specifically shielded against interference using guard rings and faradays cage. The components and the printed circuit board material should endure the high temperature and rapid temperature changes to which the measurement system is exposed in testing automotive components.

A relay card offering excellent performance can be designed using these methods. However the performance of the relay card should be confirmed with a series of test measurements.

The relay card designed and constructed in this study performed excellently in the test measurements performed using measurement techniques described earlier. There is no visible systematic relay-to-relay variation and the bias and linearity errors in the measurements are minimal. A small frequency dependent error was discovered in measurements carried out with 10 MHz. This error is induced mainly from the decreased measurement accuracy of the HP4285A instrument, which was used in the measurements, using long cables and high measurement frequency.

LIST OF REFERENCES

[1] Okada, K and Sekino, T. (2003). *Impedance Measurement Handbook.* Agilent Technologies. USA.

[2] Ott, H. (2000). *EMC Design Guide.* [WWW Document] http://www.hottconsultants.com/pdf_files/pcb_guide.pdf (Accessed April 18, 2007)

[3] Ott, H. (2000). *Grounding of Mixed Signal PCBs.* [WWW Document] http://www.hottconsultants.com/techtips/split-gnd-plane.html (Accessed April 18, 2007)

[4] O'Hara, M. (2003). *EMC at Component and PCB Level.* Newnes. UK.

[5] Brooks, D. (2003) *Signal Integrity Issues and Printed Circuit Board Design.* Prentice Hall. USA.

[6] IPC-D-317 Standard. (1989). *Design Guide For Electronic Packaging Using High-Speed Techniques. IPC. USA.*

[7] Ott, H. (1988). *Noise Reduction Techniques in Electronic Systems.* Wiley and Sons. USA.

[8] Williams, T. (2005). *The Circuit Designers Companion.* Newnes. UK.

[9] *Datasheet for Isola FR402 Laminate.* [WWW Document] http://www.isola-group.com/images/file/DSFR402rev831607.pdf (Accessed April 18, 2007)

[10] *Datasheet for Rogers RO4350B Core Material.* [WWW Document] http://www.rogerscorporation.com/mwu/pdf/ro4000ds_4.pdf (Accessed April 18, 2007)

[11] *Datasheet for Rogers RO4403 Prepreg Material.* [WWW Document] http://www.rogerscorporation.com/mwu/pdf/ro4000ds_4.pdf (Accessed April 18, 2007)

[12] *Datasheet for Atmel AT90CAN128 Microcontroller.* [WWW Document] http://www.atmel.com/dyn/resources/prod_documents/doc7682.pdf (Accessed April 18, 2007)

[13] *Datasheet for Maxim DS1631 Digital Temperature Sensor.* [WWW Document] http://datasheets.maxim-ic.com/en/ds/DS1631-DS1731.pdf (Accessed April 18, 2007)

[14] *Datasheet for Maxim MAX3075E EIA-485 Transceiver.* [WWW Document] http://datasheets.maxim-ic.com/en/ds/MAX3070E-MAX3079E.pdf (Accessed April 18, 2007)

[15] *Datasheet for Fairchild NDS351AN N-channel FET.* [WWW Document] http://www.fairchildsemi.com/ds/ND%2FNDS351AN.pdf (Accessed April 18, 2007)

[16] *Datasheet for ON-Semiconductor MC33269 Low Dropout Voltage Regulator.* [WWW Document] http://www.onsemi.com/pub/Collateral/MC33269-D.PDF (Accessed April 18, 2007)

[17] *Datasheet for ON-Semiconductor MC74HC541 Octal Non-Inverting Buffer.* [WWW Document] http://www.onsemi.com/pub/Collateral/MC74HC541A-D.PDF (Accessed April 18, 2007)

[18] *Datasheet for Teledyne Relays ER-412T DPDT Relay.* [WWW Document] http://www.teledynerelays.com/pdf/electromechanical/412.pdf (Accessed April 18, 2007)

[19] *Datasheet for Teledyne Relays RF-170 Latching DPDT Relay*. [WWW Document] http://www.teledynerelays.com/pdf/electromechanical/RF170.pdf (Accessed April 18, 2007)

[20] *Operation Manual for Agilent HP4285A Precision LCR Meter*. [WWW Document] http://cp.literature.agilent.com/litweb/pdf/04285-90010.pdf (Accessed April 18, 2007)

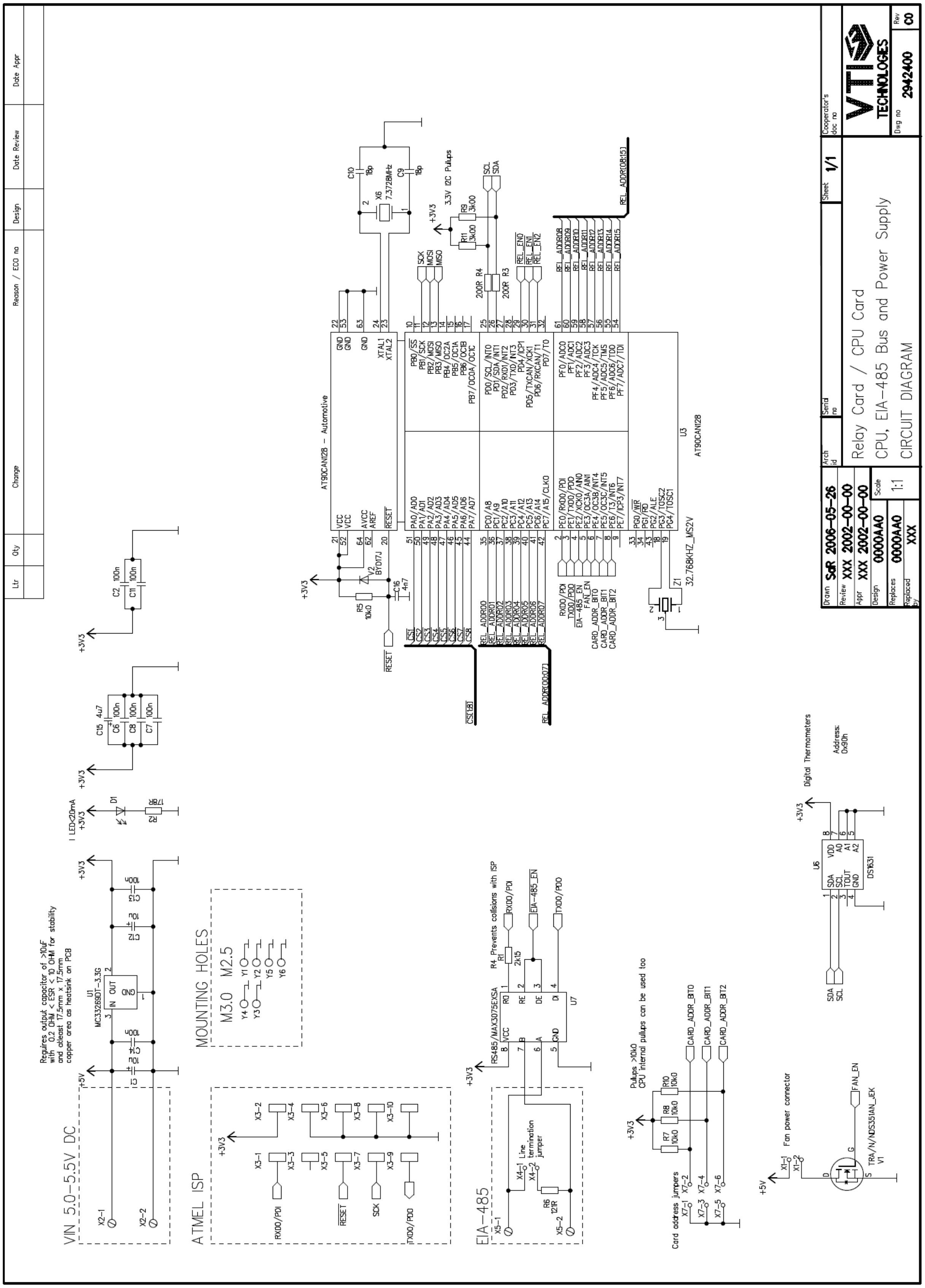
VIN 5.0-5.5V DC
X2-1
X2-2
+5V
C1 10u
C5 100n
U1 MC33269DT-3.3G
IN OUT GND
C12 10u
C13 100n
+3V3
Requires output capacitor of >10uF with 0.2 OHM < ESR < 10 OHM for stability and atleast 17.5mm x 17.5mm copper area as heatsink on PCB
I LED<20mA
D1
R2 178R
C15 4u7
C6 100n
C8 100n
C7 100n
C2 100n
C11 100n
MOUNTING HOLES
M3.0 M2.5
Y1 Y2 Y3 Y4 Y5 Y6
ATMEL ISP
X3-1 X3-2 X3-3 X3-4 X3-5 X3-6 X3-7 X3-8 X3-9 X3-10
RXD0/PDI
RESET
SCK
TXD0/PDO
EIA-485
X5-1
X5-2
X4-1 X4-2 Line termination jumper
R6 121R
RS485/MAX3075EXSA
U7
VCC RO RE DE DI GND B A
R4 Prevents collisions with ISP
R1 2k15
EIA-485_EN
Pullups >10k0
CPU internal pullups can be used too
R7 10k0
R8 10k0
R10 10k0
CARD_ADDR_BIT0
CARD_ADDR_BIT1
CARD_ADDR_BIT2
Card address jumpers
X7-1 X7-2 X7-3 X7-4 X7-5 X7-6
Fan power connector
X1-1 X1-2
FAN_EN
TRA/N/NDS351AN_JEK
V1
Digital Thermometers
Address: 0x90h
U6 DS1631
SDA SCL TOUT GND VDD A0 A1 A2
AT90CAN128 - Automotive
U3 AT90CAN128
VCC VCC AVCC AREF RESET
GND GND GND XTAL1 XTAL2
PA0/AD0 PA1/AD1 PA2/AD2 PA3/AD3 PA4/AD4 PA5/AD5 PA6/AD6 PA7/AD7
PC0/A8 PC1/A9 PC2/A10 PC3/A11 PC4/A12 PC5/A13 PC6/A14 PC7/A15/CLKO
PE0/RXD0/PDI PE1/TXD0/PDO PE2/XCK0/AIN0 PE3/OC3A/AIN1 PE4/OC3B/INT4 PE5/OC3C/INT5 PE6/T3/INT6 PE7/ICP3/INT7
PG0/WR PG1/RD PG2/ALE PG3/TOSC2 PG4/TOSC1
PB0/SS PB1/SCK PB2/MOSI PB3/MISO PB4/OC2A PB5/OC1A PB6/OC1B PB7/OC0A/OC1C
PD0/SCL/INT0 PD1/SDA/INT1 PD2/RXD1/INT2 PD3/TXD1/INT3 PD4/ICP1 PD5/TXCAN/XCK1 PD6/RXCAN/T1 PD7/T0
PF0/ADC0 PF1/ADC1 PF2/ADC2 PF3/ADC3 PF4/ADC4/TCK PF5/ADC5/TMS PF6/ADC6/TDO PF7/ADC7/TDI
R5 10k0
V2 BYD17J
C16 4n7
CS1 CS2 CS3 CS4 CS5 CS6 CS7 CS8
CS[1:8]
REL_ADDR00 … REL_ADDR07
REL_ADDR[00:07]
REL_ADDR08 … REL_ADDR15
REL_ADDR[08:15]
REL_EN0 REL_EN1 REL_EN2
Z1 32.768KHZ_MS2V
X6 7.3728MHz
C9 18p
C10 18p
R3 200R
R4 200R
R9 3k00
R11 3k00
3.3V I2C Pullups
SCL SDA
SCK MOSI MISO
Ltr Qty Change Reason / ECO no Design Date Review Date Appr
Drawn SaR 2006-05-26
Review XXX 2002-00-00
Appr XXX 2002-00-00
Design 0000AA0
Replaces 0000AA0
Replaced by XXX
Scale 1:1
Arch id
Serial no
Relay Card / CPU Card
CPU, EIA-485 Bus and Power Supply
CIRCUIT DIAGRAM
Sheet 1/1
Cooperator's doc no
VTI TECHNOLOGIES
Dwg no 2942400
Rev C0

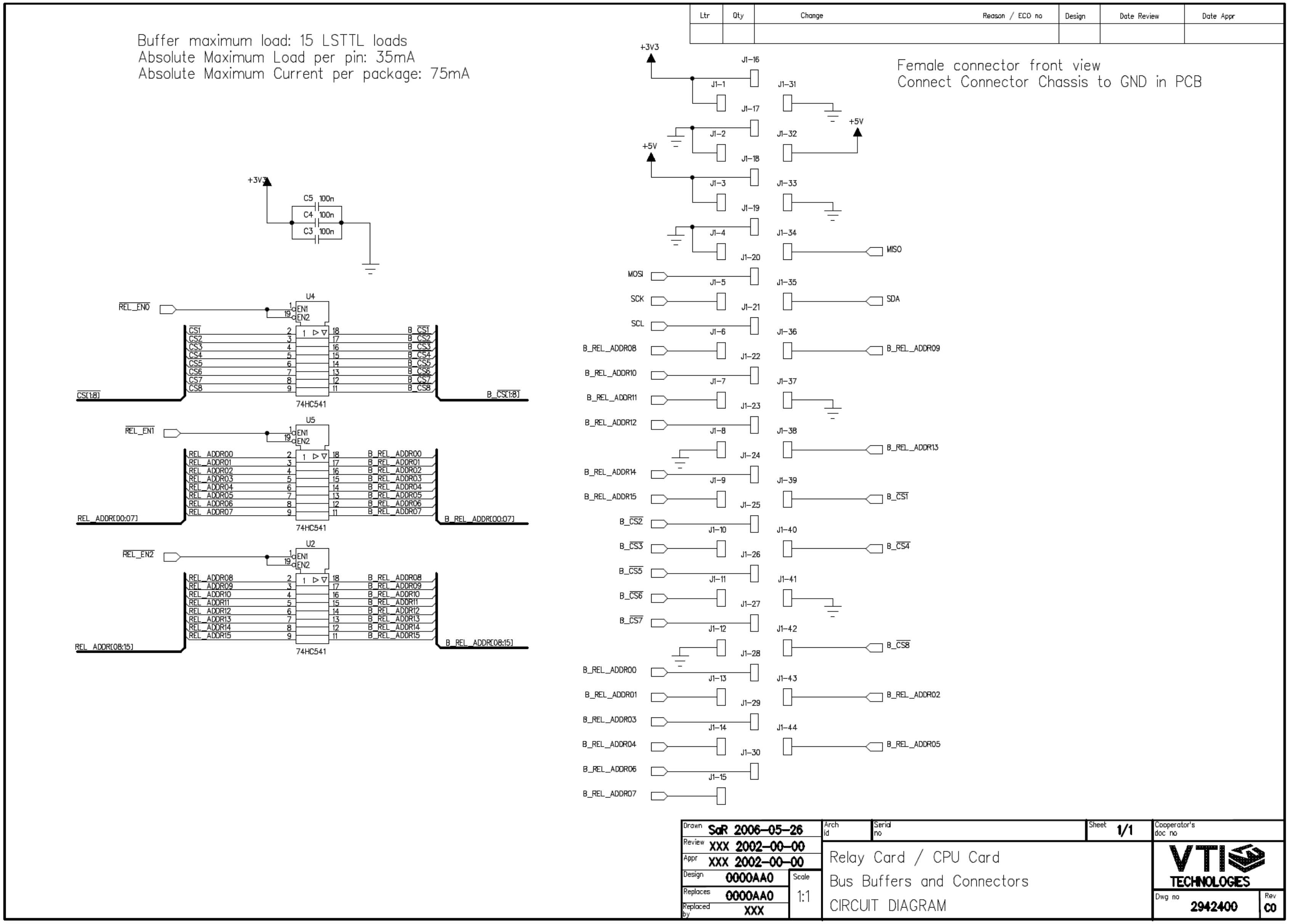

Buffer maximum load: 15 LSTTL loads
Absolute Maximum Load per pin: 35mA
Absolute Maximum Current per package: 75mA

Female connector front view
Connect Connector Chassis to GND in PCB

VTI29424C0_(CPU) Silkscreen Top

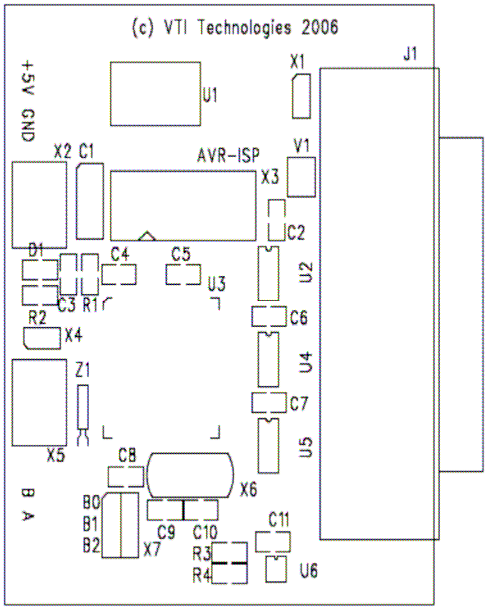

VTI29424C0_(CPU) Silkscreen Bottom

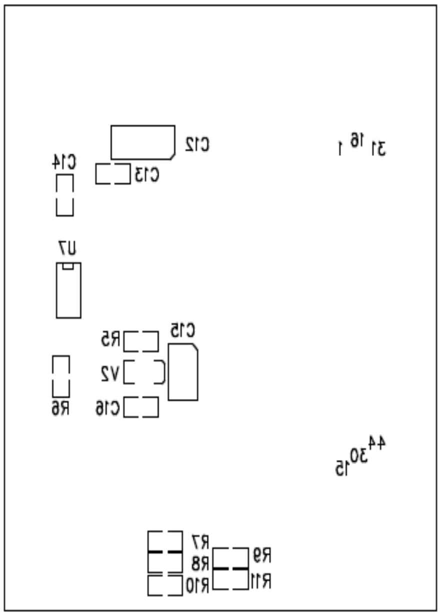

VTI29424C0_(CPU) Solder Mask Top

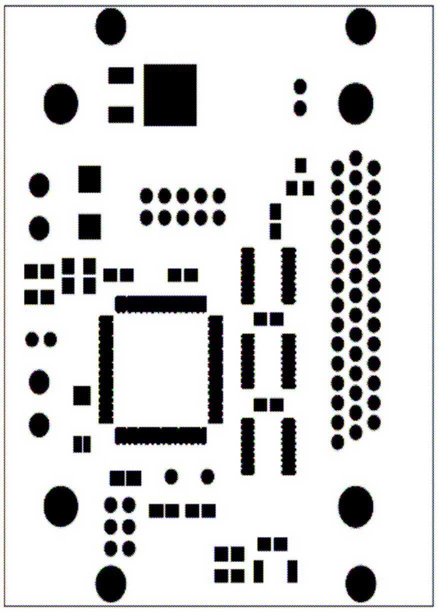

VTI29424C0_(CPU) Solder Mask Bottom

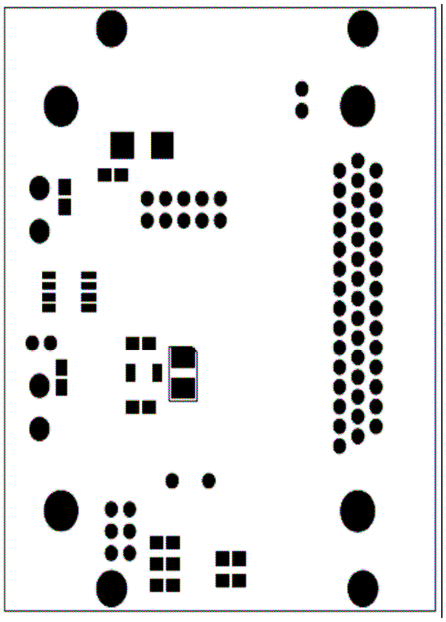

VTI29424C0_(CPU) Layer 1

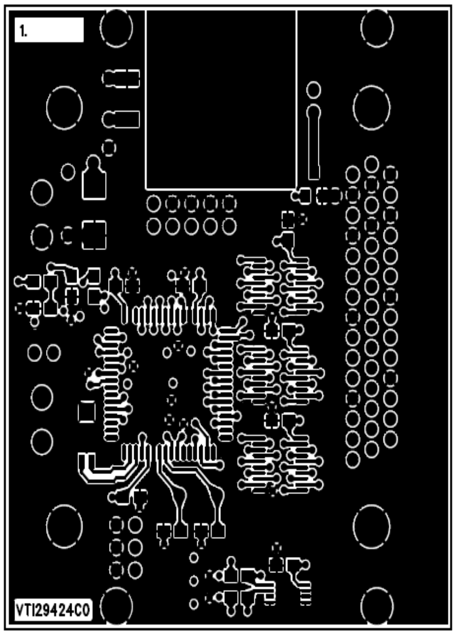

VTI29424C0_(CPU) Layer 2

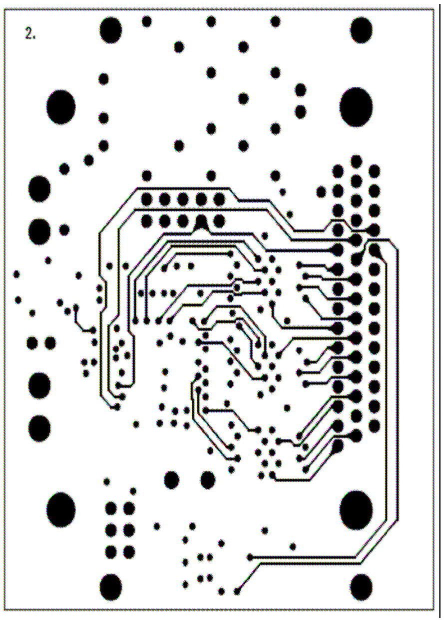

VTI29424C0_(CPU) Layer 3

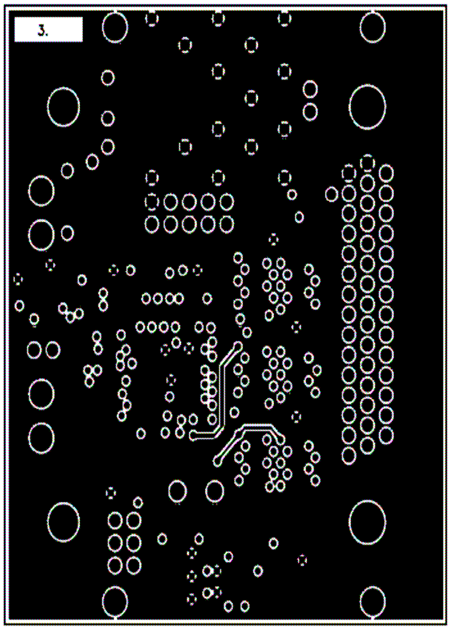

VTI29424C0_(CPU) Layer 4

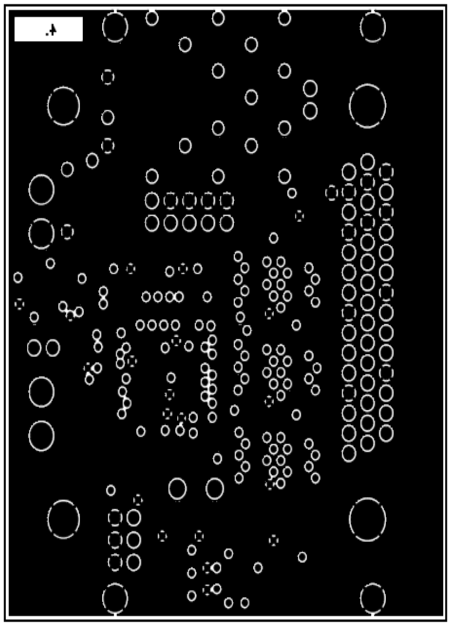

VTI29424C0_(CPU) Layer 5

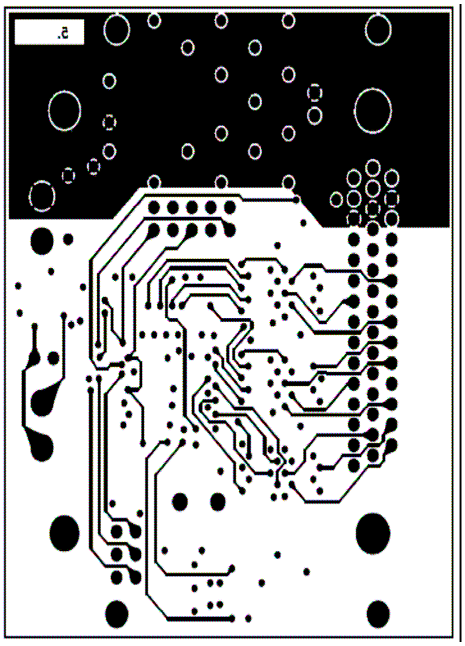

VTI29424C0_(CPU) Layer 6

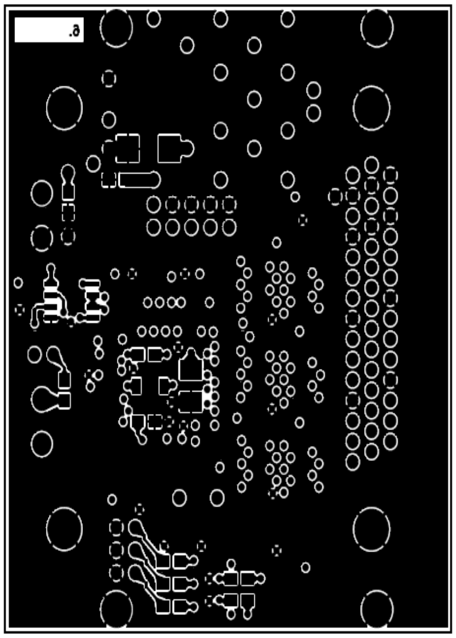

```
|-------------------------------------------------------------------------------|
|Bill Of Materials for VTI29424C0_(CPU).sch on Fri May 04 10:27:47 2007         |
|-------------------------------------------------------------------------------|
|Item|Qty |Reference|Part Name     |Manufacturer  |Description                  |
|----+----+---------+--------------+--------------+-----------------------------|
|1   |1   |Z1       |32.768KHZ_MS2V|Abracon       |Radial SMD Oscillator        |
|2   |3   |U2 U4-5  |MC74HC541ADT  |ON-Semi       |Octal TRI-STATE Buffer       |
|3   |1   |U3       |AT90CAN128-15A|Atmel         |8 bit AVR Microcontroller    |
|    |    |         |Z             |              |                             |
|4   |10  |C2-8 C11 |C/0805/100N   |AVX           |Ceramic Capacitor            |
|    |    |C13-14   |              |              |                             |
|5   |2   |C9-10    |C/0805/18P/5P |AVX           |Ceramic Capacitor            |
|6   |1   |C16      |C/0805/4N7/10P|AVX           |Ceramic Capacitor            |
|7   |2   |C1 C12   |C/EL/10U/16/60|AVX           |Tantalum Condensator         |
|    |    |         |32            |              |                             |
|8   |1   |C15      |C/EL/4U7/16/35|AVX           |Tantalum Condensator         |
|    |    |         |28            |              |                             |
|9   |1   |J1       |CON/D/SUB-44F |AMP           |44 Pin Female HD D-Connector |
|10  |1   |X3       |CON/F/10N/MALE|AMP           |Header                       |
|11  |2   |X1 X4    |CON/P/1X2     |AMP           |Header                       |
|12  |1   |X7       |CON/P/2X3     |AMP           |Header                       |
|13  |2   |X2 X5    |CON/S/2N/KRM2U|Phoenix       |Terminal Block               |
|    |    |         |L             |              |                             |
|14  |1   |V2       |DIO/BYD17J    |Philips       |Avalanche Diode              |
|15  |1   |U6       |SENS/T/DS1631 |Maxim         |Digital Temperature Sensor   |
|16  |1   |D1       |LED/0805      |Philips       |SMD LED                      |
|17  |1   |U1       |MC33269DT-3.3G|ON-Semi       |Low Dropout Regulator        |
|18  |4   |R5 R7-8  |R/0805/10K0/1P|Vishay        |Chip Resistor                |
|    |    |R10      |              |              |                             |
|19  |1   |R6       |R/0805/121R/1P|Vishay        |Chip Resistor                |
|20  |1   |R2       |R/0805/178R/1P|Vishay        |Chip Resistor                |
|21  |2   |R3-4     |R/0805/200R/1P|Vishay        |Chip Resistor                |
|22  |1   |R1       |R/0805/2K15/1P|Vishay        |Chip Resistor                |
|23  |2   |R9 R11   |R/0805/3K00/1P|Vishay        |Chip Resistor                |
|24  |1   |U7       |RS485/MAX3075E|Maxim         |EIA-485 Transceiver          |
|    |    |         |XSA           |              |                             |
|25  |1   |V1       |TRA/N/NDS351AN|ON-Semi       |N-Channel FET                |
|26  |1   |X6       |XTAL/7.3728MHZ|Abracon       |HC49/US XTAL                 |
|-------------------------------------------------------------------------------|
```

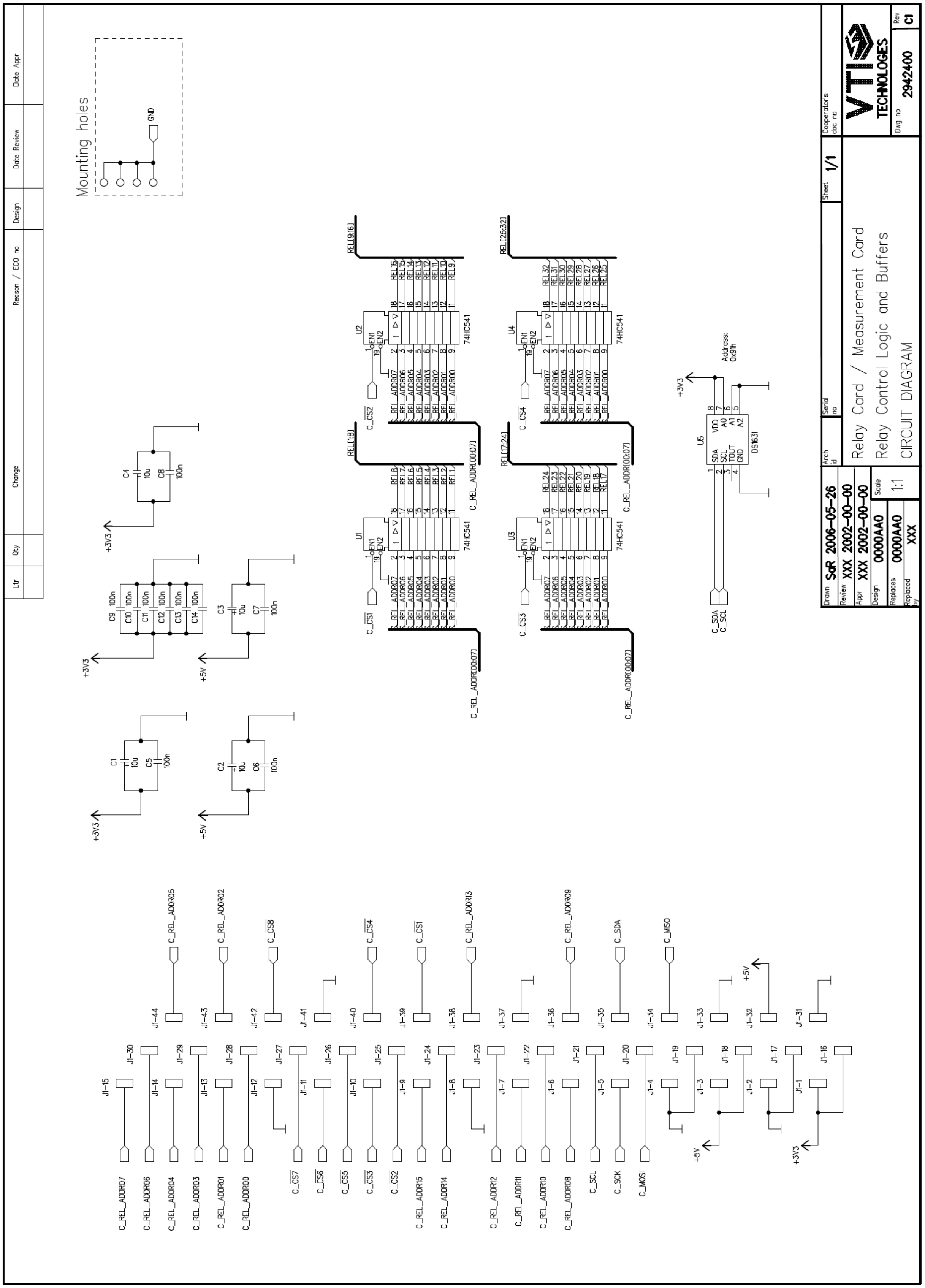
Ltr
Qty
Change
Reason / ECO no
Design
Date Review
Date Appr
Mounting holes
GND
+3V3
+5V
C1 10u
C5 100n
C2 10u
C6 100n
C3 10u
C7 100n
C4 10u
C8 100n
C9 100n
C10 100n
C11 100n
C12 100n
C13 100n
C14 100n
U1
U2
U3
U4
74HC541
EN1
EN2
C_CS1
C_CS2
C_CS3
C_CS4
C_REL_ADDR[00:07]
REL[1:8]
REL[9:16]
REL[17:24]
REL[25:32]
U5
DS1631
SDA
SCL
TOUT
GND
VDD
A0
A1
A2
Address: 0x9th
C_SDA
C_SCL
J1-1 … J1-44
C_REL_ADDR07
C_REL_ADDR06
C_REL_ADDR04
C_REL_ADDR03
C_REL_ADDR01
C_REL_ADDR00
C_CS7
C_CS6
C_CS5
C_CS3
C_CS2
C_REL_ADDR15
C_REL_ADDR14
C_REL_ADDR12
C_REL_ADDR11
C_REL_ADDR10
C_REL_ADDR08
C_SCL
C_SCK
C_MOSI
C_REL_ADDR05
C_REL_ADDR02
C_CS8
C_CS4
C_CS1
C_REL_ADDR13
C_REL_ADDR09
C_SDA
C_MISO
Drawn SaR 2006-05-26
Review XXX 2002-00-00
Appr XXX 2002-00-00
Design 0000AA0
Replaces 0000AA0
Replaced by XXX
Scale 1:1
Arch id
Serial no
Sheet 1/1
Relay Card / Measurement Card
Relay Control Logic and Buffers
CIRCUIT DIAGRAM
Cooperator's doc no
VTI TECHNOLOGIES
Dwg no 2942400
Rev C1

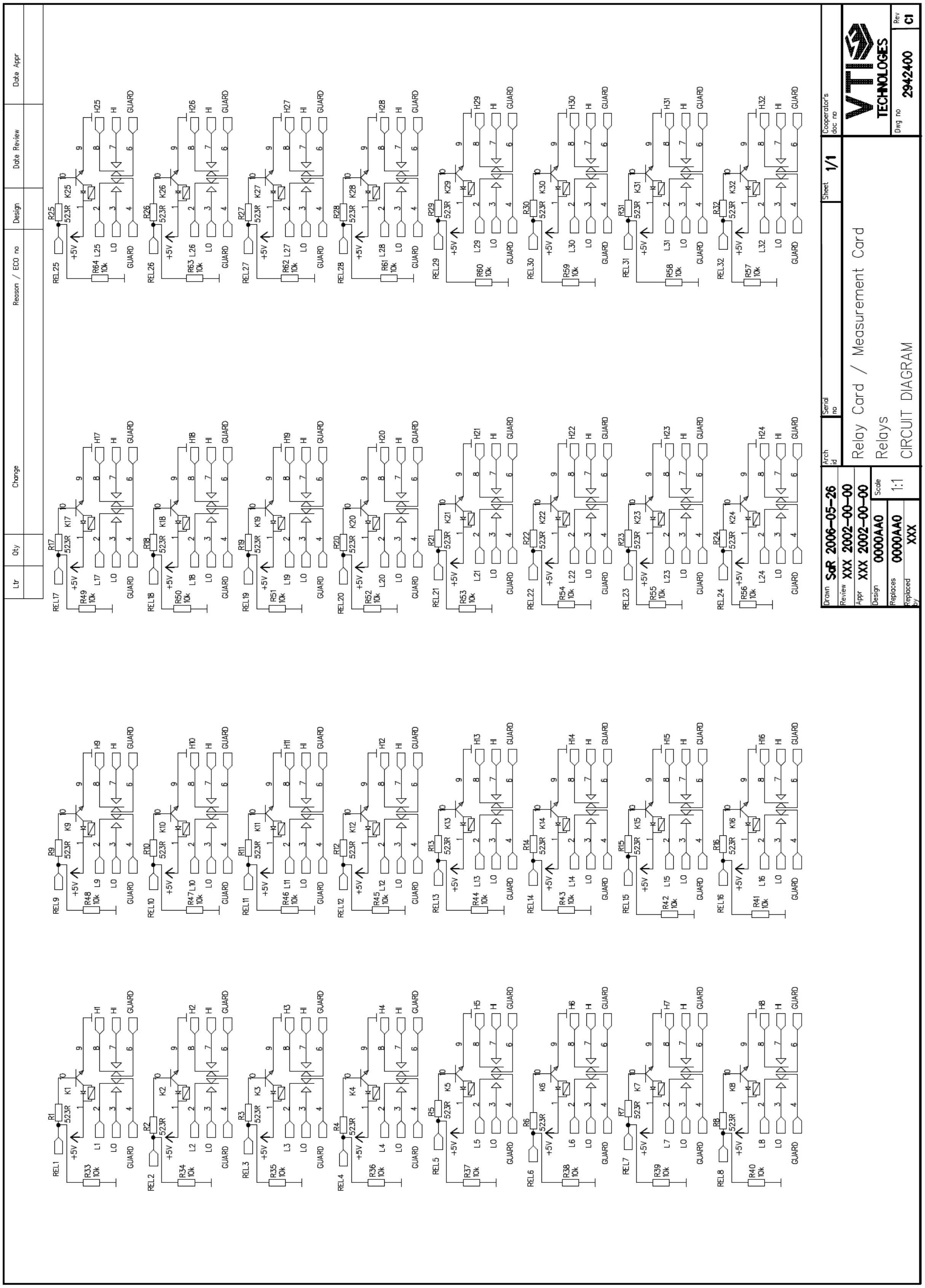

Ltr	Qty	Change	Reason / ECO no	Design	Date Review	Date Appr

Relay Card / Measurement Card

Relays

CIRCUIT DIAGRAM

Drawn	SaR	2006-05-26
Review	XXX	2002-00-00
Appr	XXX	2002-00-00
Design		0000AA0
Replaces		0000AA0
Replaced by		XXX

Scale 1:1

Sheet 1/1

Cooperator's doc no

VTI TECHNOLOGIES

Dwg no 2942400

Rev C1

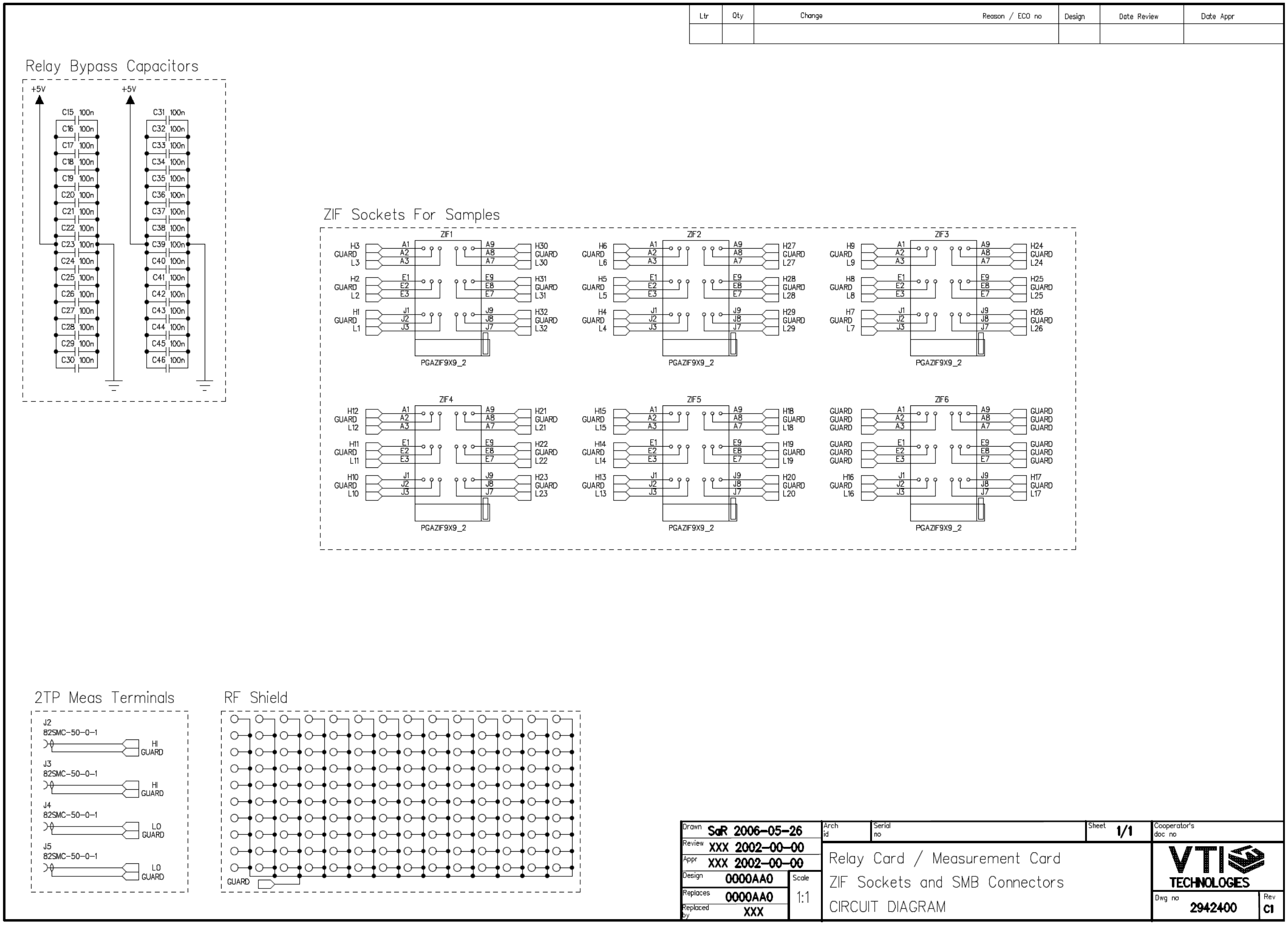
Ltr
Qty
Change
Reason / ECO no
Design
Date Review
Date Appr
Relay Bypass Capacitors
+5V
C15 100n
C16 100n
C17 100n
C18 100n
C19 100n
C20 100n
C21 100n
C22 100n
C23 100n
C24 100n
C25 100n
C26 100n
C27 100n
C28 100n
C29 100n
C30 100n
+5V
C31 100n
C32 100n
C33 100n
C34 100n
C35 100n
C36 100n
C37 100n
C38 100n
C39 100n
C40 100n
C41 100n
C42 100n
C43 100n
C44 100n
C45 100n
C46 100n
ZIF Sockets For Samples
ZIF1
H3 GUARD L3
H2 GUARD L2
H1 GUARD L1
A1 A2 A3
E1 E2 E3
J1 J2 J3
A9 A8 A7
E9 E8 E7
J9 J8 J7
H30 GUARD L30
H31 GUARD L31
H32 GUARD L32
PGAZIF9X9_2
ZIF2
H6 GUARD L6
H5 GUARD L5
H4 GUARD L4
H27 GUARD L27
H28 GUARD L28
H29 GUARD L29
PGAZIF9X9_2
ZIF3
H9 GUARD L9
H8 GUARD L8
H7 GUARD L7
H24 GUARD L24
H25 GUARD L25
H26 GUARD L26
PGAZIF9X9_2
ZIF4
H12 GUARD L12
H11 GUARD L11
H10 GUARD L10
H21 GUARD L21
H22 GUARD L22
H23 GUARD L23
PGAZIF9X9_2
ZIF5
H15 GUARD L15
H14 GUARD L14
H13 GUARD L13
H18 GUARD L18
H19 GUARD L19
H20 GUARD L20
PGAZIF9X9_2
ZIF6
GUARD GUARD GUARD
GUARD GUARD GUARD
H16 GUARD L16
GUARD GUARD GUARD
GUARD GUARD GUARD
H17 GUARD L17
PGAZIF9X9_2
2TP Meas Terminals
J2 82SMC-50-0-1 HI GUARD
J3 82SMC-50-0-1 HI GUARD
J4 82SMC-50-0-1 LO GUARD
J5 82SMC-50-0-1 LO GUARD
RF Shield
GUARD
Drawn SaR 2006-05-26
Review XXX 2002-00-00
Appr XXX 2002-00-00
Design 0000AA0
Replaces 0000AA0
Replaced by XXX
Scale 1:1
Arch id
Serial no
Sheet 1/1
Cooperator's doc no
Relay Card / Measurement Card
ZIF Sockets and SMB Connectors
CIRCUIT DIAGRAM
VTI TECHNOLOGIES
Dwg no 2942400
Rev C1

VTI29424C1_(Measurement) Silkscreen Top

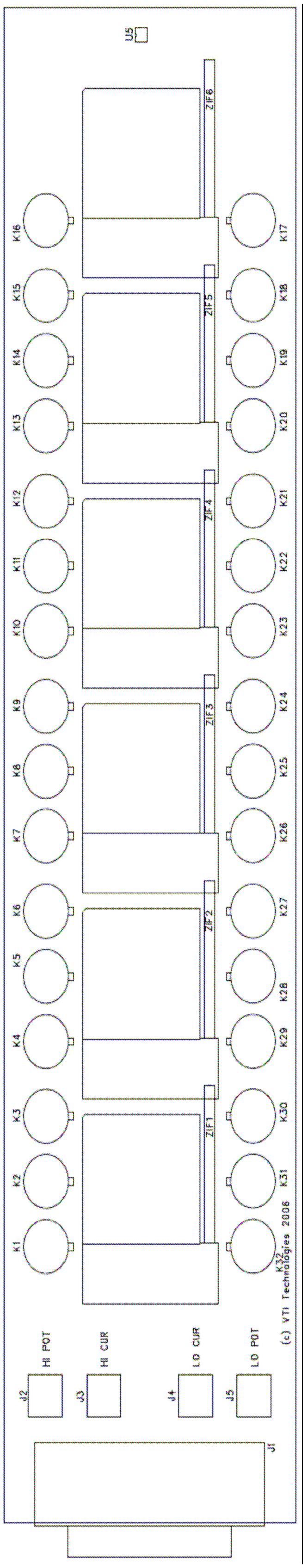

VTI29424C1_(Measurement) Silkscreen Bottom

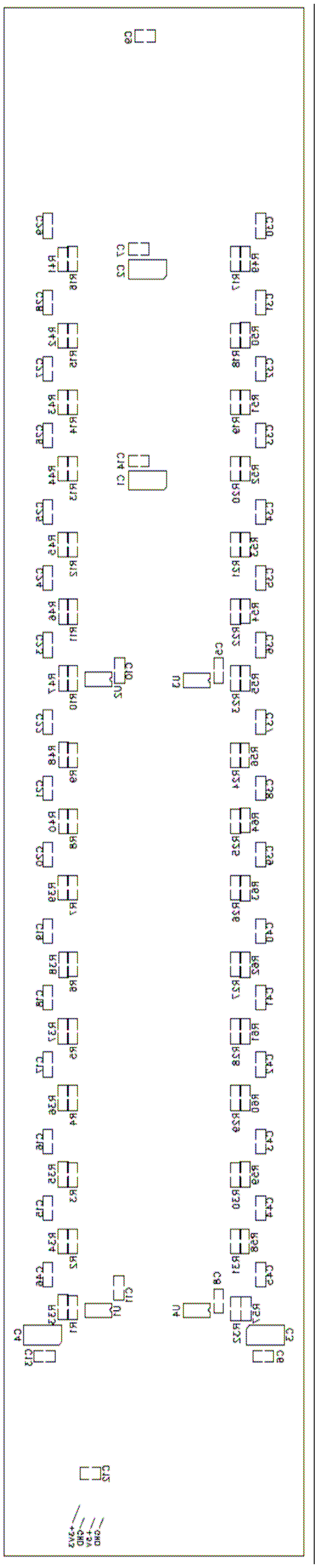

VTI29424C1_(Measurement) Solder Mask Top

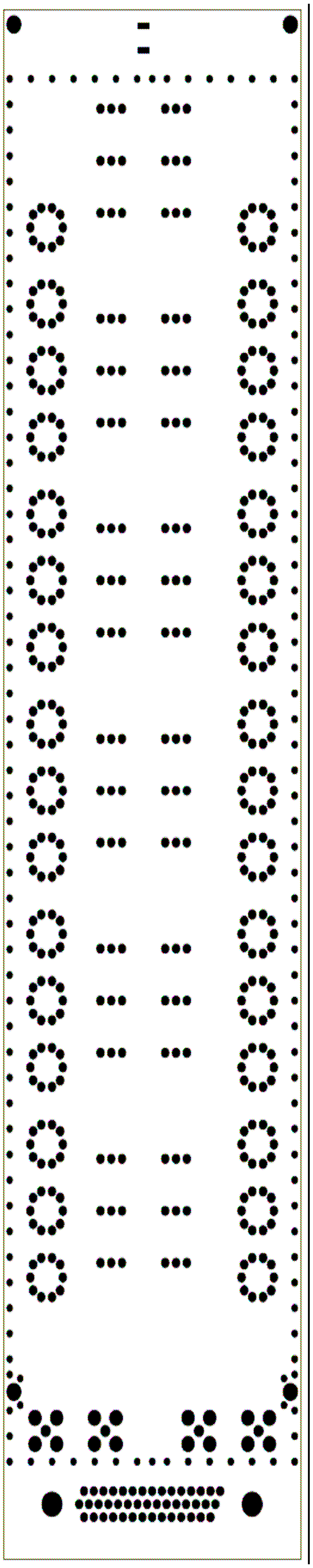

VTI29424C1_(Measurement) Solder Mask Bottom

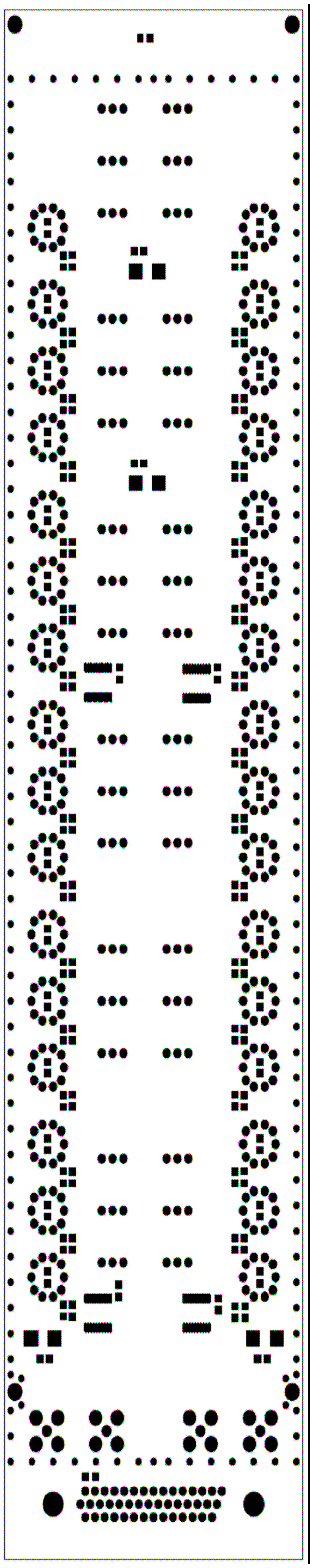

VTI29424C1_(Measurement) Layer 1

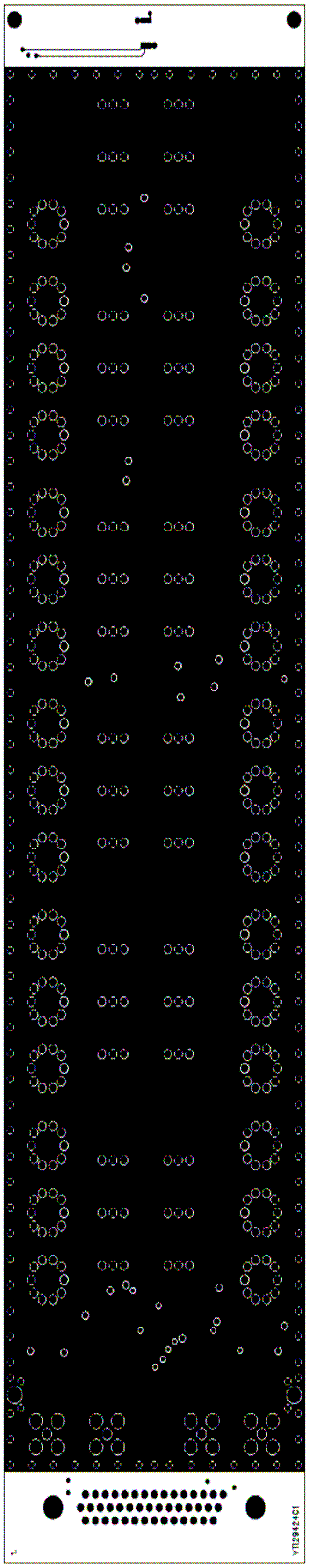

VTI29424C1_(Measurement) Layer 2

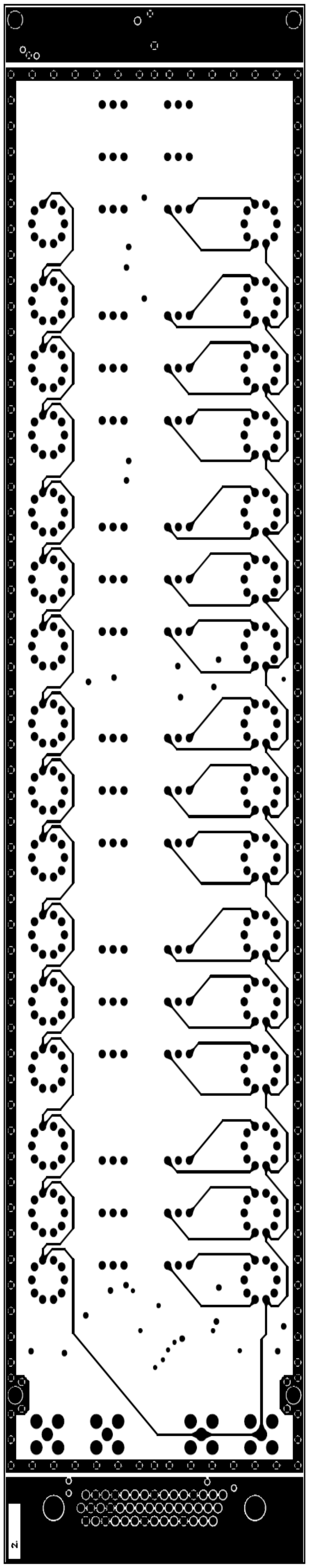

VTI29424C1_(Measurement) Layer 3

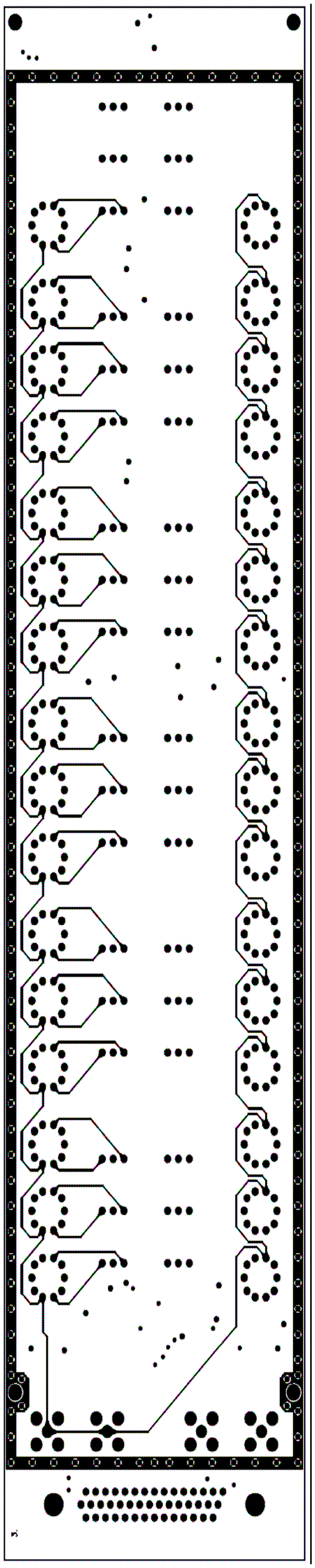

VTI29424C1_(Measurement) Layer 4

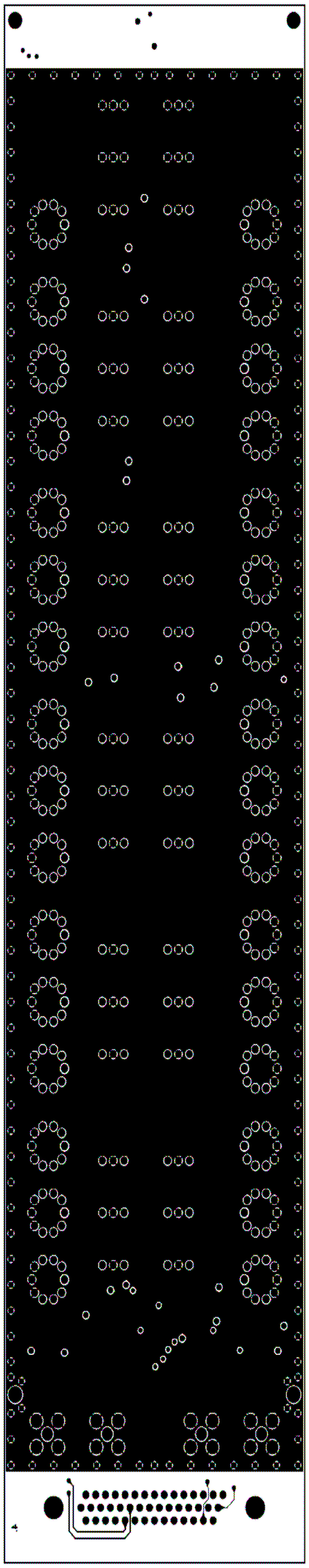

VTI29424C1_(Measurement) Layer 5

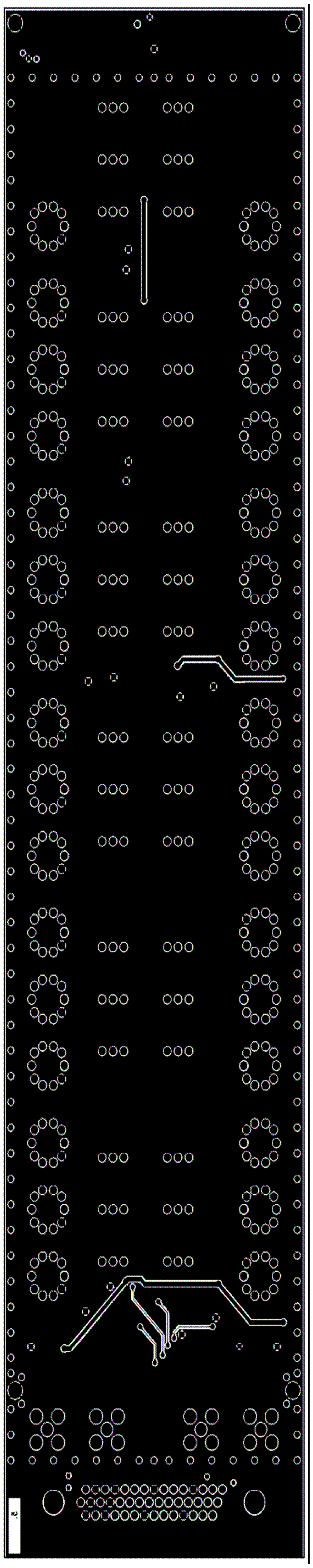

VTI29424C1_(Measurement) Layer 6

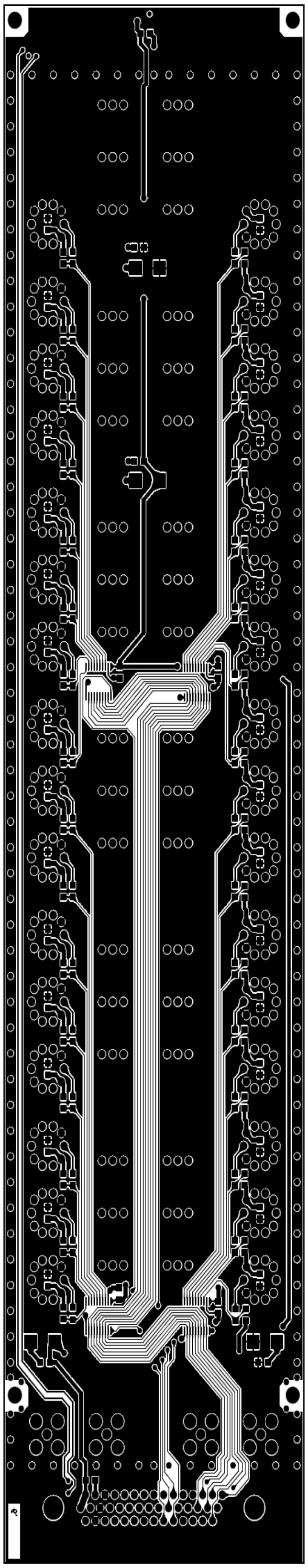

```
|--------------------------------------------------------------------------------|
|Bill Of Materials for VTI29424C1_(Measurement).sch on Fri May 04 11:15:42 2007 |
|--------------------------------------------------------------------------------|
|Item|Qty |Reference|Part Name     |Manufacturer  |Description                   |
|----+----+---------+--------------+--------------+------------------------------|
|1   |4   |U1-4     |MC74HC541ADT  |ON-Semi       |Octal TRI-STATE Buffer        |
|2   |42  |C5-46    |C/0805/100N   |AVX           |Ceramic Capacitor             |
|3   |4   |C1-4     |C/EL/10U/35/60|AVX           |Tantalum Capacitor            |
|    |    |         |32            |              |                              |
|4   |1   |J1       |CON/D/SUB-44M |AMP           |44 Pin Male HD D-Connector    |
|5   |4   |J2-5     |CON/K/82SMB500|Huber Suhner  |SMB Connector                 |
|6   |1   |U5       |DS1631        |Maxim         |Digital Temperature Sensor    |
|7   |6   |ZIF1-6   |PGAZIF9X9     |Aries         |ZIF Socket                    |
|8   |32  |R1-32    |R/0805/523R/1P|Vishay        |Chip Resistor                 |
|9   |32  |R33-64   |R/0805/10k/1P |Vishay        |Chip Resistor                 |
|10  |32  |K1-32    |REL/ER-412TN  |Teledyne      |DPDT Relay                    |
|--------------------------------------------------------------------------------|
```

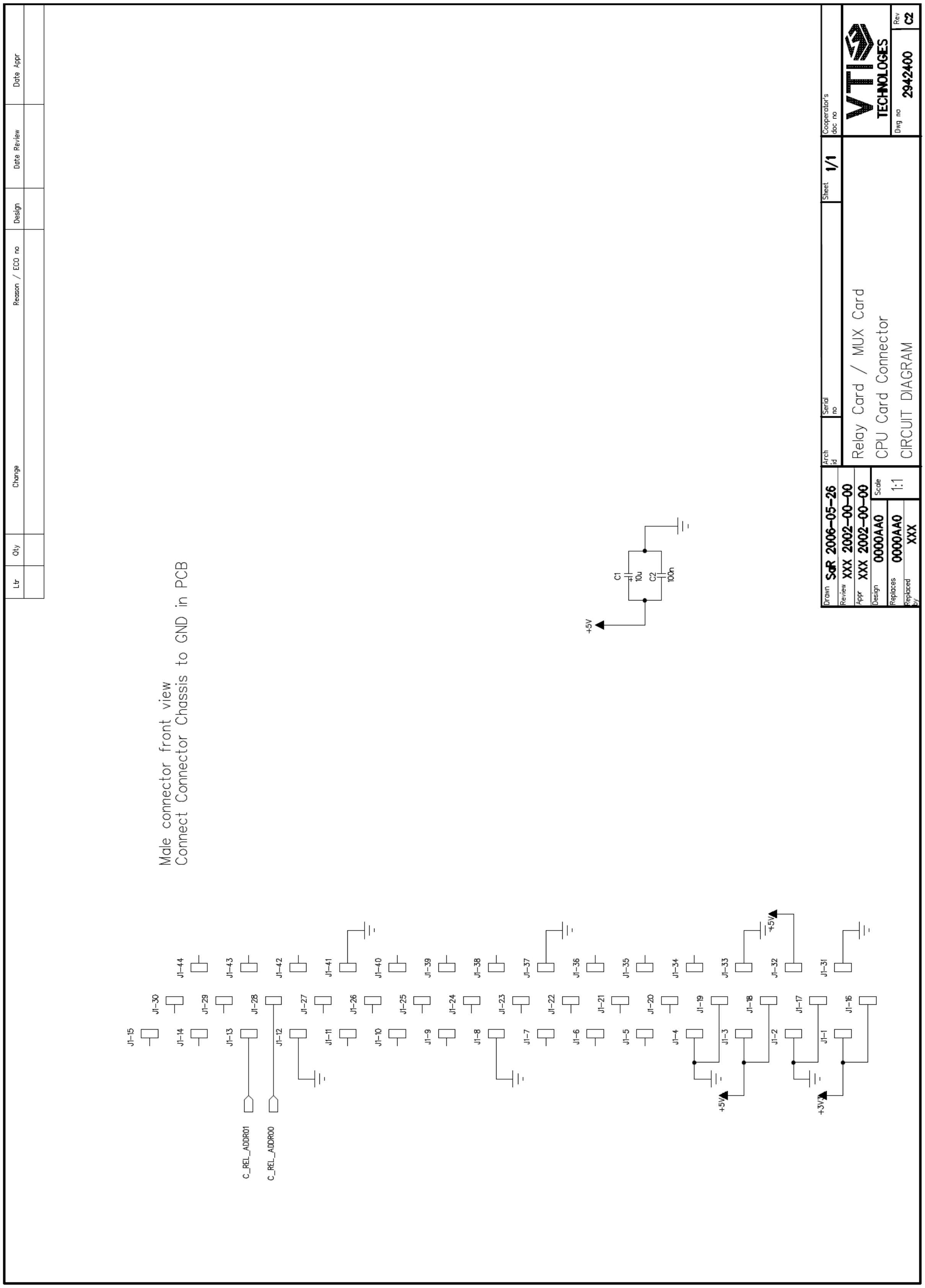
Ltr
Qty
Change
Reason / ECO no
Design
Date Review
Date Appr
Male connector front view
Connect Connector Chassis to GND in PCB
C1
10u
C2
100n
+5V
J1-1
J1-2
J1-3
J1-4
J1-5
J1-6
J1-7
J1-8
J1-9
J1-10
J1-11
J1-12
J1-13
J1-14
J1-15
J1-16
J1-17
J1-18
J1-19
J1-20
J1-21
J1-22
J1-23
J1-24
J1-25
J1-26
J1-27
J1-28
J1-29
J1-30
J1-31
J1-32
J1-33
J1-34
J1-35
J1-36
J1-37
J1-38
J1-39
J1-40
J1-41
J1-42
J1-43
J1-44
+5V
+5V
+3V3
C_REL_ADDR01
C_REL_ADDR00
Drawn SaR 2006-05-26
Review XXX 2002-00-00
Appr XXX 2002-00-00
Design 0000AA0
Replaces 0000AA0
Replaced by XXX
Scale 1:1
Arch id
Serial no
Relay Card / MUX Card
CPU Card Connector
CIRCUIT DIAGRAM
Sheet 1/1
Cooperator's doc no
VTI TECHNOLOGIES
Dwg no 2942400
Rev C2

Ltr	Qty	Change	Reason / ECO no	Design	Date Review	Date Appr

Layers 1–2, 3–4, 5–6 separated by 0.18mm
Layers 2–3 and 4–5 separated by 0.47mm
Core and Prepreg ek is 4.3
50 ohm Striplines Between (Width 0.15mm) layers 1 and 3 or 4 and 6
For other configurations Consult:
Martin O'Hara – EMC at component and PCB level, Chapter 7. (Book)
Polar Si8000 Controlled Impedance Solver (Software)

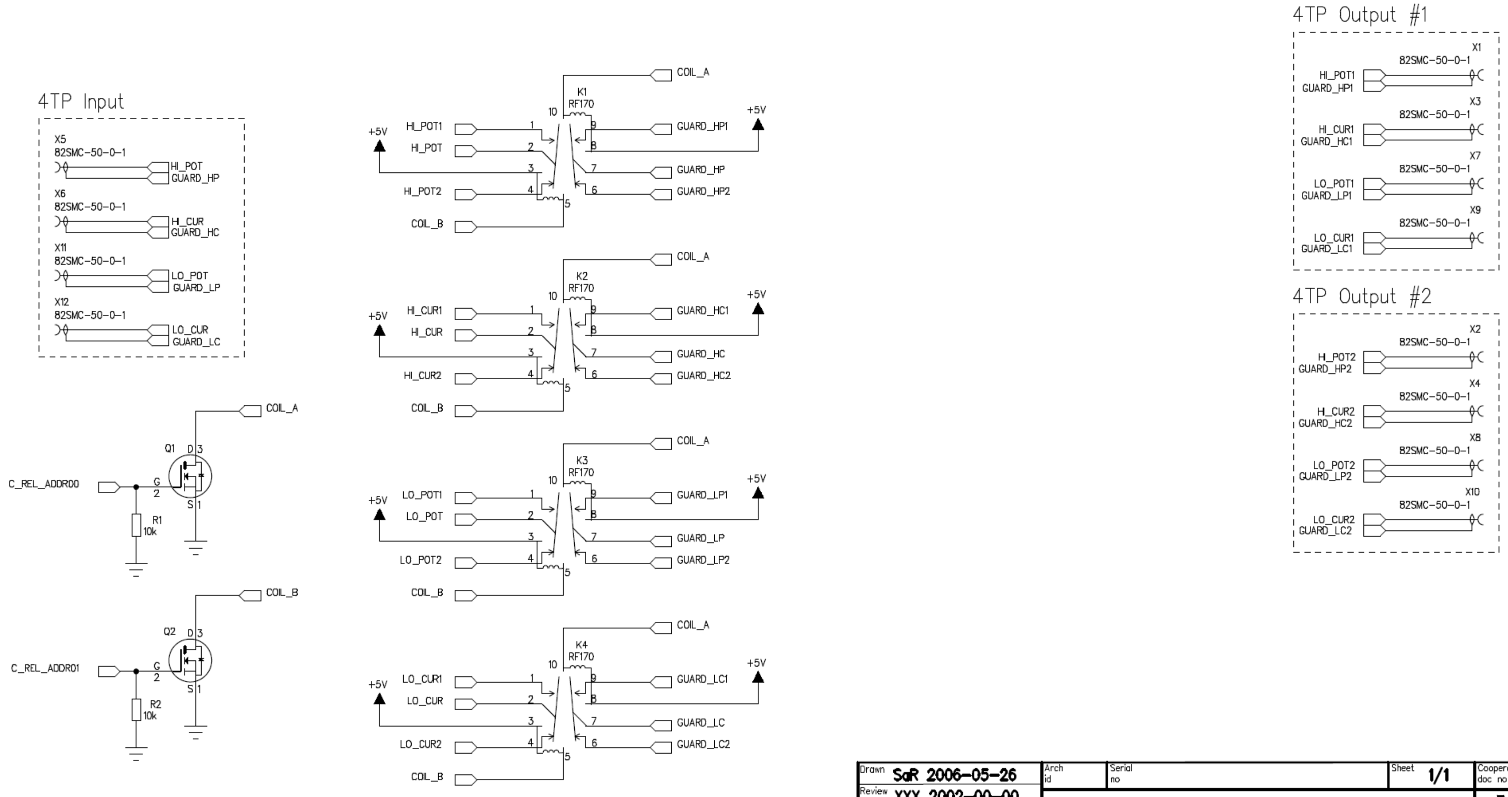

Drawn	SaR 2006-05-26	Arch id	Serial no
Review	XXX 2002-00-00	Sheet	1/1
Appr	XXX 2002-00-00	Cooperator's doc no	
Design	0000AA0	Scale	1:1
Replaces	0000AA0	Dwg no	2942400
Replaced by	XXX	Rev	C2

Relay Card / MUX Card
Relay Control Logic and Relays
CIRCUIT DIAGRAM

VTI TECHNOLOGIES

VTI29424C2_(MUX) Silkscreen Top

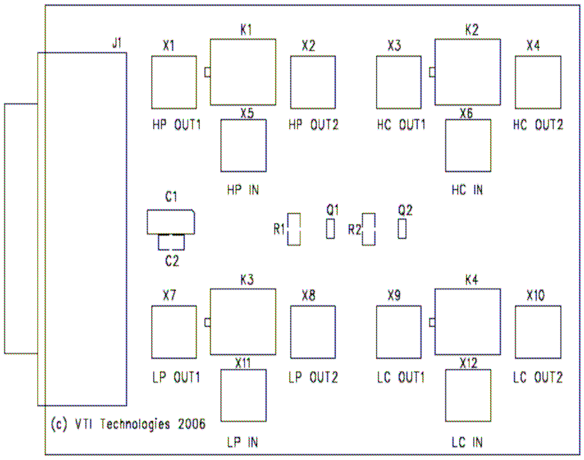

VTI29424C2_(MUX) Silkscreen Bottom

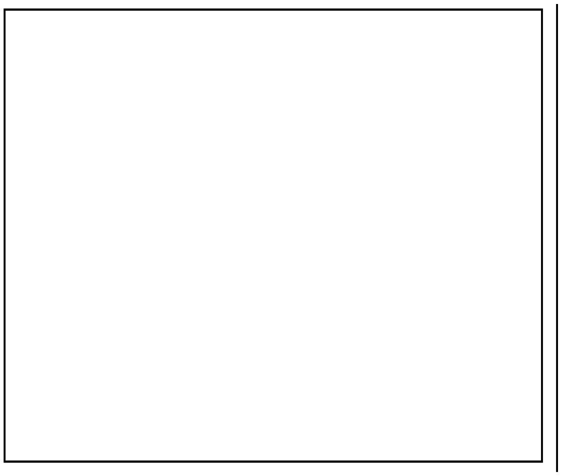

VTI29424C2_(MUX) Solder Mask Top

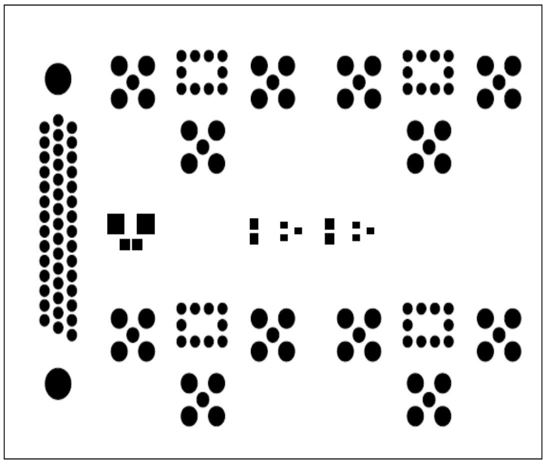

VTI29424C2_(MUX) Solder Mask Bottom

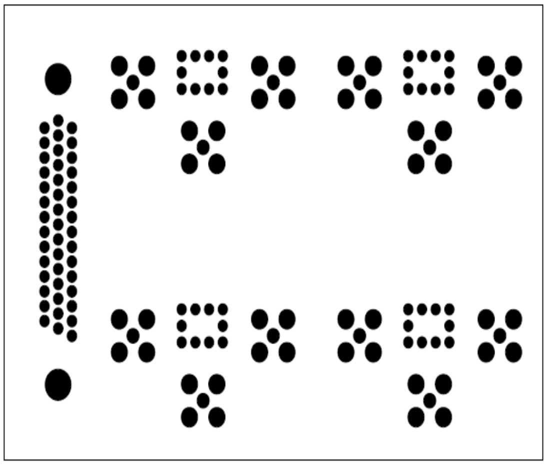

VTI29424C2_(MUX) Layer 1

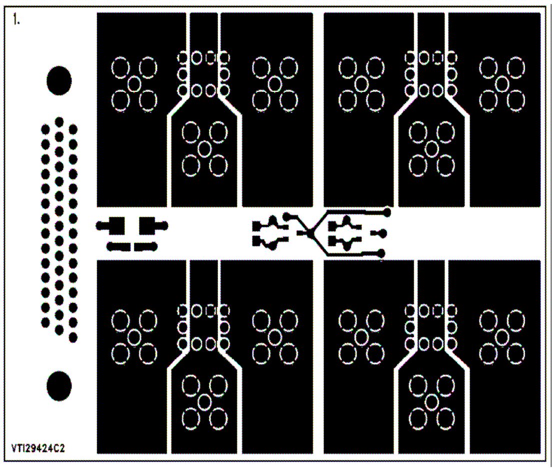

VTI29424C2_(MUX) Layer 2

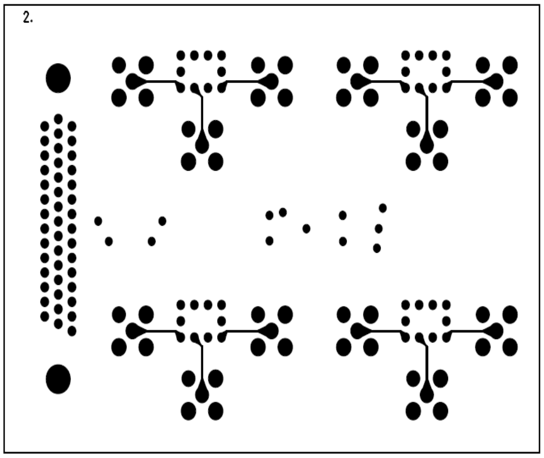

VTI29424C2_(MUX) Layer 3

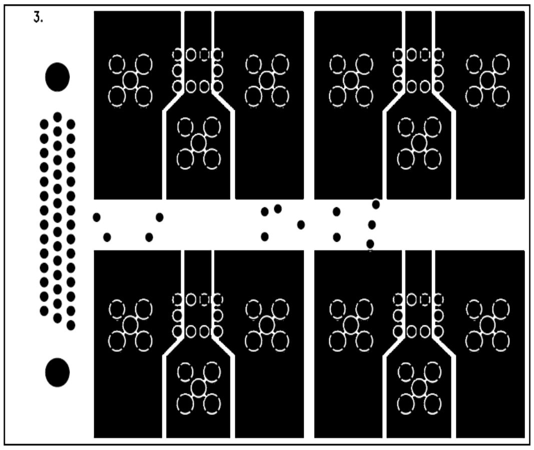

VTI29424C2_(MUX) Layer 4

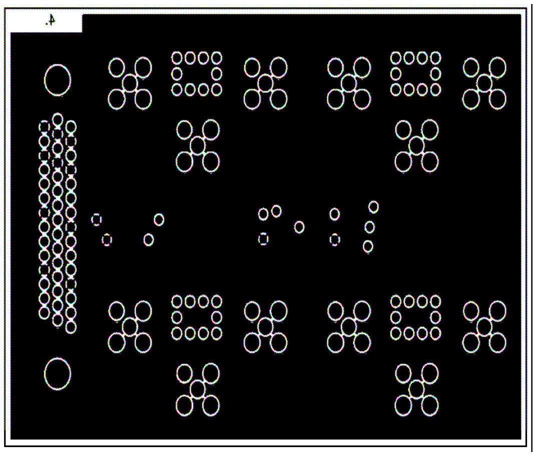

VTI29424C2_(MUX) Layer 5

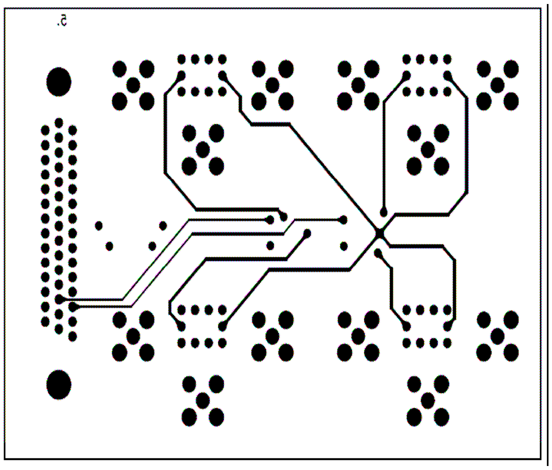

VTI29424C2_(MUX) Layer 6

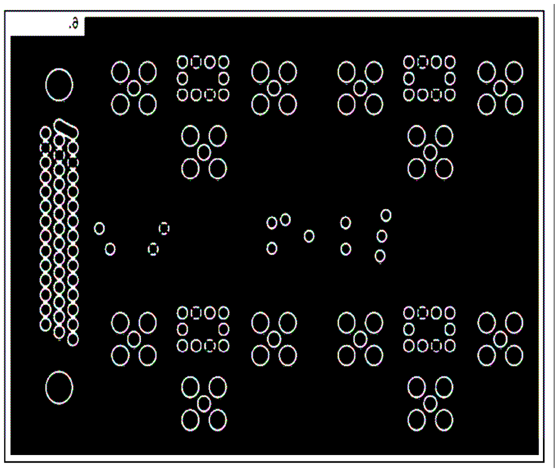

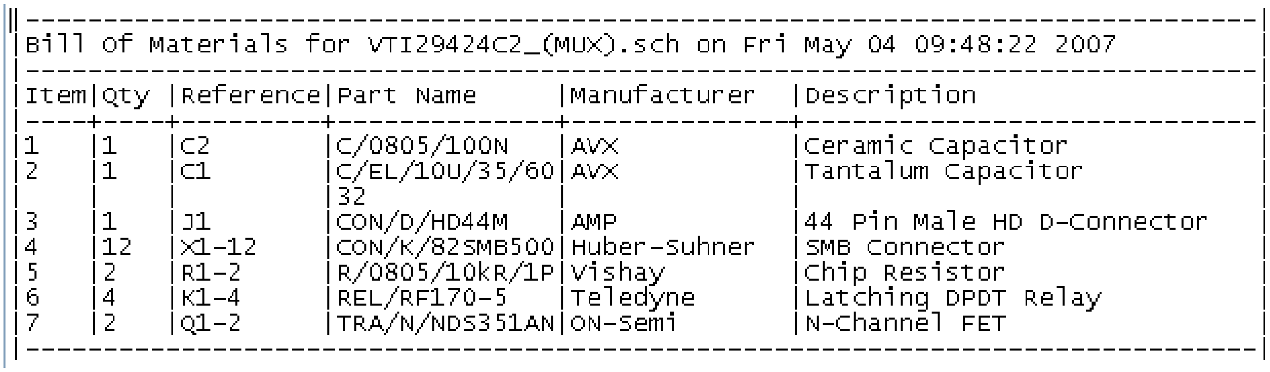

```
|--------------------------------------------------------------------------------|
|Bill Of Materials for VTI29424C2_(MUX).sch on Fri May 04 09:48:22 2007          |
|--------------------------------------------------------------------------------|
|Item|Qty |Reference|Part Name     |Manufacturer  |Description                   |
|----+----+---------+--------------+--------------+------------------------------|
|1   |1   |C2       |C/0805/100N   |AVX           |Ceramic Capacitor             |
|2   |1   |C1       |C/EL/10U/35/60|AVX           |Tantalum Capacitor            |
|    |    |         |32            |              |                              |
|3   |1   |J1       |CON/D/HD44M   |AMP           |44 Pin Male HD D-Connector    |
|4   |12  |X1-12    |CON/K/82SMB500|Huber-Suhner  |SMB Connector                 |
|5   |2   |R1-2     |R/0805/10kR/1P|Vishay        |Chip Resistor                 |
|6   |4   |K1-4     |REL/RF170-5   |Teledyne      |Latching DPDT Relay           |
|7   |2   |Q1-2     |TRA/N/NDS351AN|ON-Semi       |N-Channel FET                 |
|--------------------------------------------------------------------------------|
```

Test Measurement 1

Cable	Part	C(75 kHz)	C(100 kHz)	C(1 MHz)	C(3 MHz)	C(7 MHz)	C(10 MHz)
0	3	3.13724	3.13692	3.13320	3.12166	3.06607	2.99617
0	6	5.87294	5.87228	5.87089	5.84534	5.74735	5.61749
0	9	9.01299	9.01260	9.01115	8.97219	8.82245	8.62370
0	12	11.78410	11.78320	11.78190	11.73070	11.53610	11.27670

Test Measurement 2

Cable	Part	C(75 kHz)	C(100 kHz)	C(1 MHz)	C(3 MHz)	C(7 MHz)	C(10 MHz)
1.5	3	3.13634	3.13622	3.13263	3.12069	3.06528	2.98834
1.5	6	5.87152	5.87146	5.87032	5.84411	5.74631	5.61500
1.5	9	9.01054	9.01074	9.00942	8.97041	8.82054	8.62408
1.5	12	11.78240	11.78240	11.78140	11.73010	11.53530	11.28100

Test Measurement 3

Relay	Part	C(75 kHz)	C(100 kHz)	C(1 MHz)	C(3 MHz)	C(7 MHz)	C(10 MHz)
1	0	-0.00045	0.00039	0.00013	0.00016	0.00005	0.00341
1	3	3.14750	3.14777	3.14373	3.13230	3.07642	3.00633
1	6	5.88111	5.88160	5.88002	5.85436	5.75661	5.62458
1	9	9.01879	9.01901	9.01746	8.97822	8.82882	8.63117
1	12	11.78830	11.78890	11.78690	11.73580	11.54080	11.28180
2	0	-0.00007	0.00007	0.00010	-0.00095	0.00009	-0.00368
2	3	3.14577	3.14572	3.14168	3.13009	3.07416	3.00885
2	6	5.87978	5.87968	5.87882	5.85279	5.75429	5.61768
2	9	9.01743	9.01702	9.01632	8.97706	8.82665	8.62101
2	12	11.78770	11.78760	11.78700	11.73510	11.53910	11.27300
3	0	0.00049	0.00027	0.00016	0.00027	0.00014	-0.00263
3	3	3.14828	3.14855	3.14452	3.13323	3.07697	3.00705
3	6	5.88206	5.88171	5.88065	5.85510	5.75658	5.62641
3	9	9.01953	9.01921	9.01773	8.97893	8.82793	8.62740
3	12	11.78930	11.78930	11.78770	11.74710	11.54070	11.28060
4	0	0.00433	-0.00082	-0.00051	-0.00082	-0.00046	-0.00818
4	3	3.14583	3.14533	3.14127	3.12955	3.07360	3.00185
4	6	5.87860	5.87808	5.87721	5.85121	5.75262	5.61860
4	9	9.01535	9.01510	9.01403	8.97473	8.82402	8.62423
4	12	11.78510	11.78490	11.78360	11.74330	11.53520	11.26840
5	0	-0.00085	-0.00021	-0.00028	-0.00043	-0.00025	0.01113
5	3	3.14555	3.14578	3.14135	3.13021	3.07382	3.00831
5	6	5.87914	5.87914	5.87770	5.85212	5.75335	5.62770
5	9	9.01684	9.01697	9.01517	8.97608	8.82482	8.62453
5	12	11.78750	11.78750	11.78530	11.74390	11.53800	11.28520
6	0	-0.00049	-0.00020	0.00018	0.00026	0.00007	0.00496
6	3	3.14729	3.14696	3.14305	3.13154	3.07541	3.01431
6	6	5.88097	5.88064	5.87934	5.85392	5.75522	5.62944
6	9	9.01854	9.01840	9.01705	8.97773	8.82685	8.62866
6	12	11.78920	11.78910	11.78740	11.74560	11.53930	11.28020
7	0	-0.00109	-0.00104	-0.00091	-0.00105	-0.00089	0.01680
7	3	3.14449	3.14458	3.14063	3.12931	3.07288	3.00301
7	6	5.87822	5.87823	5.87697	5.85095	5.75263	5.62182
7	9	9.01614	9.01617	9.01487	8.97547	8.82454	8.62184
7	12	11.78680	11.78680	11.78530	11.74350	11.53680	11.27460
8	0	-0.00027	-0.00094	-0.00013	-0.00335	-0.00014	0.00679
8	3	3.14574	3.14551	3.14147	3.13010	3.07365	3.00511
8	6	5.87916	5.87868	5.87749	5.85157	5.75309	5.62692
8	9	9.01574	9.01561	9.01444	8.97521	8.82411	8.62099
8	12	11.78600	11.78580	11.78450	11.74340	11.53580	11.27780

Test Measurement 3 (continued)

Relay	Part	C(75 kHz)	C(100 kHz)	C(1 MHz)	C(3 MHz)	C(7 MHz)	C(10 MHz)
9	0	-0.00067	-0.00042	-0.00008	-0.00062	-0.00005	0.00658
9	3	3.14687	3.14673	3.14265	3.13119	3.07495	3.00795
9	6	5.88087	5.88065	5.87938	5.85339	5.75493	5.62765
9	9	9.01845	9.01838	9.01655	8.97764	8.82669	8.62606
9	12	11.78810	11.78840	11.78610	11.74540	11.53820	11.27740
10	0	0.00064	0.00012	0.00004	0.00023	0.00004	-0.00622
10	3	3.14495	3.14453	3.14056	3.12917	3.07268	3.00814
10	6	5.87812	5.87797	5.87660	5.85088	5.75222	5.61969
10	9	9.01573	9.01575	9.01381	8.97453	8.82347	8.62449
10	12	11.78530	11.78540	11.78360	11.74100	11.53450	11.27130
11	0	-0.00009	0.00020	-0.00002	0.00024	-0.00004	0.00244
11	3	3.14524	3.14525	3.14116	3.13000	3.07331	3.00034
11	6	5.87862	5.87919	5.87768	5.85208	5.75291	5.61710
11	9	9.01628	9.01655	9.01528	8.97587	8.82411	8.61801
11	12	11.78680	11.78710	11.78510	11.74390	11.53590	11.27350
12	0	0.00013	0.00337	-0.00016	-0.00040	-0.00008	-0.00131
12	3	3.14732	3.14733	3.14314	3.13133	3.07494	3.00883
12	6	5.87994	5.87976	5.87843	5.85260	5.75328	5.61958
12	9	9.01765	9.01787	9.01613	8.97626	8.82466	8.62374
12	12	11.78720	11.78700	11.78560	11.74290	11.53560	11.27370
13	0	-0.00054	-0.00039	-0.00010	-0.00062	-0.00008	0.00561
13	3	3.14655	3.14654	3.14251	3.13072	3.07462	3.00698
13	6	5.88046	5.88027	5.87900	5.85297	5.75421	5.61999
13	9	9.01744	9.01710	9.01588	8.97639	8.82496	8.61882
13	12	11.78800	11.78750	11.78630	11.74660	11.53730	11.26720
14	0	-0.00070	-0.00073	-0.00059	-0.00082	-0.00061	-0.00493
14	3	3.14362	3.14384	3.13983	3.12869	3.07197	3.00956
14	6	5.87744	5.87774	5.87631	5.85071	5.75168	5.61969
14	9	9.01491	9.01452	9.01331	8.97414	8.82200	8.61947
14	12	11.78490	11.78490	11.78320	11.74440	11.53410	11.27030
15	0	-0.00083	-0.00086	-0.00058	-0.00065	-0.00054	-0.00675
15	3	3.14717	3.14730	3.14338	3.13190	3.07493	3.00418
15	6	5.87782	5.87777	5.87638	5.85021	5.75077	5.61798
15	9	9.01462	9.01475	9.01297	8.97380	8.82108	8.61719
15	12	11.78650	11.78620	11.78480	11.74400	11.53480	11.27380
16	0	-0.00043	-0.00046	-0.00052	-0.00078	-0.00041	-0.00586
16	3	3.14515	3.14484	3.14103	3.12948	3.07269	3.00306
16	6	5.87811	5.87807	5.87705	5.85086	5.75147	5.61808
16	9	9.01519	9.01539	9.01410	8.97406	8.82200	8.62352
16	12	11.78510	11.78520	11.78390	11.74170	11.53330	11.27450

Test Measurement 3 (continued)

Relay	Part	C(75 kHz)	C(100 kHz)	C(1 MHz)	C(3 MHz)	C(7 MHz)	C(10 MHz)
17	0	0.00059	0.00043	0.00035	0.00016	0.00029	0.00697
17	3	3.14763	3.14739	3.14346	3.13188	3.07499	3.00874
17	6	5.88116	5.88104	5.87975	5.85344	5.75414	5.62402
17	9	9.01819	9.01774	9.01705	8.97734	8.82500	8.62216
17	12	11.78750	11.78730	11.78590	11.74670	11.53530	11.27360
18	0	-0.00073	-0.00058	-0.00051	-0.00056	-0.00048	-0.00620
18	3	3.14578	3.14604	3.14207	3.13065	3.07392	3.00421
18	6	5.87774	5.87809	5.87661	5.85056	5.75142	5.61644
18	9	9.01503	9.01525	9.01380	8.97442	8.82210	8.61682
18	12	11.78500	11.78530	11.78380	11.74480	11.53370	11.27020
19	0	0.00022	-0.00022	-0.00021	0.00031	-0.00014	0.00446
19	3	3.14281	3.14238	3.13875	3.12736	3.07076	3.00444
19	6	5.87703	5.87655	5.87538	5.84966	5.75032	5.62176
19	9	9.01846	9.01789	9.01691	8.97734	8.82553	8.62834
19	12	11.78490	11.78440	11.78290	11.74300	11.53330	11.27050
20	0	0.00050	0.00066	0.00044	0.00050	0.00041	0.00337
20	3	3.14527	3.14566	3.14171	3.13015	3.07347	3.01091
20	6	5.87967	5.87963	5.87860	5.85277	5.75339	5.62561
20	9	9.01673	9.01676	9.01533	8.97597	8.82396	8.62692
20	12	11.78610	11.78610	11.78460	11.74310	11.53500	11.27250
21	0	0.00059	0.00012	-0.00016	-0.00051	-0.00013	-0.00264
21	3	3.14404	3.14371	3.13992	3.12823	3.07185	3.00781
21	6	5.87779	5.87764	5.87639	5.85052	5.75131	5.61979
21	9	9.01536	9.01514	9.01394	8.97453	8.82247	8.61791
21	12	11.78720	11.78680	11.78530	11.74350	11.53610	11.26880
22	0	-0.00053	-0.00030	-0.00048	-0.00087	-0.00051	-0.00420
22	3	3.14332	3.14352	3.13918	3.12793	3.07149	3.00741
22	6	5.87709	5.87676	5.87561	5.84972	5.75124	5.62394
22	9	9.01690	9.01676	9.01512	8.97619	8.82494	8.62957
22	12	11.78680	11.78680	11.78470	11.74520	11.53680	11.27800
23	0	0.00056	0.00078	0.00039	0.00027	0.00041	0.00218
23	3	3.14570	3.14573	3.14159	3.13015	3.07374	3.00486
23	6	5.87989	5.87989	5.87901	5.85276	5.75413	5.62540
23	9	9.01778	9.01762	9.01639	8.97708	8.82559	8.62392
23	12	11.78870	11.78840	11.78710	11.74530	11.53820	11.27500
24	0	-0.00071	-0.00076	-0.00053	-0.00038	-0.00042	0.01950
24	3	3.14487	3.14524	3.14111	3.12993	3.07342	3.00412
24	6	5.87976	5.88014	5.87861	5.85316	5.75416	5.62023
24	9	9.01783	9.01777	9.01661	8.97777	8.82595	8.62714
24	12	11.78860	11.78890	11.78740	11.74830	11.53870	11.28050

Test Measurement 3 (continued)

Relay	Part	C(75 kHz)	C(100 kHz)	C(1 MHz)	C(3 MHz)	C(7 MHz)	C(10 MHz)
25	0	-0.00041	-0.00055	-0.00043	-0.00059	-0.00045	-0.00471
25	3	3.14638	3.14616	3.14230	3.13111	3.07449	3.00569
25	6	5.87710	5.87696	5.87585	5.85043	5.75133	5.62126
25	9	9.01377	9.01419	9.01275	8.97353	8.82213	8.62458
25	12	11.78340	11.78330	11.78210	11.74010	11.53320	11.27560
26	0	0.00030	-0.00024	0.00006	0.00044	0.00007	0.00343
26	3	3.14842	3.14814	3.14385	3.13236	3.07615	3.01204
26	6	5.88217	5.88229	5.88069	5.85478	5.75637	5.62321
26	9	9.01870	9.01907	9.01688	8.97785	8.82681	8.62561
26	12	11.78830	11.78900	11.78680	11.74420	11.53870	11.27270
27	0	0.00036	0.00027	0.00037	-0.00016	0.00035	-0.00500
27	3	3.14827	3.14793	3.14425	3.13251	3.07649	3.00657
27	6	5.87954	5.87934	5.87851	5.85258	5.75433	5.62491
27	9	9.01664	9.01673	9.01526	8.97597	8.82502	8.62915
27	12	11.78650	11.78640	11.78560	11.74570	11.53720	11.28130
28	0	-0.00118	-0.00023	-0.00031	-0.00037	-0.00033	0.00377
28	3	3.14683	3.14687	3.14299	3.13162	3.07534	3.00930
28	6	5.87846	5.87869	5.87702	5.85109	5.75291	5.62564
28	9	9.01909	9.01935	9.01771	8.97860	8.82833	8.62896
28	12	11.78680	11.78700	11.78560	11.74630	11.53780	11.27470
29	0	-0.00045	-0.00069	-0.00053	-0.00079	-0.00051	-0.00778
29	3	3.14631	3.14613	3.14226	3.13095	3.07470	3.01131
29	6	5.87984	5.87985	5.87853	5.85268	5.75420	5.62152
29	9	9.01710	9.01712	9.01535	8.97639	8.82580	8.62126
29	12	11.78720	11.78800	11.78570	11.74700	11.53800	11.27770
30	0	0.00022	0.00030	0.00026	0.00055	0.00026	0.00632
30	3	3.14572	3.14566	3.14179	3.13058	3.07430	3.01257
30	6	5.87971	5.87997	5.87876	5.85276	5.75468	5.62048
30	9	9.01708	9.01755	9.01577	8.97672	8.82610	8.62773
30	12	11.78800	11.78830	11.78610	11.74600	11.53890	11.28360
31	0	-0.00228	-0.00033	-0.00030	-0.00012	-0.00030	-0.00559
31	3	3.14390	3.14366	3.13985	3.12879	3.07243	3.00381
31	6	5.87744	5.87747	5.87646	5.85074	5.75239	5.61886
31	9	9.01524	9.01550	9.01377	8.97468	8.82402	8.63006
31	12	11.78550	11.78580	11.78400	11.74600	11.53670	11.28190
32	0	-0.00014	-0.00357	-0.00006	-0.00040	-0.00005	0.00126
32	3	3.14750	3.14756	3.14373	3.13187	3.07603	3.01083
32	6	5.88066	5.88042	5.87949	5.85316	5.75500	5.62801
32	9	9.01637	9.01634	9.01527	8.97555	8.82525	8.62678
32	12	11.78490	11.78520	11.78440	11.73270	11.53630	11.27540